

Electronic Supplementary Information for

Palladium–Peptide Oxidative Addition Complexes for Bioconjugation

Anthony J. Rojas,^{a,b,‡} Justin M. Wolfe,^{a,‡} Heemal H. Dhanjee,^a Ivan Buslov,^a Nicholas L. Truex,^a
Richard Y. Liu,^c Walter Masefski,^a Bradley L. Pentelute,^{a,d,e,f,*} Stephen L. Buchwald^{a,*}

^{a.} Department of Chemistry, Massachusetts Institute of Technology, 77 Massachusetts Avenue, Cambridge, MA 02139, USA.

^{b.} Department of Chemistry and Biochemistry, Kennesaw State University, 1000 Chastain Road NW, Kennesaw, GA 30144, USA.

^{c.} Department of Chemistry and Chemical Biology, Harvard University, 12 Oxford Street, Cambridge, MA 02138, USA.

^{d.} The Koch Institute for Integrative Cancer Research, Massachusetts Institute of Technology, 500 Main Street, Cambridge, MA 02142, USA.

^{e.} Center for Environmental Health Sciences, Massachusetts Institute of Technology, 77 Massachusetts Avenue, Cambridge, MA 02139, USA.

^{f.} Broad Institute of MIT and Harvard, 415 Main Street, Cambridge, MA 02142, USA.

*Email: blp@mit.edu, sbuchwal@mit.edu

‡These authors contributed equally to this work.

SUPPORTING INFORMATION

1. General Experimental Details	S2-5
2. Peptide Synthesis and LC-MS Characterization	S6-12
3. Oxidative Addition Complex Synthesis and LC-MS Characterization	S13-21
4. Palladium-Peptide Reactions with Small Molecule Thiols	S22-26
5. Studies of pH Dependence of the Bioconjugation Reaction	S27-28
6. Studies of Halide Dependence of the Bioconjugation Reaction	S29-30
7. Peptide-Peptide Ligation Reactions and LC-MS Characterization	S31-38
8. Peptide-Protein Ligation Reactions and LC-MS Characterization	S39-47
9. Oxidative Addition Complex Stability	S48-50
10. Complex 1B MS/MS Characterization	S51-52
11. NMR Structure Analysis of Peptide-OAC	S53-62
12. Conformational Analysis of a Tripeptide Oxidative Addition Complex via DFT	S63-71
13. NMR Spectra	S72-86
14. References	S87-88

1. GENERAL EXPERIMENTAL DETAILS

General Reagent Information

1-[Bis(dimethylamino)methylene]-1H-1,2,3-triazolo[4,5-b]pyridinium 3-oxide hexafluorophosphate (HATU), Fmoc-L-Gly-OH, Fmoc-L-Leu-OH, Fmoc-L-Ile-OH, Fmoc-L-Lys(Boc)-OH, Fmoc-L-Ala-OH, Fmoc-L-Cys(Trt)-OH, Fmoc-L-Gln(Trt)-OH, Fmoc-L-Asn(Trt)-OH, Fmoc-L-Glu(*Ot*Bu)-OH, Fmoc-L-Asp-OH, Fmoc-L-Arg(Pbf)-OH, Fmoc-L-Phe-OH, Fmoc-L-Ser(*t*Bu)-OH, Fmoc-L-Trp-OH, Fmoc-L-Thr(*t*Bu)-OH, Fmoc-L-Tyr(*t*Bu)-OH, and Fmoc-L-His(Trt)-OH were purchased from CreoSalus, Inc (Louisville, KY). Fmoc-4-iodo-L-phenylalanine, Fmoc-4-bromo-L-phenylalanine, and Fmoc-4-chloro-L-phenylalanine were purchased from Chem-Impex International (Wood Dale, IL). H-Rink Amide-ChemMatrix resin was obtained from PCAS BioMatrix Inc. (St-Jean-sur-Richelieu, Quebec, Canada). PyAOP was purchased from P3 BioSystems (Louisville, KY). Peptide synthesis-grade *N,N*-dimethylformamide (DMF), dichloromethane (CH₂Cl₂), diethyl ether, and HPLC-grade acetonitrile were obtained from VWR International (Philadelphia, PA). Small molecule thiols were purchased from Aldrich Chemical Co., Alfa Aesar, or Matrix Scientific and were used without additional purification. All deuterated solvents were purchased from Cambridge Isotopes and used without further purification. All other reagents were purchased from Sigma-Aldrich and used as received.

All reactions with peptides were set up on the bench top and carried out under ambient conditions. Dimethylsulfoxide (DMSO), pentane, and cyclohexane were purchased from Aldrich Chemical Company in SureSeal™ bottles and were purged with argon before use. The ligand used during this study, sSPhos, was generously gifted from Aldrich Chemical Company.

All small-molecule organic and organometallic compounds were characterized by ¹H, ¹³C NMR, and IR spectroscopy, as well as high-resolution mass spectrometry (unless otherwise noted). ³¹P NMR spectroscopy was used for characterization of palladium complexes. Copies of the ¹H, ¹³C, and ³¹P NMR spectra can be found at the end of the Supporting Information. Nuclear Magnetic Resonance spectra were recorded on a Bruker 400 MHz instrument and a Varian 300 MHz instrument. Unless otherwise stated, all ¹H NMR experiments are reported in δ units, parts per million (ppm), and were measured relative to the signals of the residual proton resonances methanol-d₄ (4.78 and 3.31 ppm) in the deuterated solvents. High resolution mass spectra were obtained on a Bruker Daltonics APEXIV 4.7 Tesla Fourier transform ion cyclotron resonance mass spectrometer (FT-ICR-MS). Matrix assisted laser desorption/ionization time of flight mass spectrometry (MALDI-TOF-MS) analysis was performed on a Bruker MicroFlex using positive reflector mode.

LC-MS chromatograms and associated mass spectra were acquired using Agilent 6520 ESI-Q-TOF mass spectrometer. Solvent compositions used in the LC-MS are 0.1% formic acid in H₂O (solvent A) and 0.1% formic acid in acetonitrile (solvent B). **Method A was used for all samples unless otherwise noted.**

Note: When calculating the mass of peptide-based substrates, TFA salts were not considered in the molecular weight calculation both for experimental set up and for yield determination.

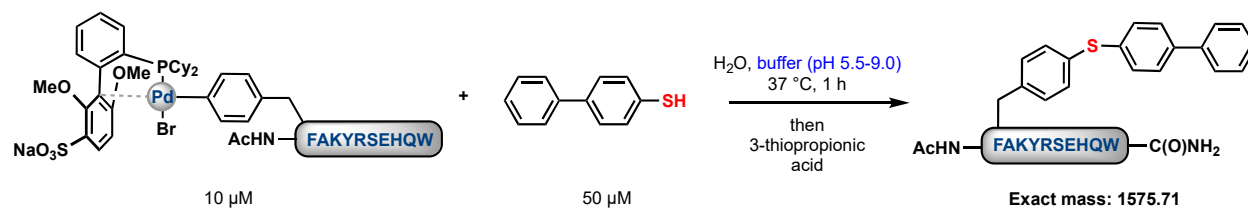
Method A LC conditions: Zorbax 300SB C3 column: 2.1 x 150 mm, 5 μ m, column temperature: 40 °C, gradient: 0-2 min 1% B, 2-11 min 1-61% B, flow rate: 0.8 mL/min. MS conditions: positive electrospray ionization (ESI) extended dynamic mode in mass range 300 – 3000 m/z , temperature of drying gas = 350 °C, flow rate of drying gas = 11 L/min, pressure of nebulizer gas = 60 psi, the capillary, fragmentor, and octapole rf voltages were set at 4000, 175, and 750, respectively.

Method B: Select LC-MS chromatograms and associated mass spectra were acquired using an Agilent 6550 ESI-Q-TOF mass spectrometer. The solvent compositions used were 0.1% formic acid in H₂O (solvent A) and 0.1% formic acid in acetonitrile (solvent B). The column was a Phenomenex Jupiter C4 column 150 x 1.0 mm ID, 5 μ m 300Å silica. The method started at 1% B, and after 4 minutes, the gradient ramped to 91% over 16 minutes. Flowrate was 100 μ l/min. MS acquired from 4 to 18 minutes.

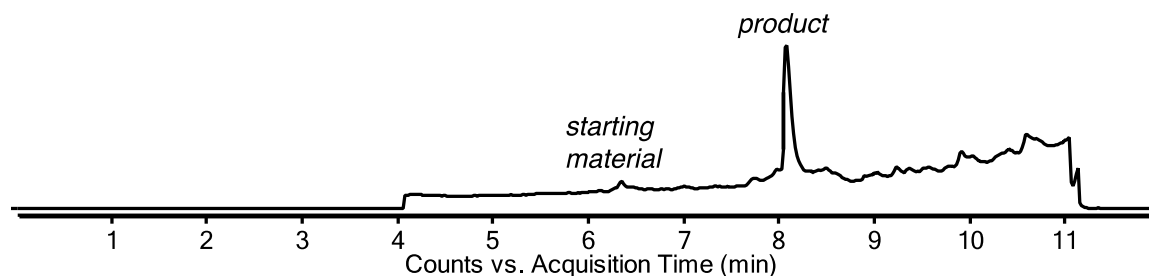
Method C: LC-MS chromatograms and associated mass spectra for protein ligation reactions were acquired using and Agilent 6550 ESI-Q-TOF mass spectrometer. The conditions were: Zorbax 300SB C3 column: 2.1 x 150 mm, 5 μ m, column temperature: 40 °C, gradient: 0-2 min 25% B, 2-34 min 25-95% B, flow rate: 0.5 mL/min. MS conditions: positive electrospray ionization (ESI) extended dynamic mode in mass range 100 – 3000 m/z , sheath gas temperature = 350 °C, flow rate of drying gas = 11 L/min, pressure of nebulizer gas = 55 psi, the capillary, fragmentor, and nozzle voltages were set at 3500, 175, and 1000, respectively.

Determination of Bioconjugation Conversions

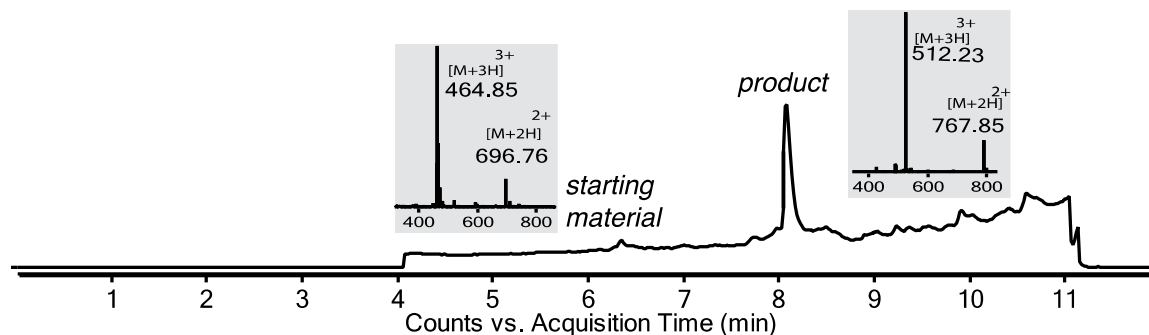
Data were processed using Agilent MassHunter software package. All reported yields were determined by integrating total ion current (TIC) spectra. First, the peak areas for all relevant peptide-containing species on the chromatogram were integrated using Agilent MassHunter software package. Since no peptide-based side products were generated in the experiments, the yields shown in **Schemes 1, 2, and 3** were determined as follows: %yield = S_{pr}/S_{total} where S_{pr} is the peak area of the product and S_{total} is the peak area of combined peptide-containing species (product and starting material). For protein bioconjugation, deconvoluted masses of proteins were obtained using maximum entropy algorithm. LC-MS data shown were acquired using Method A, unless otherwise noted. Mass spectrum insets correspond to the integration of the TIC peak unless otherwise noted. In order to provide clarity, an example of how bioconjugation conversion is detailed below:



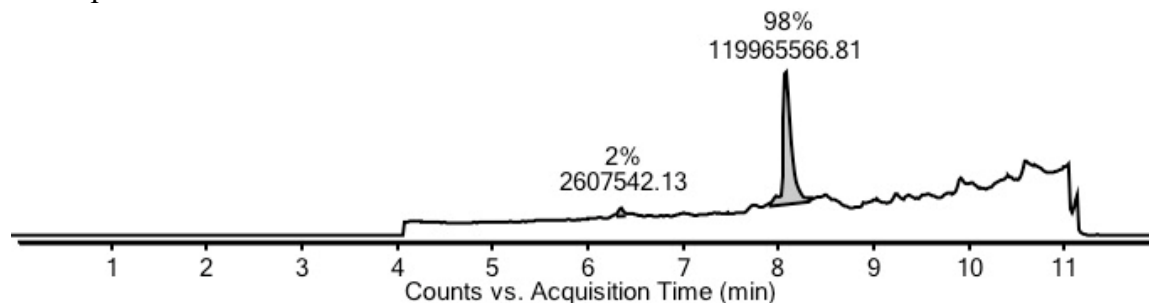
The crude reaction mixture is depicted below:



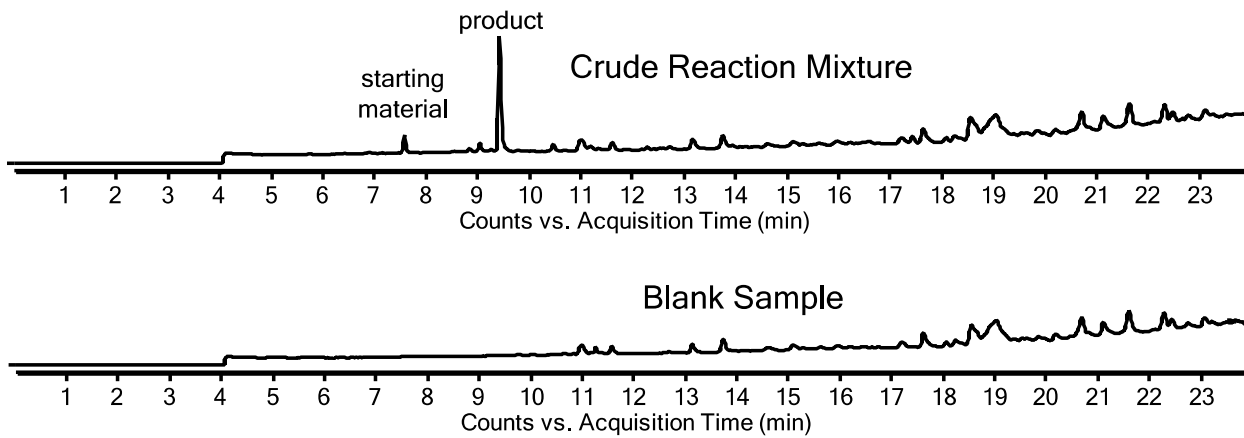
This mixture was analyzed by LC-MS using Agilent MassHunter software package. The peptide-containing peaks that correspond to the starting material and product were identified by mass as can be seen from the insets depicted below.



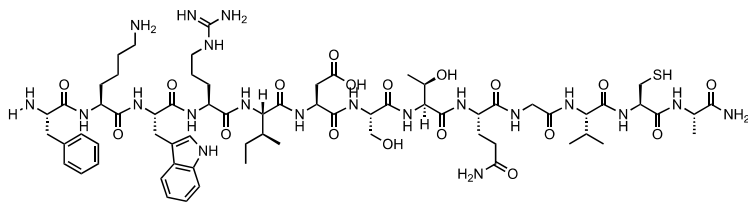
Finally, using the calculation described above, the Agilent MassHunter software package was used to integrate below the starting material and product peaks to determine the percent of conversion to the product.



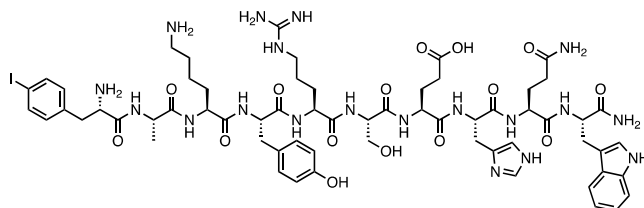
In some cases, a small non-peptidic impurity near the starting material was found, resulting in an additional peak. This peak was omitted from conversion calculations because it does not correspond to total peptide-containing species.



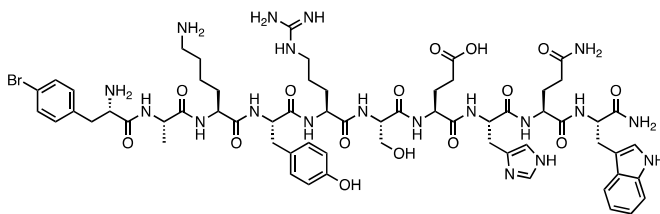
A longer, 26-minute LC-MS method was also performed to confirm the lack of byproducts produced from the crude reaction.



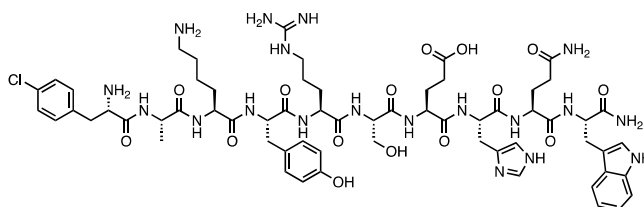
P3
Phe Lys Trp Arg Ile Asp Ser Thr Gln Gly Val Cys Ala
 mass: 1508.76



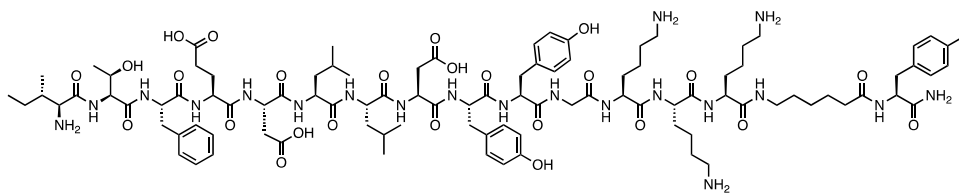
P4
4-iodoPhe Ala Lys Tyr Arg Ser Glu His Gln Trp
 mass: 1475.56



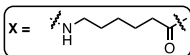
P5
4-bromoPhe Ala Lys Tyr Arg Ser Glu His Gln Trp
 mass: 1427.52

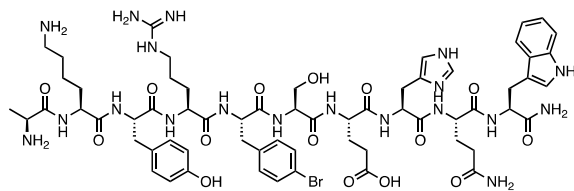


P6
4-chloroPhe Ala Lys Tyr Arg Ser Glu His Gln Trp
 mass: 1383.62

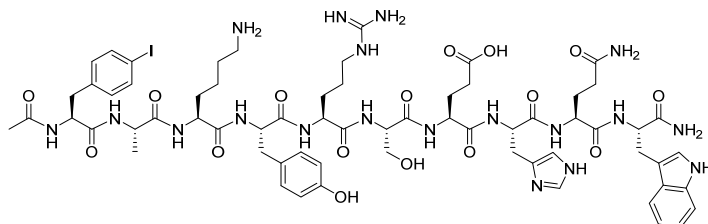


P7
Ile Thr Phe Glu Asp Leu Leu Asp Tyr Tyr Gly Lys Lys X 4-iodoPhe
 mass: 2116.97

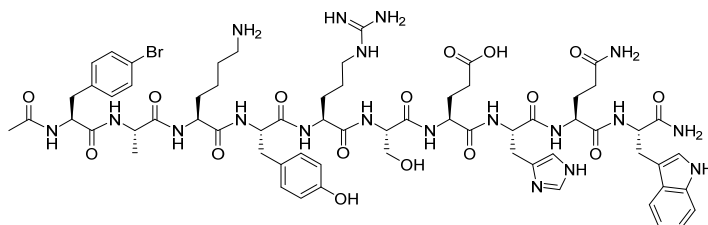




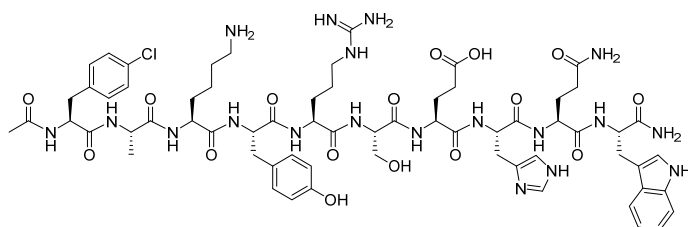
P8
Ala Lys Tyr Arg 4-bromoPhe Ser Glu His Gln Trp
mass: 1427.57



P9
Acetyl 4-iodoPhe Ala Lys Tyr Arg Ser Glu His Gln Trp
Exact Mass: 1517.57



P10
Acetyl 4-bromoPhe Ala Lys Tyr Arg Ser Glu His Gln Trp
Exact Mass: 1469.58



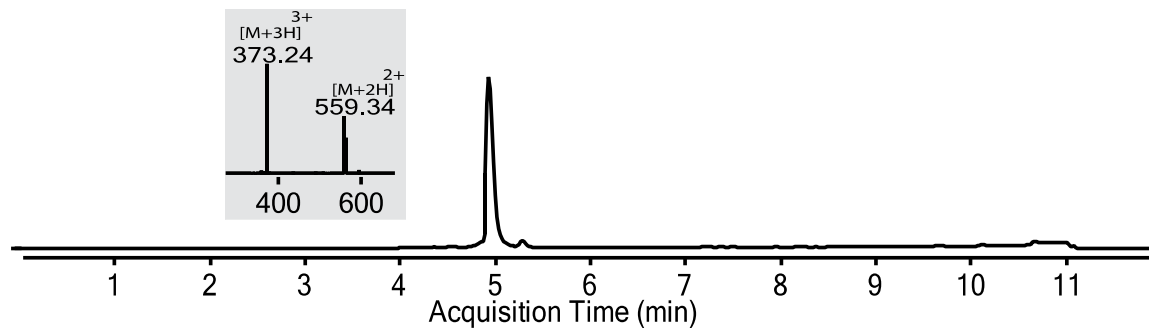
P11
Acetyl 4-chloroPhe Ala Lys Tyr Arg Ser Glu His Gln Trp
Exact Mass: 1425.63

Peptide Purification

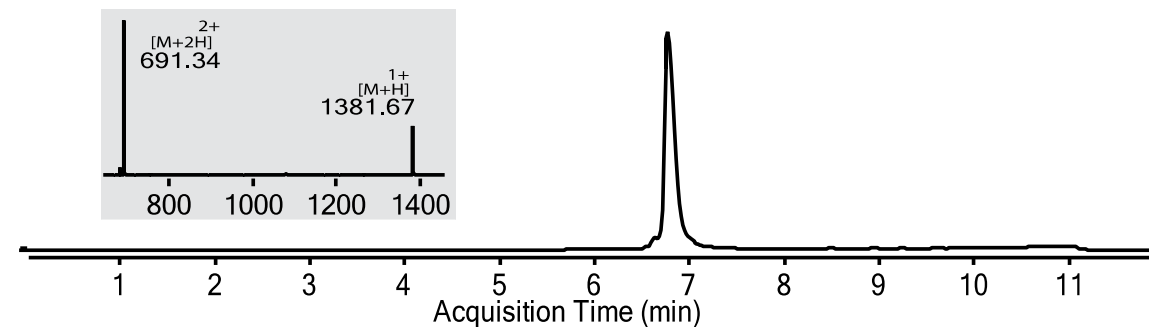
Peptides were dissolved in water and acetonitrile containing 0.1% TFA, filtered through a 0.22 μm nylon filter and purified by mass-directed semi-preparative reversed-phase HPLC (RP-HPLC). Solvent **A** was water with 0.1% TFA additive and Solvent **B** was acetonitrile with 0.1% TFA additive. A linear gradient from 5-45% **B** changing a rate of 0.5% **B**/min was used. The peptides were purified on an Agilent Zorbax SB C3 column: 9.4 x 250 mm, 5 μm . Using the mass data collected for each fraction from the instrument, only pure fractions were combined and

lyophilized. The purity of the fraction pool was confirmed by LC-MS. Total-ion current chromatograms for each peptide is shown below.

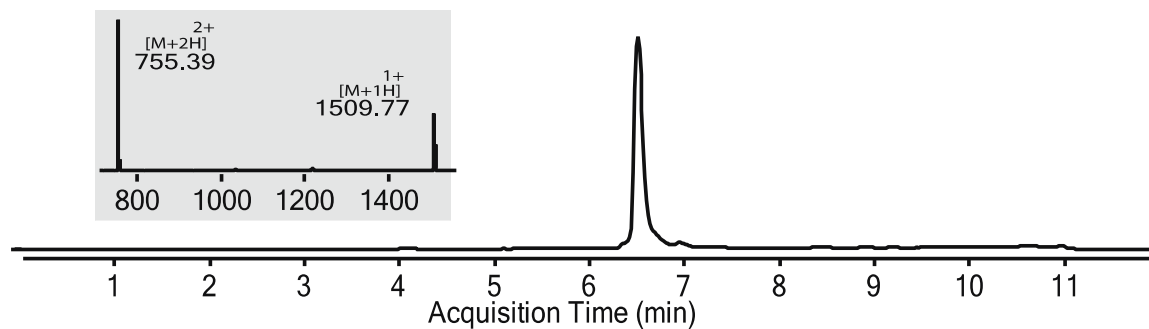
P1:



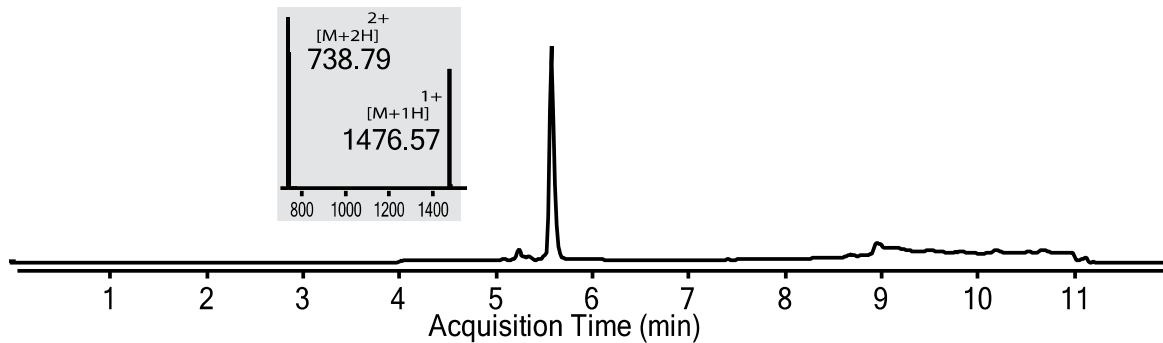
P2:



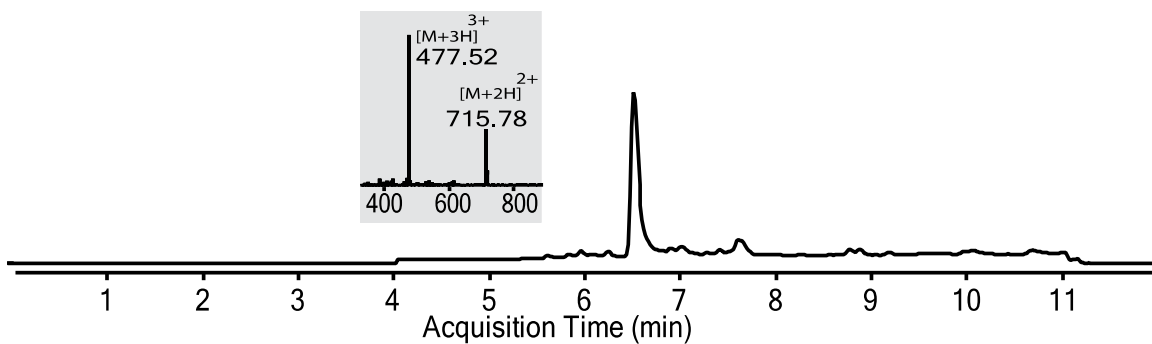
P3:



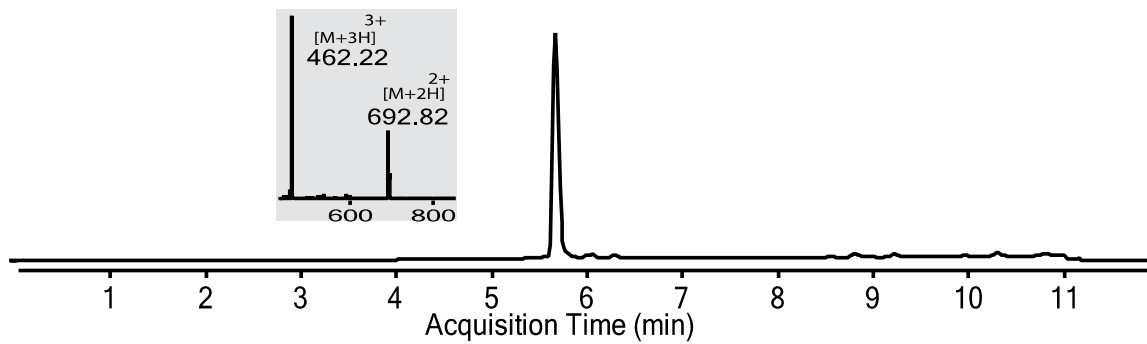
P4:



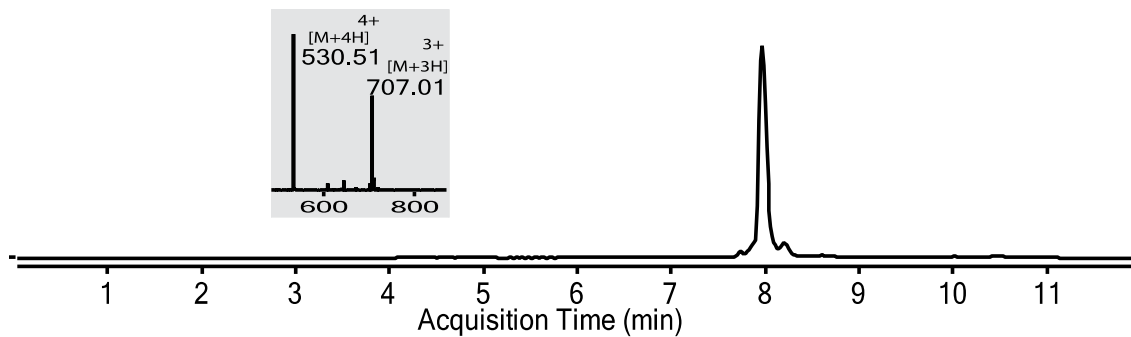
P5:



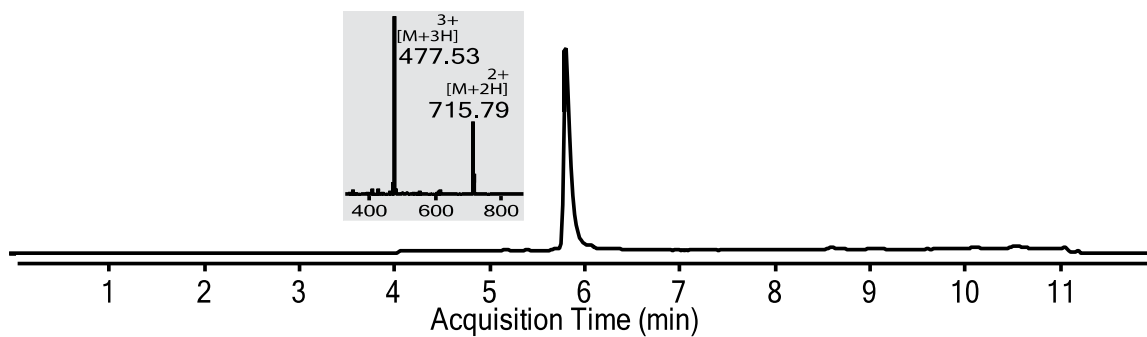
P6:



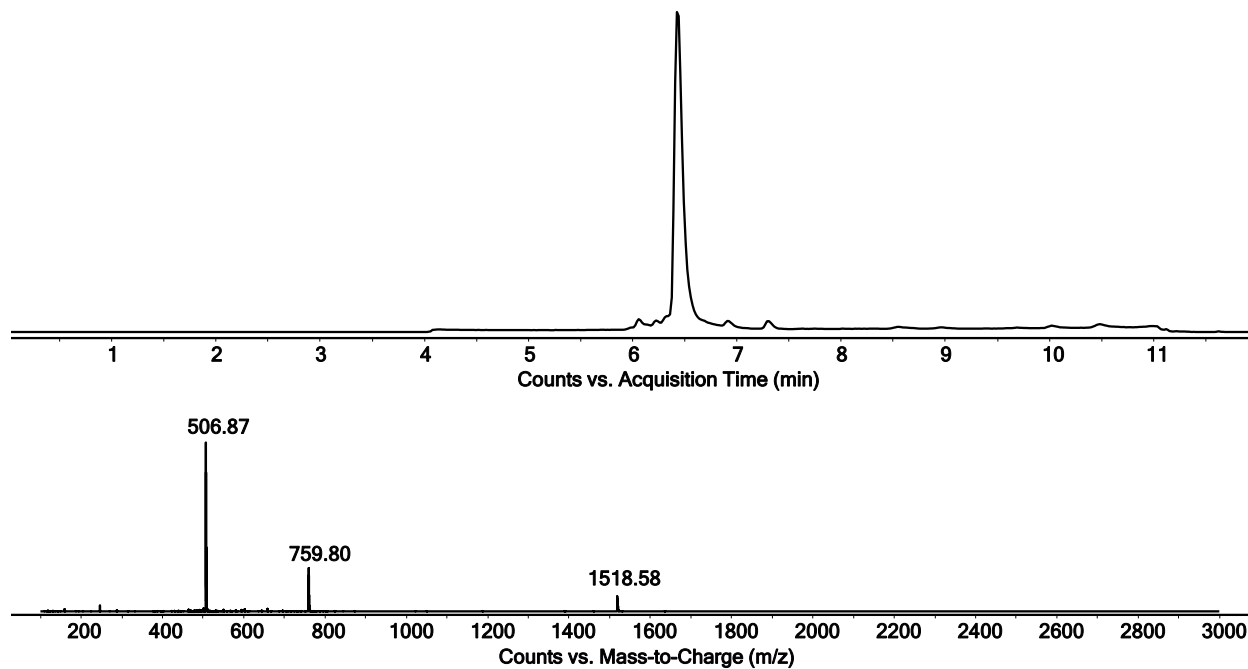
P7:



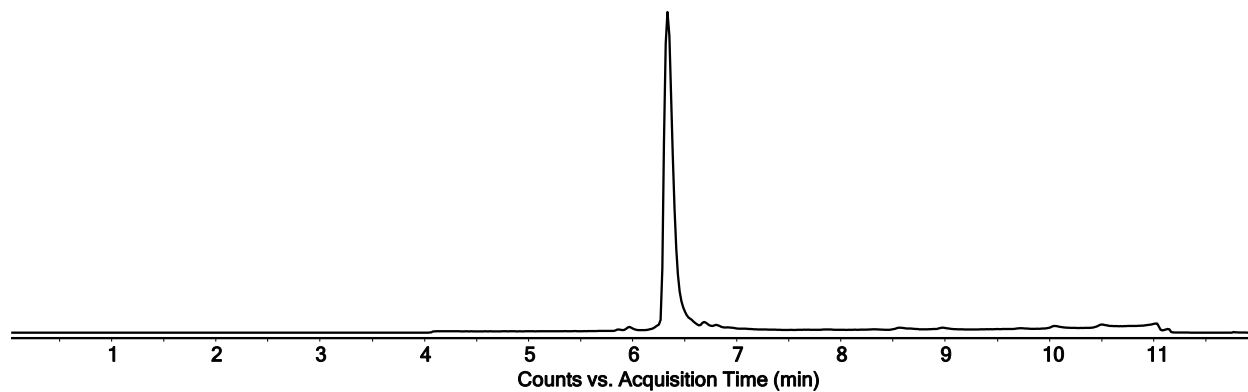
P8:

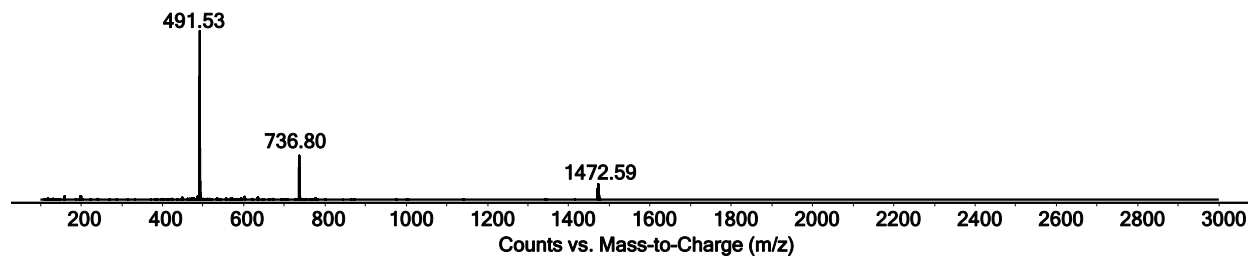


P9:

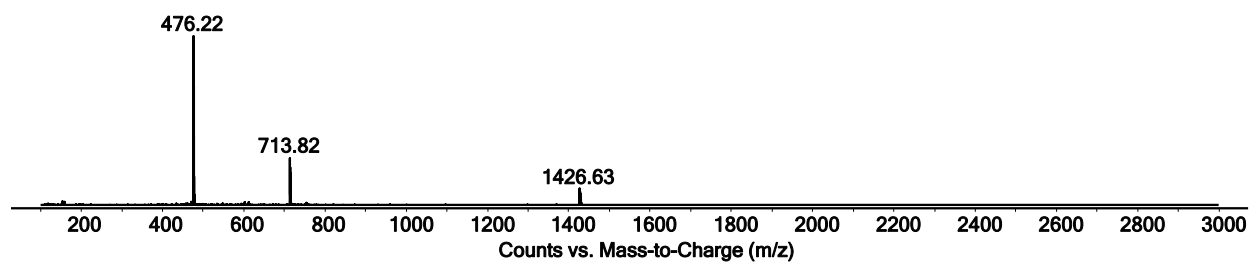
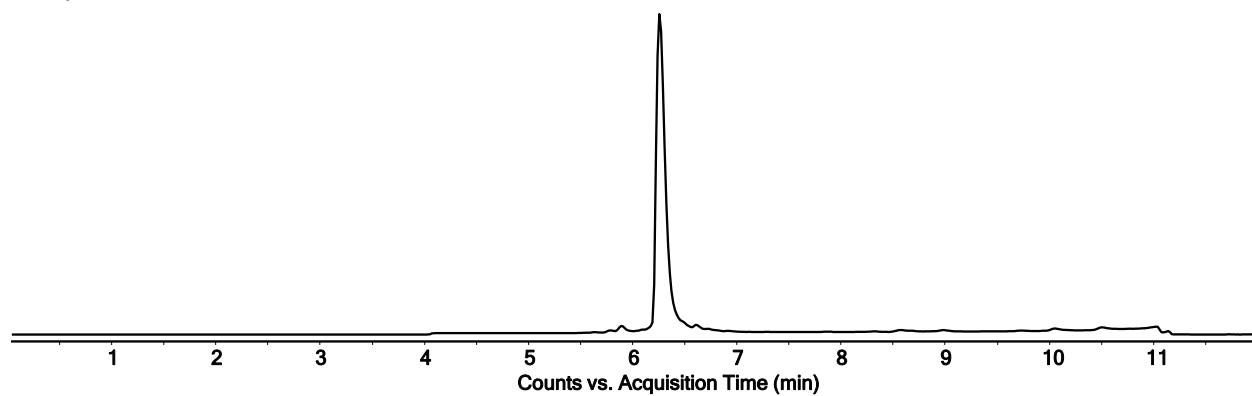


P10:





P11:

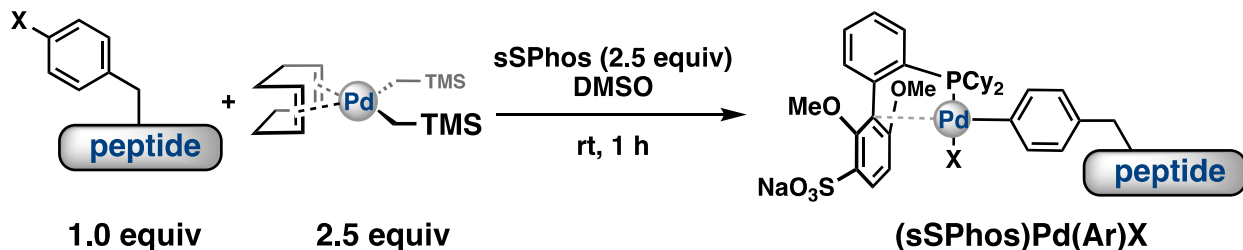


3. OXIDATIVE ADDITION COMPLEXES AND SYNTHETIC PROCEDURES

Synthesis of Pd-Peptide Oxidative Addition Complexes

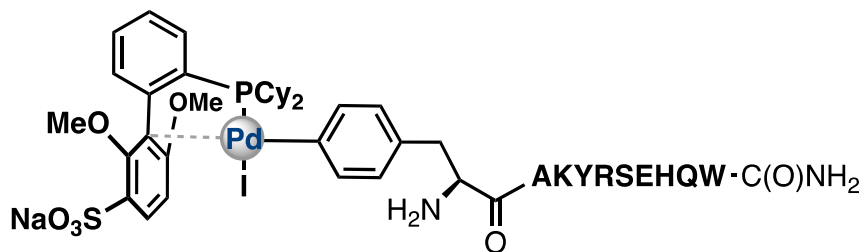
Synthesis of [(1,5-COD)Pd(CH₂TMS)₂]. This compound was synthesized according to the procedure reported in the literature.¹ The ¹H and ¹³C NMR spectra of the obtained material are identical to those reported in the literature.¹ The title compound was stored in a freezer at -20 °C.

General Procedure for the Synthesis of Palladium-Peptide Oxidative Addition Complexes.



In a scintillation vial (10 mL) open to the air and equipped with a magnetic stir bar, the vial was charged with sSPhos ligand (2.5 equiv), peptide-Ar-X (1 equiv), and DMSO (1 mL). Solid (1,5-COD)Pd(CH₂SiMe₃)₂ (2.5 equiv) was added rapidly in one portion and the resulting solution was stirred for 1 h at rt.* After this time, the solution was frozen by placing the capped vial into a liquid nitrogen bath and subsequently lyophilized to remove the DMSO. The Pd-Peptide oxidative addition complexes were purified via mass-directed preparative RP-HPLC.

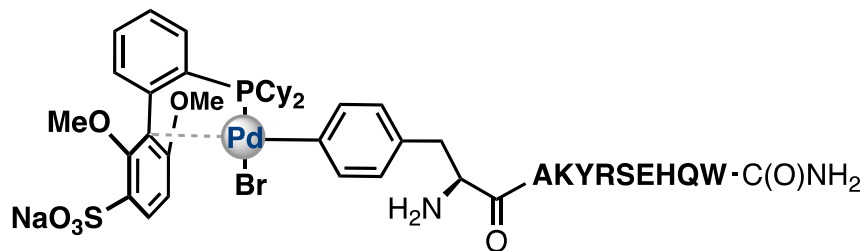
*The synthesis of the OA complex containing the ArCl (**1C**) requires 5 equiv of (1,5-COD)Pd(CH₂SiMe₃)₂ to reach full conversion in 1 h.



1A

Following the general procedure, a mixture containing peptide **P4** (10 mg, 0.0068 mmol), sSPhos (8.7 mg, 0.017 mmol), and (1,5-COD)Pd(CH₂TMS)₂ (6.5 mg, 0.017 mmol) was stirred at rt in DMSO (1.5 mL) for 1 h. General work-up afforded **1A** as a white solid (7.60 mg, 54%).

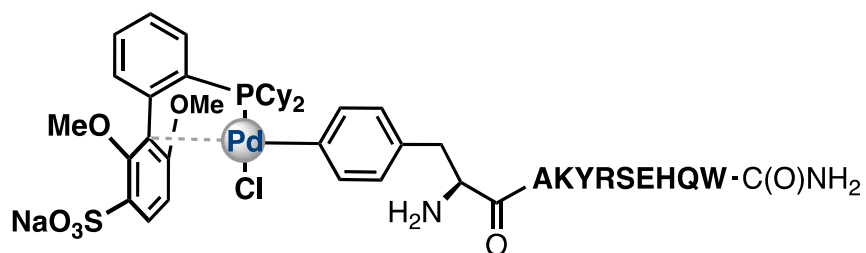
HRMS (ESI on Agilent 6520): calc. C₈₉H₁₂₂N₁₉O₂₀PPdS²⁺ [M-NaI+2H]²⁺: 972.88, found 972.89.



1B

Following the general procedure, a mixture containing peptide **P5** (10 mg, 0.0070 mmol), sSPhos (8.7 mg, 0.017 mmol), and (1,5-COD)Pd(CH₂TMS)₂ (6.5 mg, 0.017 mmol) was stirred at rt in DMSO (1.5 mL) for 1 h. General work-up afforded **1B** as a white solid (5.60 mg, 39%).

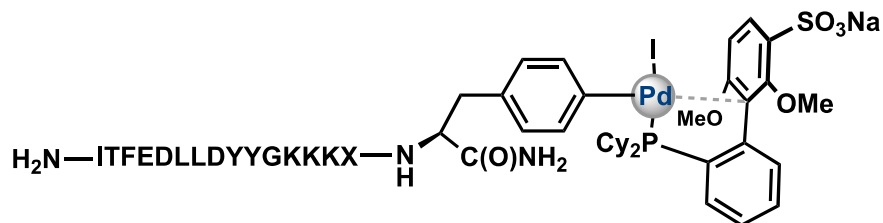
HRMS (ESI on Agilent 6520): calc. C₈₉H₁₂₂N₁₉O₂₀PPdS²⁺ [M-NaBr+2H]²⁺: 972.88, found 972.88.



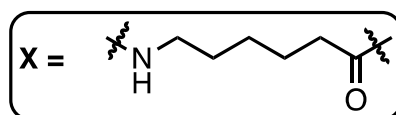
1C

Following the general procedure, a mixture containing peptide **P6** (10 mg, 0.0072 mmol), sSPhos (8.7 mg, 0.017 mmol), and (1,5-COD)Pd(CH₂TMS)₂ (13 mg, 0.034 mmol) was stirred at rt in DMSO (1.5 mL) for 1 h. General work-up afforded **1C** as a white solid (1.60 mg, 11%).

HRMS (ESI on Agilent 6520): calc. C₈₉H₁₂₂N₁₉O₂₀PPdS²⁺ [M-NaCl+2H]²⁺: 972.88, found 972.88.

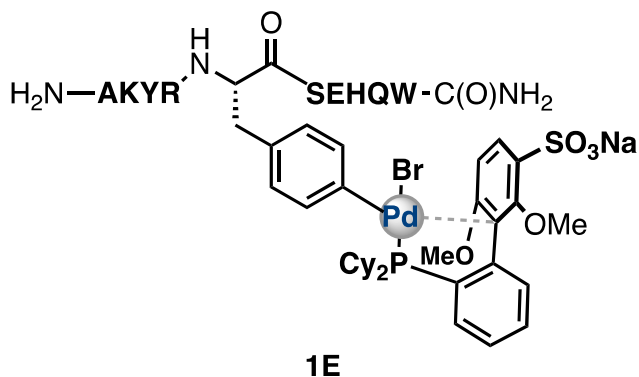


1D



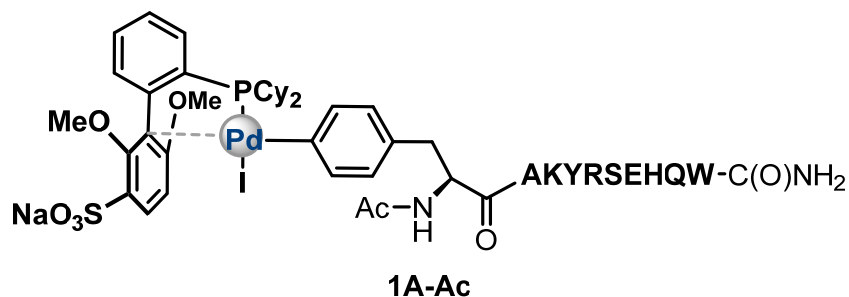
Following the general procedure, a mixture containing peptide **P7** (10 mg, 0.0047 mmol), sSPhos (4.8 mg, 0.0095 mmol), and (1,5-COD)Pd(CH₂TMS)₂ (3.7 mg, 0.0095 mmol) was stirred at rt in DMSO (1.5 mL) for 1 h. General work-up afforded **1D** as a white solid (7.72 mg, 60%).

HRMS (ESI on Agilent 6520): calc. C₁₂₃H₁₈₁N₂₀O₃₀PPdS²⁺ [M-NaI+2H]²⁺: 1293.59, found 1293.59.



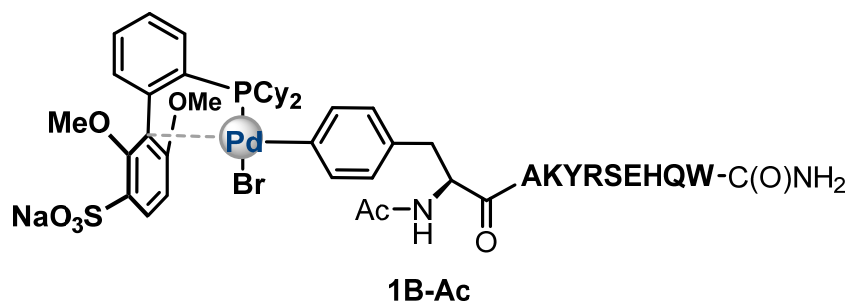
Following the general procedure, a mixture containing peptide **P8** (10 mg, 0.0070 mmol), sSPhos (8.7 mg, 0.017 mmol), and (1,5-COD)Pd(CH₂TMS)₂ (6.5 mg, 0.017 mmol) was stirred at rt in DMSO (1.5 mL) for 1 h. General work-up afforded **1E** as a white solid (3.80 mg, 27%).

HRMS (ESI on Agilent 6520): calc. C₈₉H₁₂₂N₁₉O₂₀PPdS²⁺ [M-NaBr+2H]²⁺: 972.88, found 972.89.



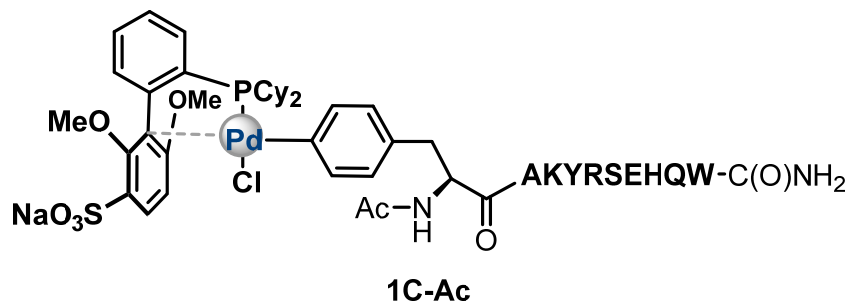
1A-Ac Following a modified general procedure, a mixture containing peptide **P9** (15 mg, 0.0099 mmol), sSPhos (5.6 mg, 0.011 mmol), and (1,5-COD)Pd(CH₂TMS)₂ (4.3 mg, 0.011 mmol) was stirred at rt in DMSO (1.5 mL) for 6 h. General work-up afforded **1A-Ac** as a white solid (3.0 mg, 14%).

LCMS (ESI on Agilent 6550): calc. C₉₁H₁₂₄N₁₉O₂₁PPdS²⁺ [M-NaI+2H]²⁺: 993.89, found 993.89



1B-Ac Following a modified general procedure, a mixture containing peptide **P10** (5 mg, 0.003 mmol), sSPhos (1.1 equiv, 0.0033 mmol), and (1,5-COD)Pd(CH₂TMS)₂ (1.1 equiv, 0.0033 mmol) was stirred at rt in DMSO (1.5 mL) for 2 h. General work-up afforded **1B-Ac** as a white solid (0.42 mg, 6%).

LCMS (ESI on Agilent 6550): calc. C₉₁H₁₂₄N₁₉O₂₁PPdS²⁺ [M-NaBr+2H]²⁺: 993.89, found 993.89



1C-Ac Following a modified general procedure, a mixture containing peptide **P11** (5 mg, 0.004 mmol), sSPhos (1.1 equiv, 0.0033 mmol), and (1,5-COD)Pd(CH₂TMS)₂ (1.1 equiv 0.0033 mmol) was stirred at rt in DMSO (1.5 mL) for 2 h. General work-up afforded **1C-Ac** as a white solid (0.47 mg, 7%).

LCMS (ESI on Agilent 6550): calc. C₉₁H₁₂₄N₁₉O₂₁PPdS²⁺ [M-NaCl+2H]²⁺: 993.89, found 993.89

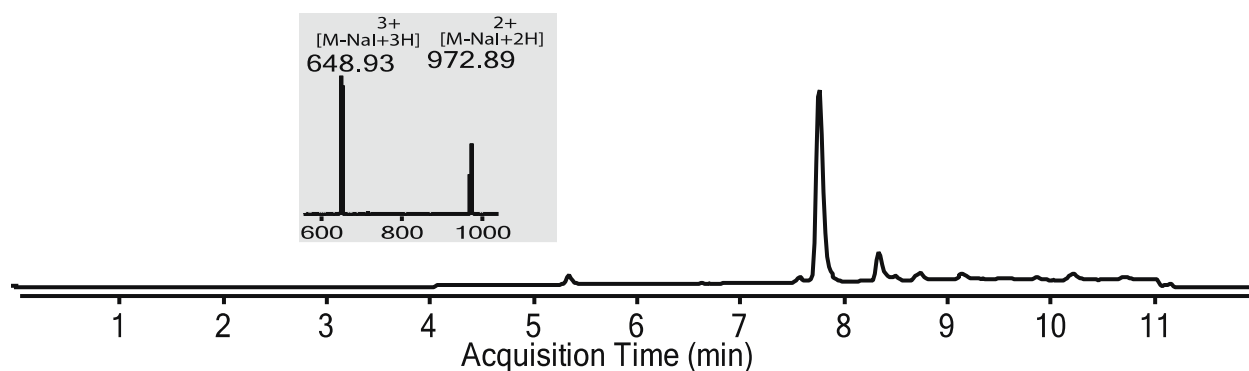
Palladium-Peptide Oxidative Addition Complex Purification

Although the purified palladium-peptide oxidative addition complexes are readily soluble in aqueous solutions, we found that the crude palladium-peptide oxidative complexes exhibited limited solubility, likely due to the excess ligand. Therefore, after lyophilization, the palladium-peptide oxidative addition complexes were dissolved in 2 mL of a 50:50 (v/v) mix of water and acetonitrile containing 0.1% TFA. The solution was diluted with 1 mL of water containing 0.1% TFA, filtered through a 0.22 μm nylon filter, and purified by mass-directed semi-preparative

reversed-phase HPLC (RP-HPLC). Solvent A was water with 0.1% TFA additive and Solvent B was acetonitrile with 0.1% TFA additive. A linear gradient from 15-50% B changing at a rate of 0.5% B/min was used. The peptides were purified on an Agilent Zorbax SB C3 column: 9.4 x 250 mm, 5 μ m.

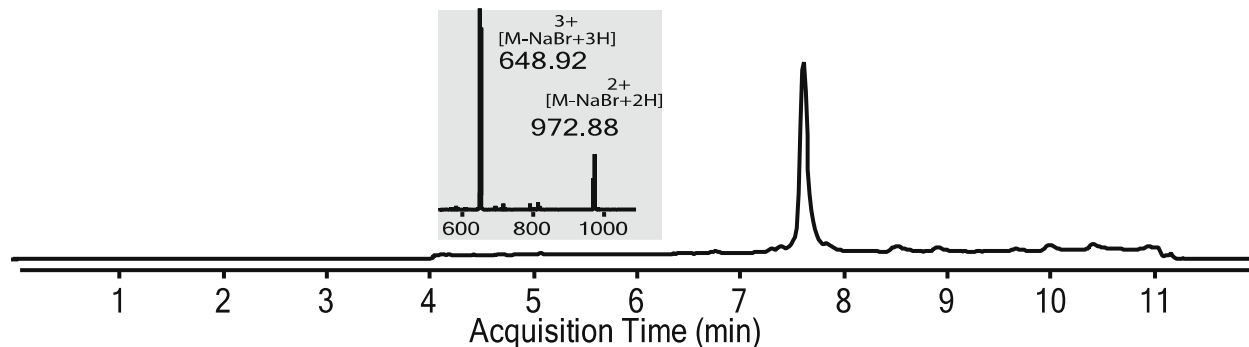
Using mass data from the instrument about each fraction, pure fractions were pooled and lyophilized. Despite different retention times, peptide OA complexes and ligand often co-elute, which can reduce overall yield (particularly for 1C). The purity of the fraction pool was confirmed by LC-MS. Total-ion current chromatograms for each complex is shown below. With electrospray ionization, we observe ions corresponding to each palladium-peptide oxidative addition complex without sodium and halide. An additional characterization of OA complex 1B using MALDI-TOF-MS is also presented, and we also observe the loss of sodium and halide.

1A:

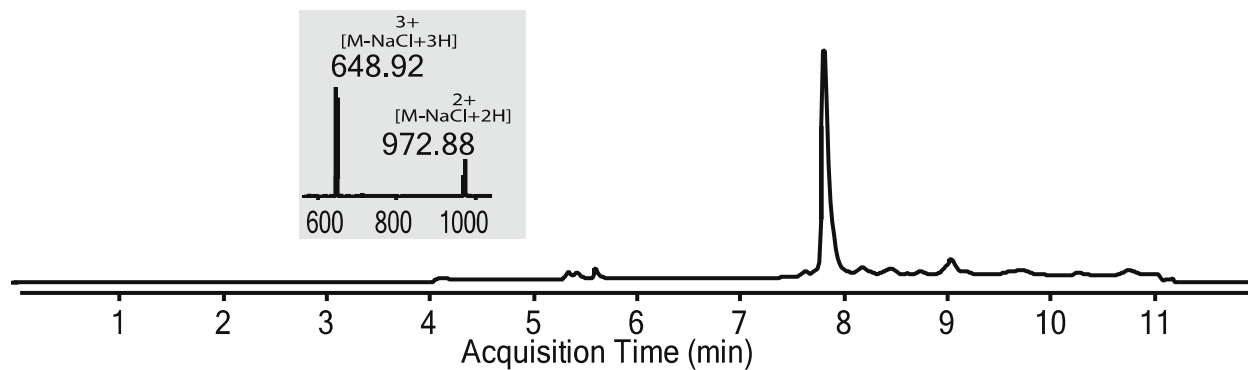


The LC-MS chromatogram of OA complex 1A has a peak at 8.4 min that corresponds to free ligand. HPLC purification fails to fully resolve the complex from the ligand, and techniques to improve the purification have been unsuccessful but the subsequent reactivity of the complex is identical to that of the other Pd-peptide complexes.

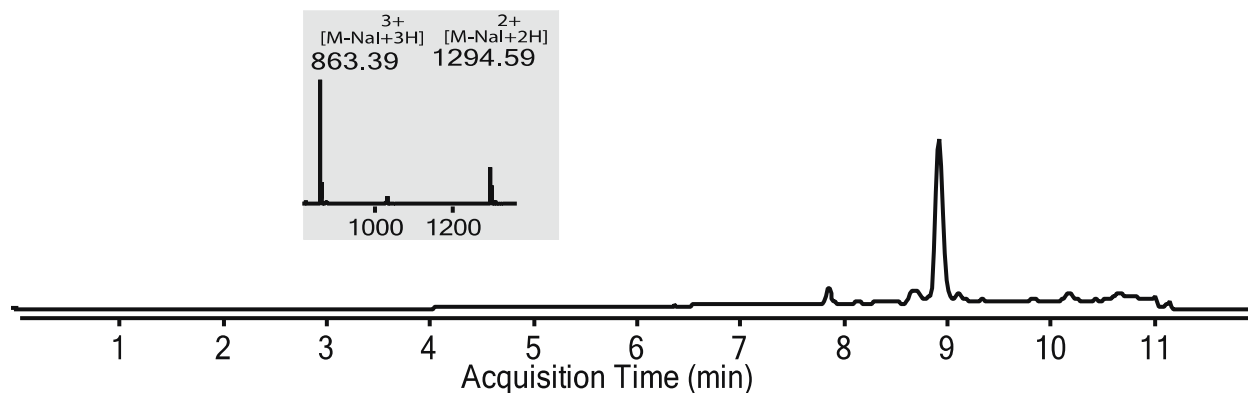
1B:



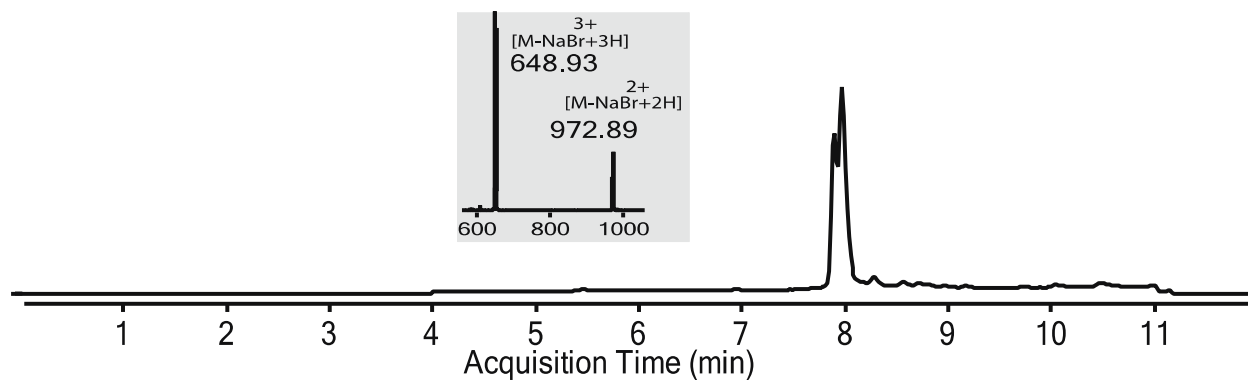
1C:



1D:

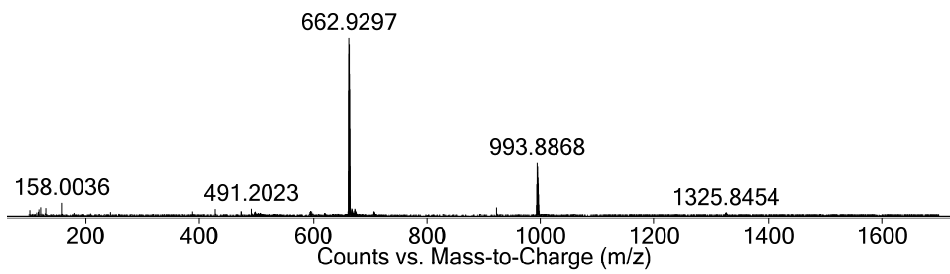
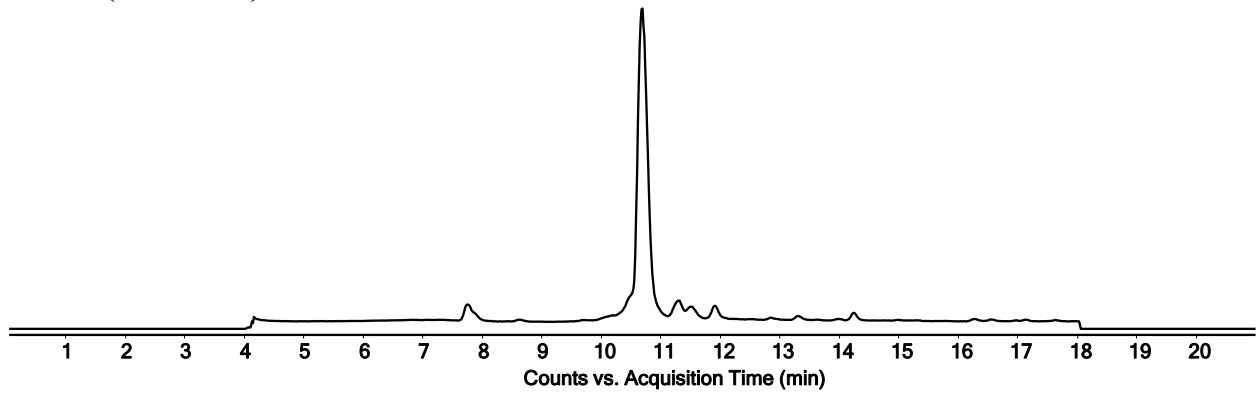


1E:

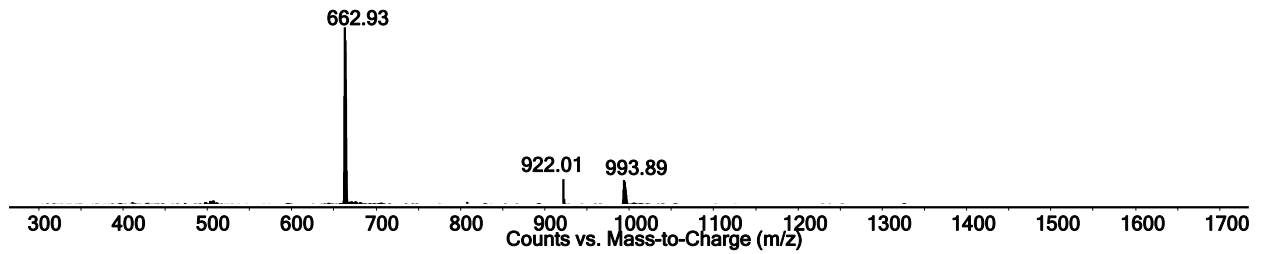
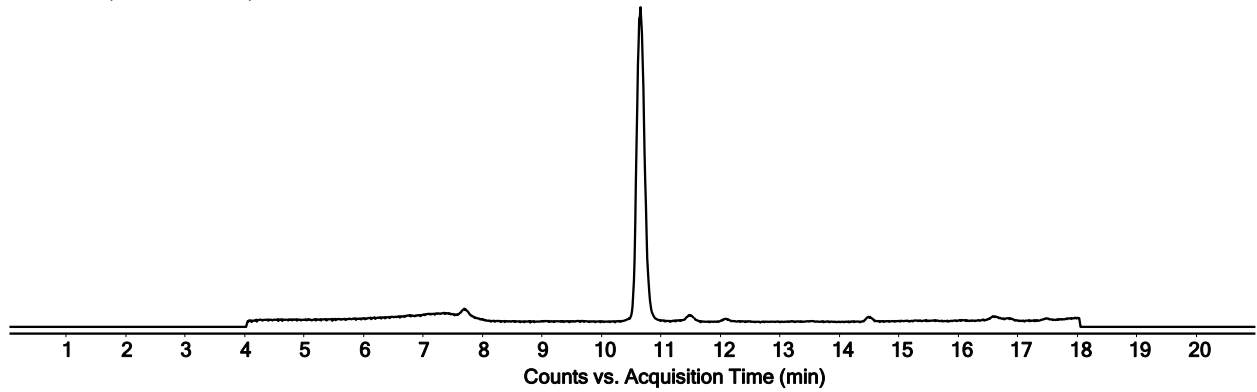


For the LC-MS chromatogram of OA complex **1E**, there are two peaks observed at 8 min. These peaks both have the same mass, and we hypothesize they arise due to two distinct conformations of the ligand when the bromophenylalanine is in the middle of the peptide (i.e. rotamers).

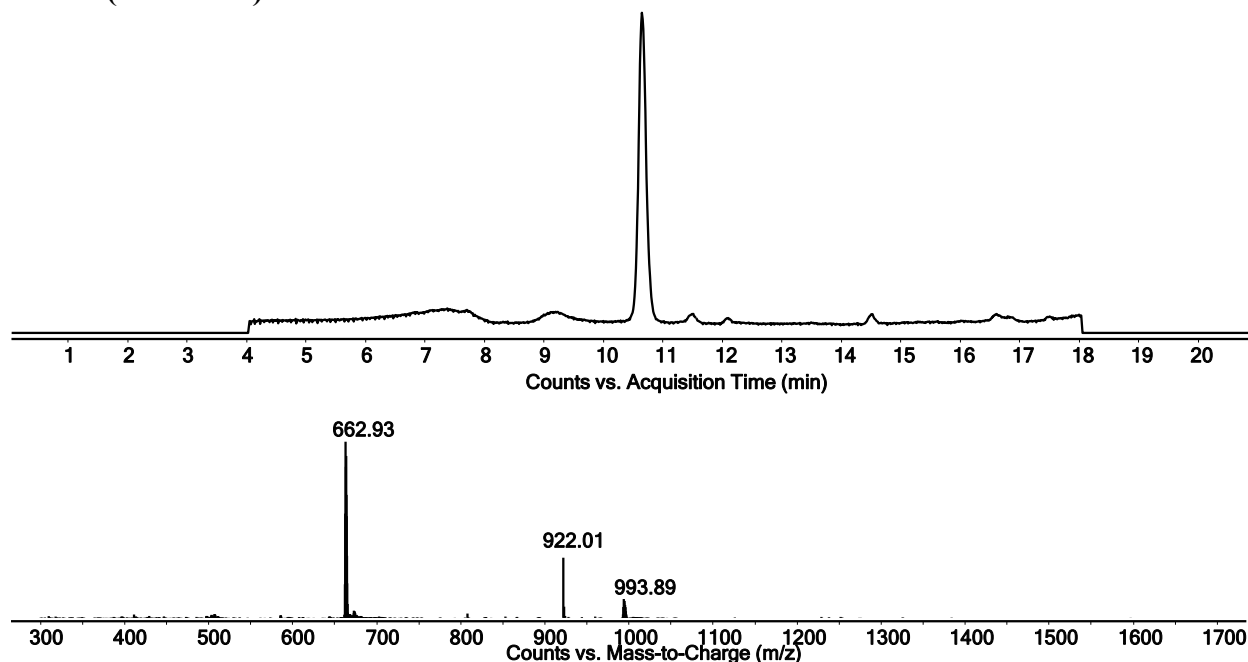
1A-Ac (Method B)



1B-Ac (Method B)

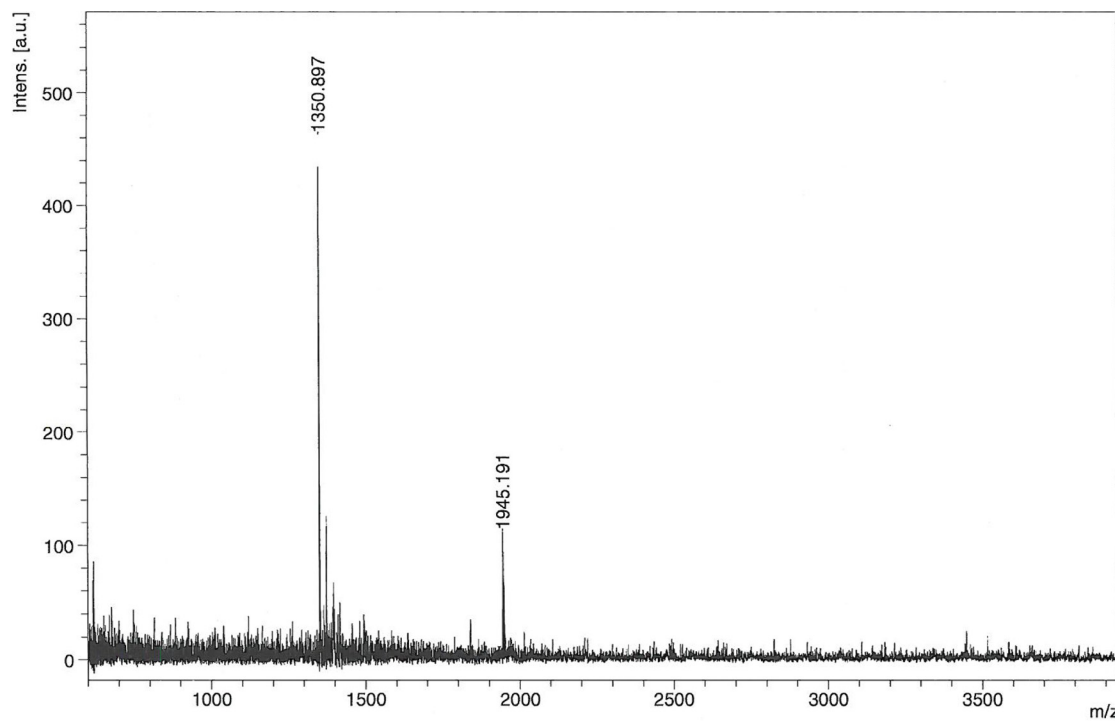


1C-Ac (Method B)

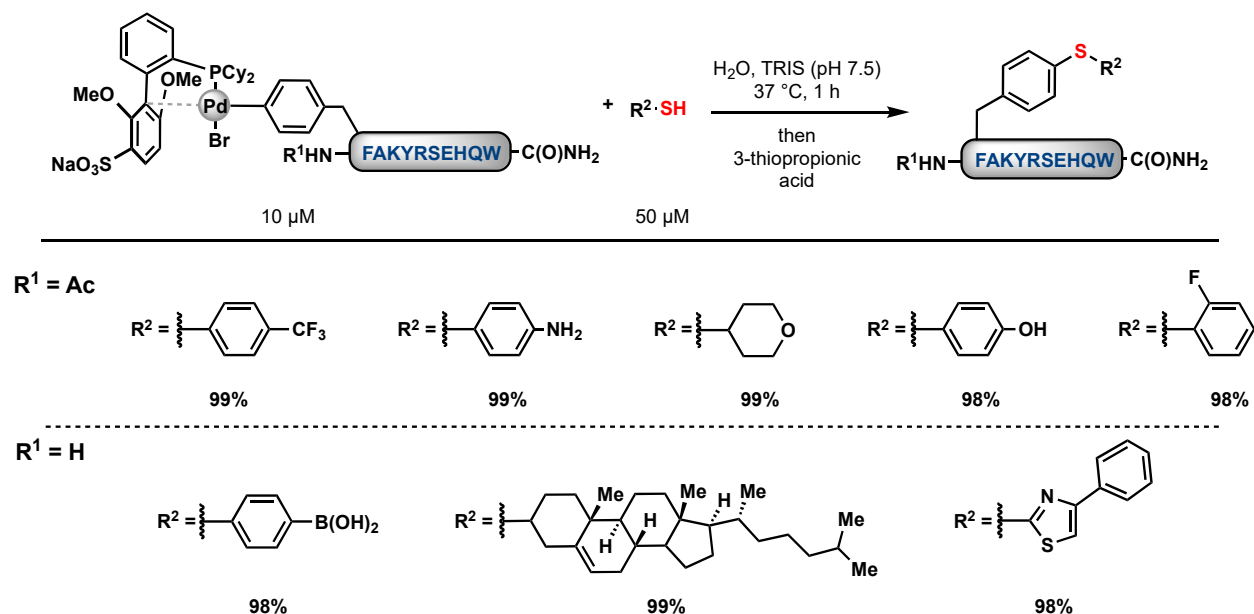


MALDI-TOF-MS Analysis

For purified OA complex **1B**, the compound was also analyzed using MALDI-TOF-MS. Shown below is the spectrum obtained after preparing the sample in α -cyano-4-hydroxycinnamic acid matrix. The spectrum was acquired in positive reflector mode, with PIE delay set to 240 ns, laser repetition rate set to 60 Hz, reflector detector voltage set to 1.854 kV, ion source voltage 1 set to 19 kV, ion source voltage 2 set to 15.9 kV, ion source lens voltage set to 9.1 kV, and the number of shots set to 400. Mass calculated $C_{89}H_{121}N_{19}O_{20}PPdS^+ [M-NaBr+H]^+$: 1944.75. Mass observed: 1944.19. The additional peak at 1350.9 corresponds to $M -Na, -Br, -Pd, -ligand, +H$.

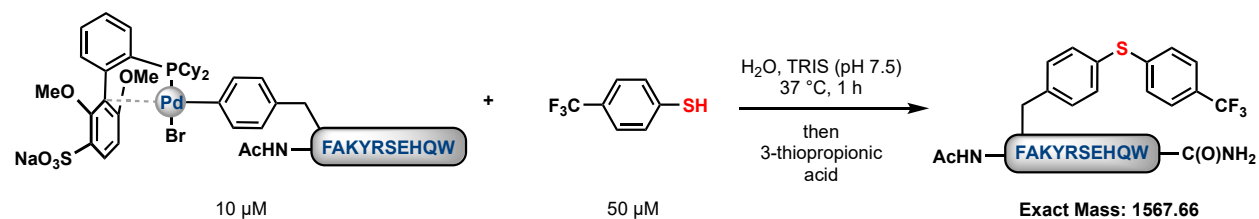


4. PALLADIUM-PEPTIDE REACTIONS WITH SMALL MOLECULE THIOLS

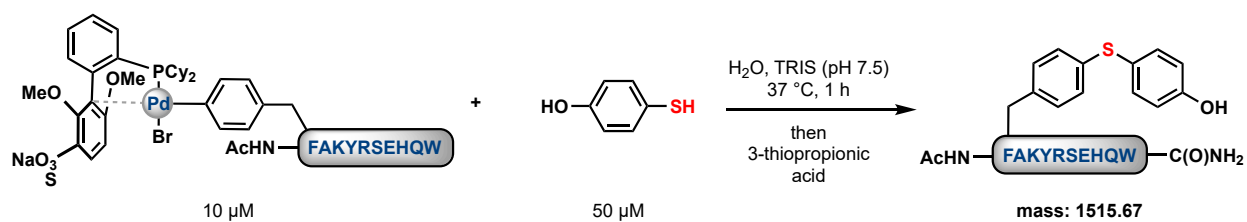
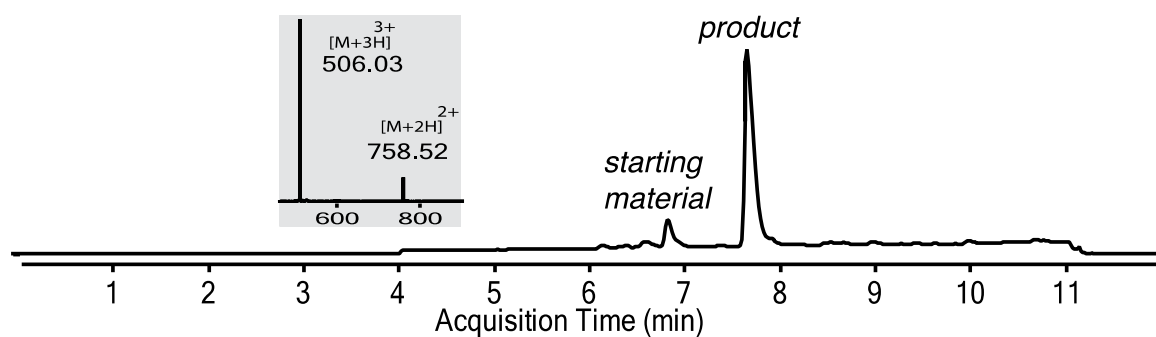


General Bioconjugation Procedure

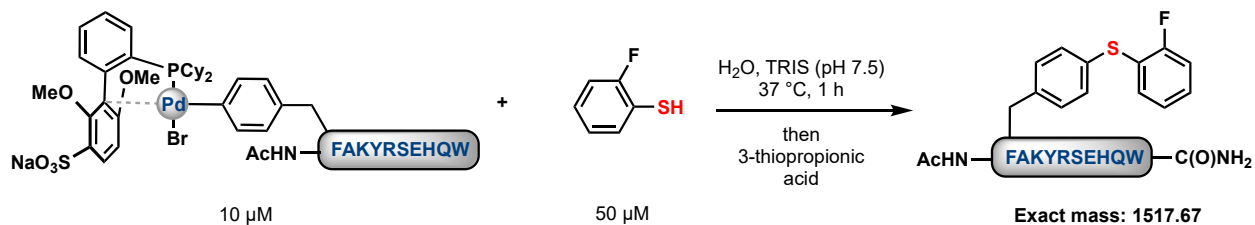
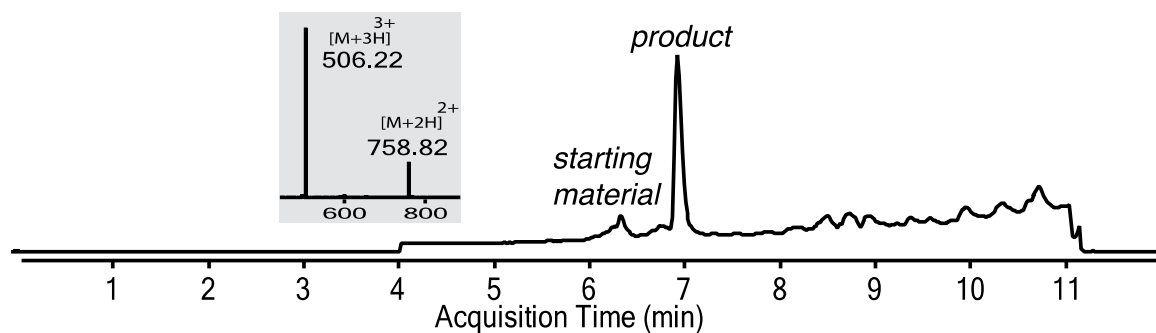
A solution of the palladium-peptide reagent **1B** (20 μM) in water was added to an equal volume of a solution containing the small molecule thiol (100 μM) in 0.1 M TRIS buffer at pH 7.5. The palladium reagents were sonicated for 10 s to ensure the reagents were fully dissolved. Final conditions: $[\text{Pd}] = 10 \mu\text{M}$; $[\text{R-SH}] = 50 \mu\text{M}$; After 1 h at 37°C , of 3-mercaptopropionic acid (3 equiv) dissolved in H_2O was added to the reaction mixture to quench the remaining palladium species. The reaction was allowed to stand for 5 min and subsequently characterized by LC-MS.



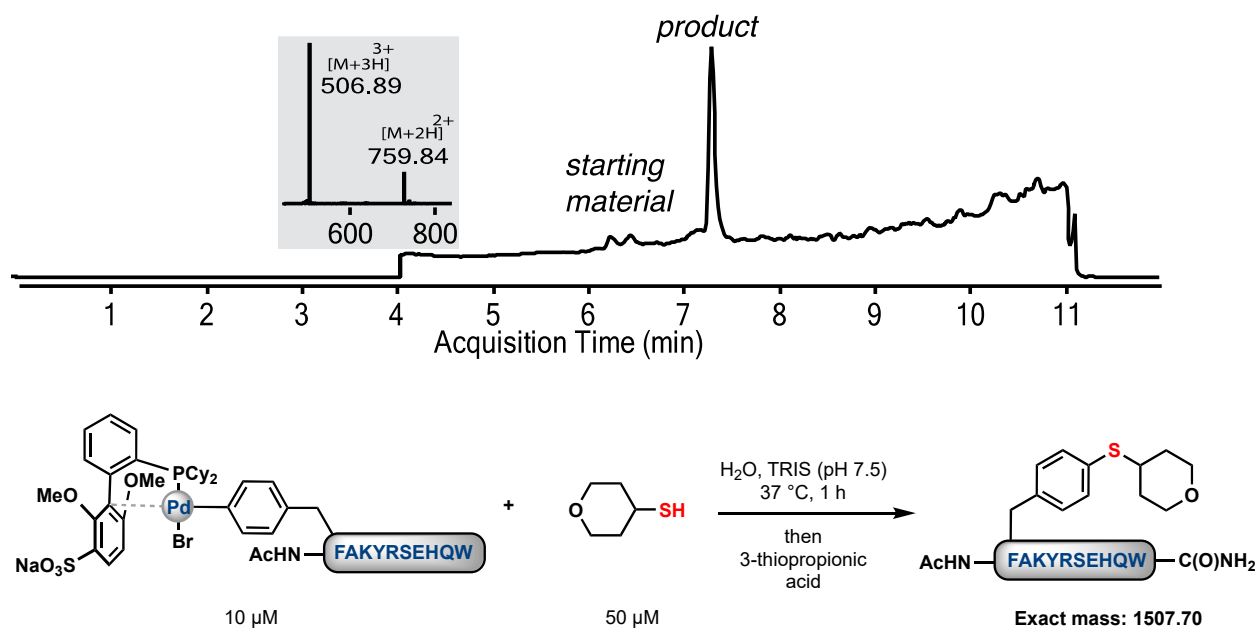
Following the general bioconjugation procedure with the N-acetylated palladium-peptide depicted (10 μM) 4-(trifluoromethyl)benzenethiol (50 μM) resulted in a 99% conversion to the desired product as determined by LC-MS analysis.



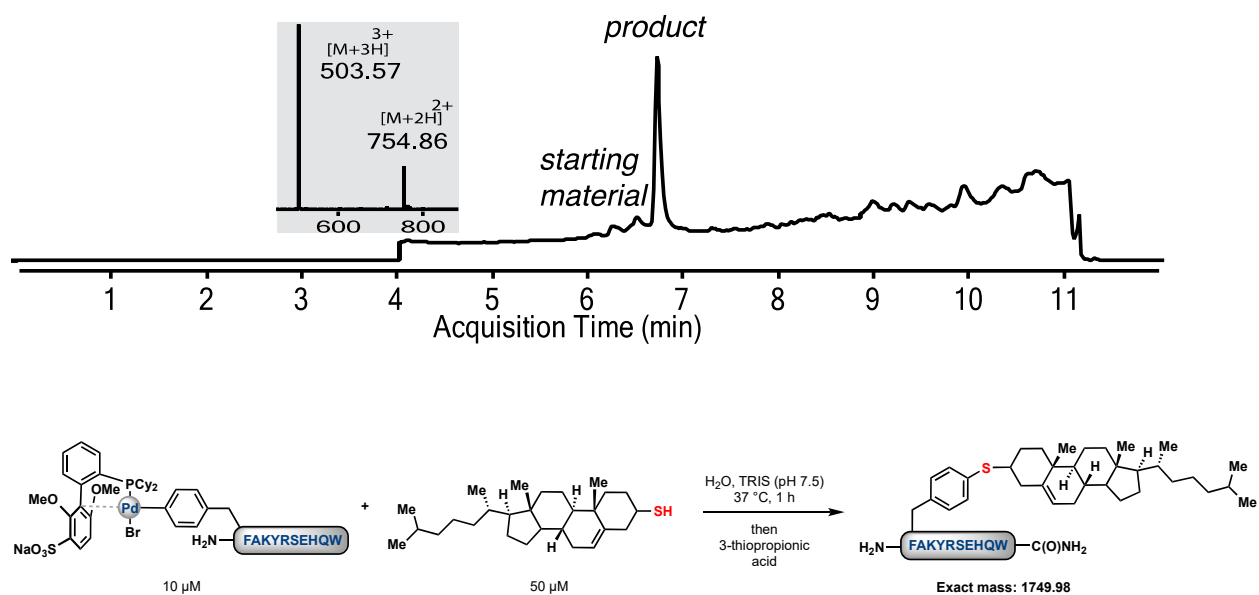
Following the general bioconjugation procedure with the depicted N-acetylated palladium-peptide (10 μM) and 4-mercaptophenol (50 μM) resulted in a 98% conversion to the desired product as determined by LC-MS analysis.



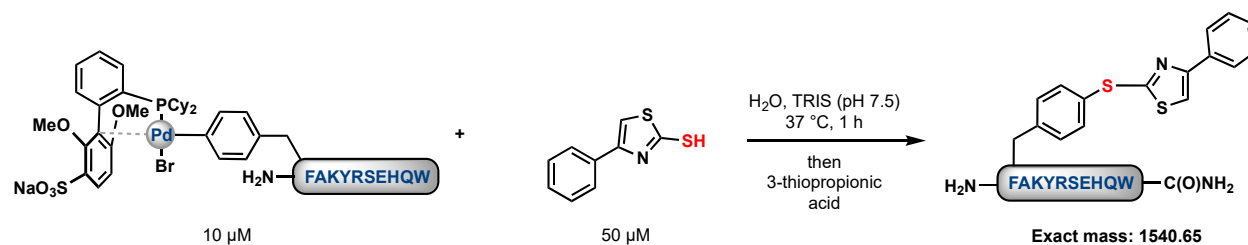
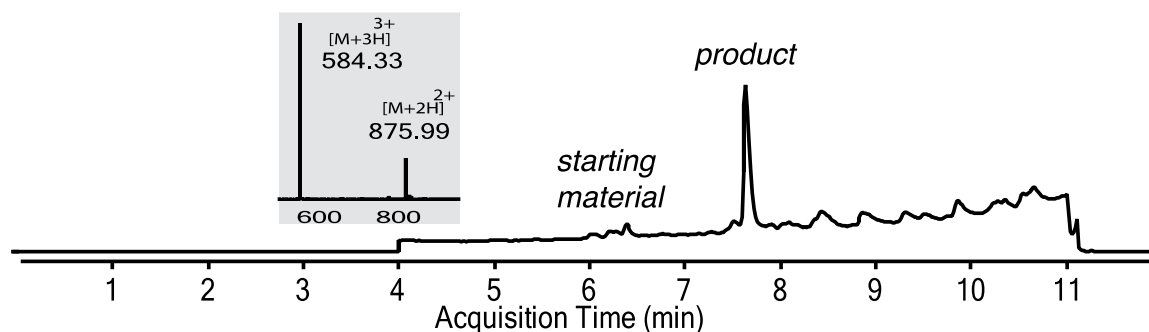
Following the general bioconjugation procedure with the depicted N-acetylated palladium-peptide (10 μ M) and 2-fluorothiophenol (50 μ M) resulted in a 98% conversion to the desired product as determined by LC-MS analysis.



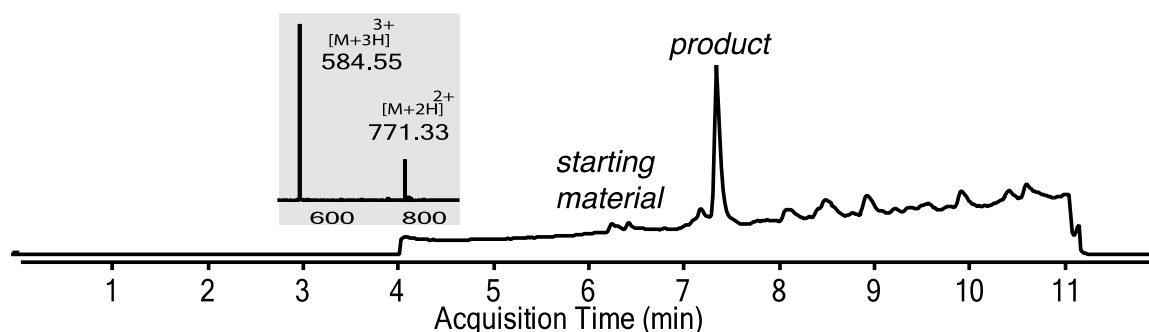
Following the general bioconjugation procedure with the depicted N-acetylated palladium-peptide (10 μ M) and 4-mercaptotetrahydropyran (50 μ M) resulted in a 99% conversion to the desired product as determined by LC-MS analysis.



Following the general bioconjugation procedure with the depicted palladium-peptide with free N-terminus (10 μ M) and thiocholesterol (50 μ M) resulted in a 99% conversion to the desired product as determined by LC-MS analysis.

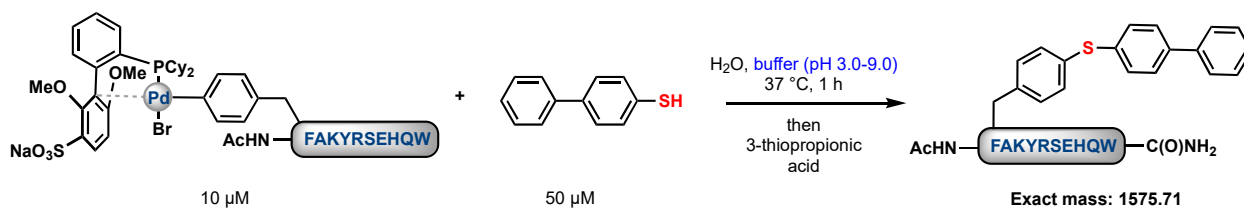


Following the general bioconjugation procedure with the depicted palladium-peptide with free N-terminus (10 μ M) and 4-phenylthiazole-2-thiol (50 μ M) resulted in a 98% conversion to the desired product as determined by LC-MS analysis.

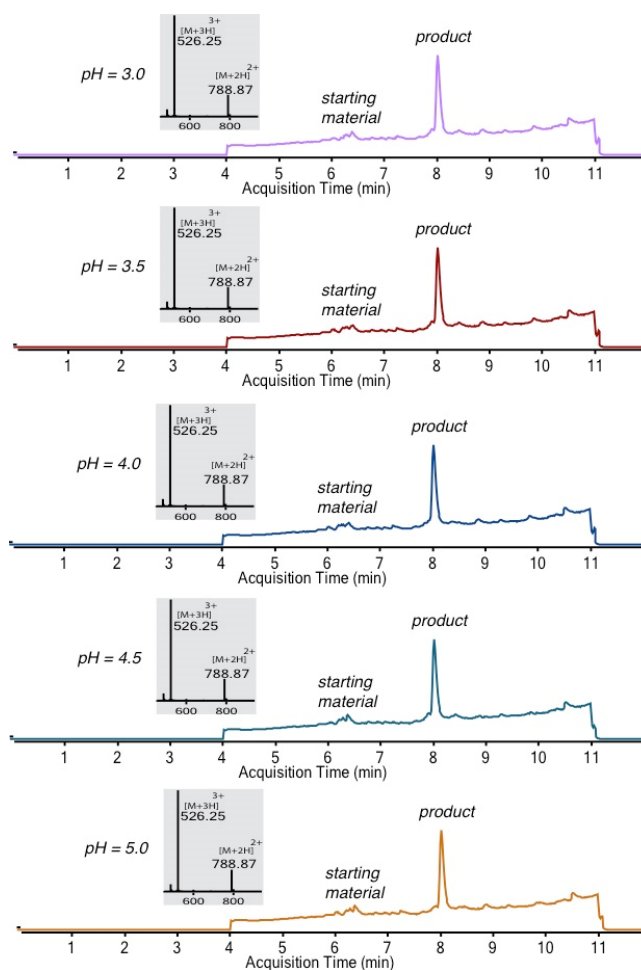


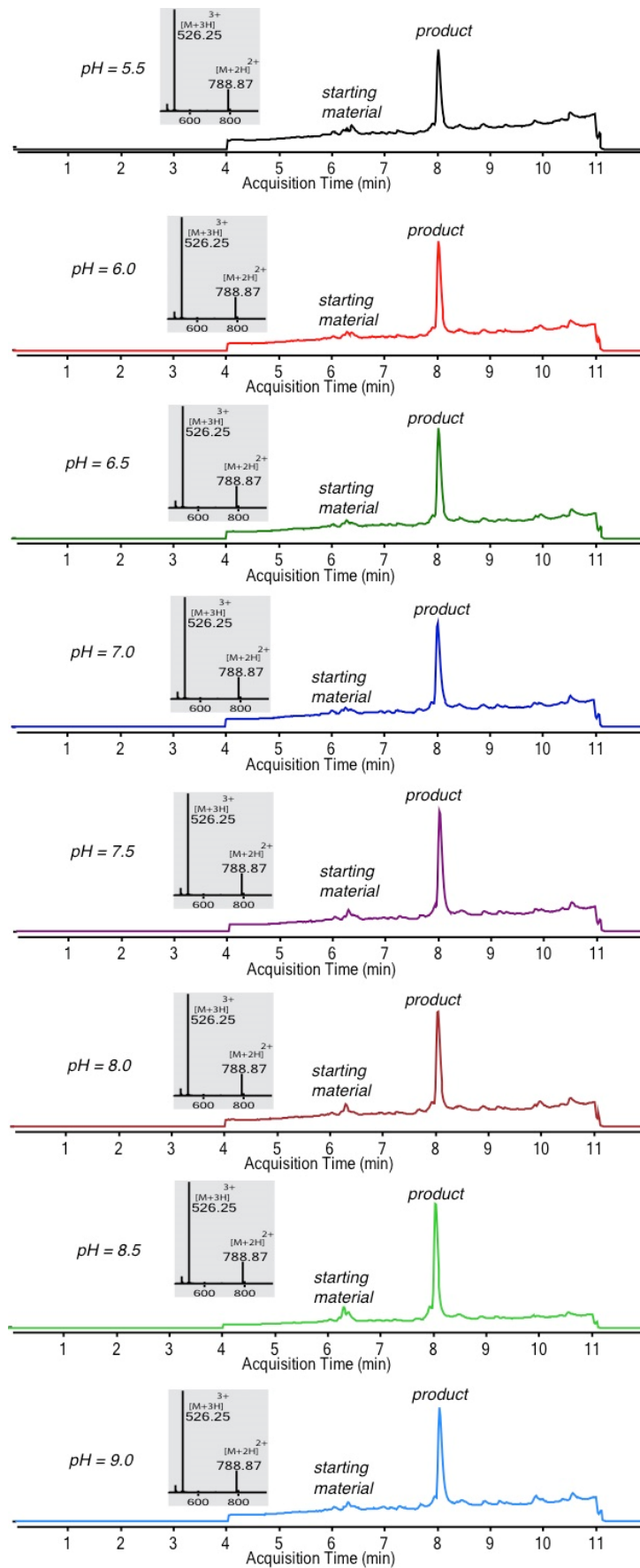
5. STUDIES OF pH DEPENDENCE OF THE BIOCONJUGATION REACTIONS

General pH Study Procedure – (Buffer Experiments)



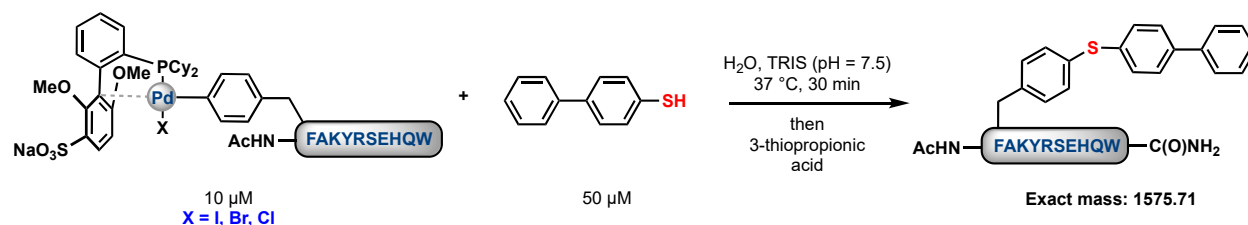
A solution of the depicted N-acetylated palladium-peptide reagent (20 μM) in water was added to a equal volume of a solution containing biphenyl-4-thiol (100 μM) in buffer (0.1 M, Citrate buffer = pH 3.0-5.0, Phosphate buffer = pH 5.5-7.0, TRIS buffer = pH 7.5-9.0). The palladium reagents were sonicated for 10 s to ensure the reagents were fully dissolved. Final conditions: $[\text{Pd}] = 10 \mu\text{M}$; $[\text{biphenyl-SH}] = 50 \mu\text{M}$; After 1 h at 37 $^{\circ}\text{C}$, 3-mercaptopropionic acid (3 equiv) dissolved in H_2O was added to the reaction mixture to quench the remaining palladium species. The reaction was allowed to stand for 5 min and subsequently characterized by LC-MS.



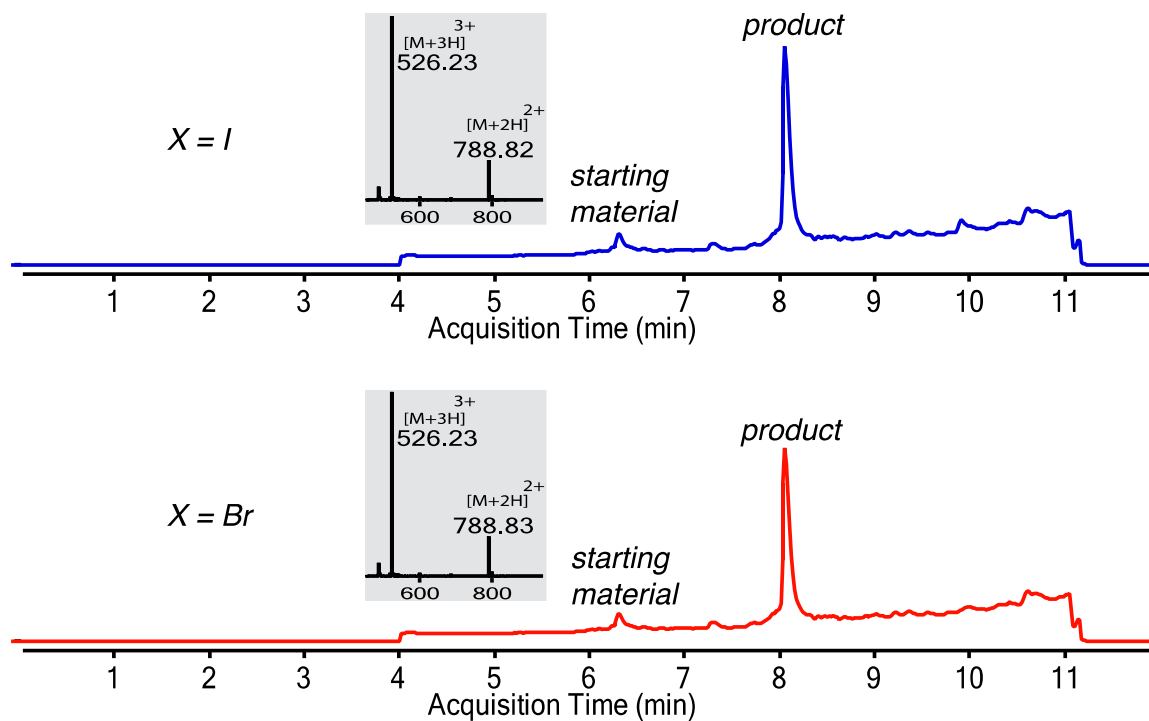


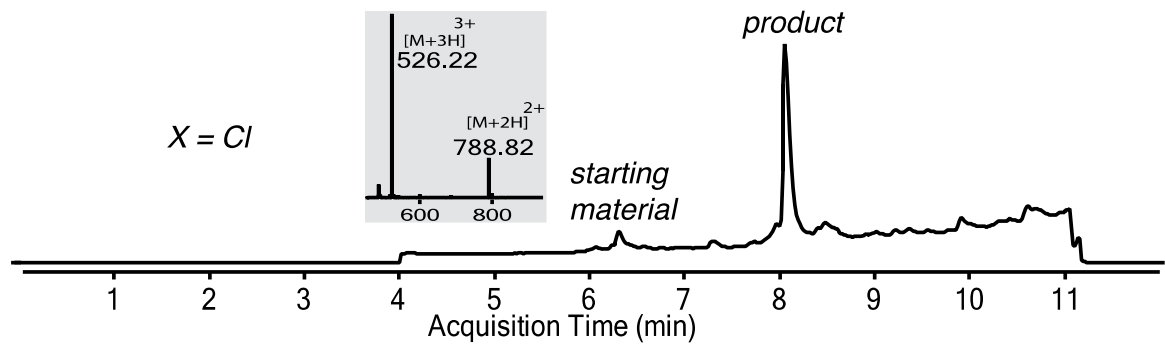
6. STUDIES OF HALIDE DEPENDENCE OF THE BIOCONJUGATION REACTIONS

General Halide Study Procedure – (Halide Effect Experiments)



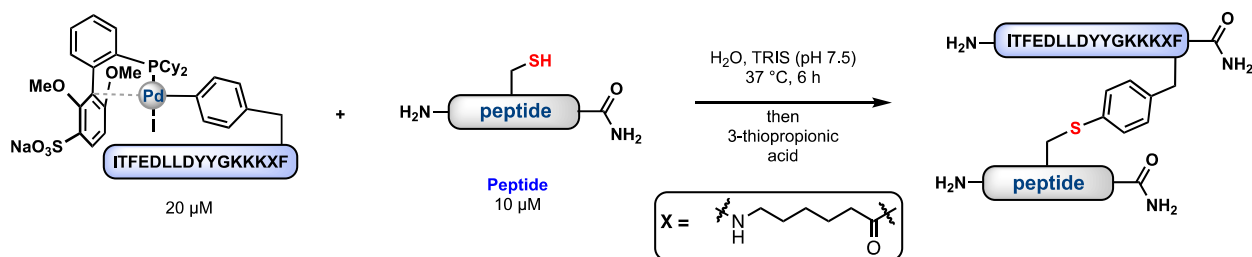
A solution of the depicted N-acetylated palladium-peptide reagent [$\text{X} = \text{I, Br, or Cl}$] (20 μM) in water was added to an equal volume of a solution containing biphenyl-4-thiol (100 μM) in in buffer (0.1 M TRIS buffer = pH 7.5). The palladium reagents were sonicated for 10 s to ensure the reagents were fully dissolved. Final conditions: $[\text{Pd}] = 10 \mu\text{M}$; $[\text{biphenyl-SH}] = 50 \mu\text{M}$; After 1 h at 37 °C, 3-mercaptopropionic acid (3 equiv) dissolved in H_2O was added to the reaction mixture to quench the remaining palladium species. The reaction was allowed to stand for 5 min and subsequently characterized by LC-MS.





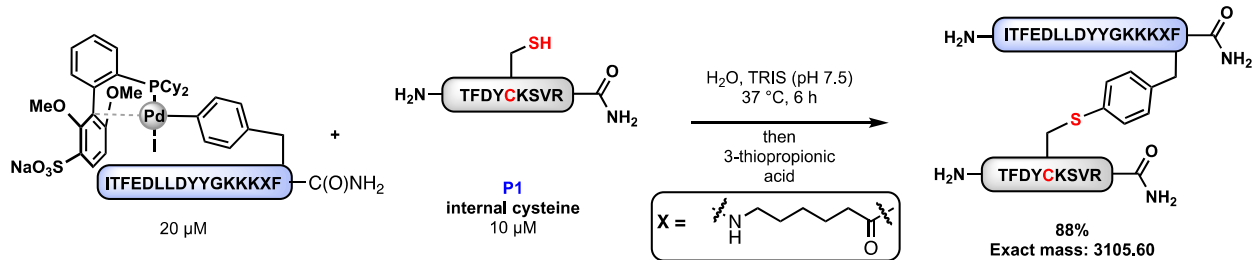
7. PEPTIDE-PEPTIDE LIGATION REACTIONS AND LC-MS CHARACTERIZATION

General Peptide-Peptide Ligation Procedure

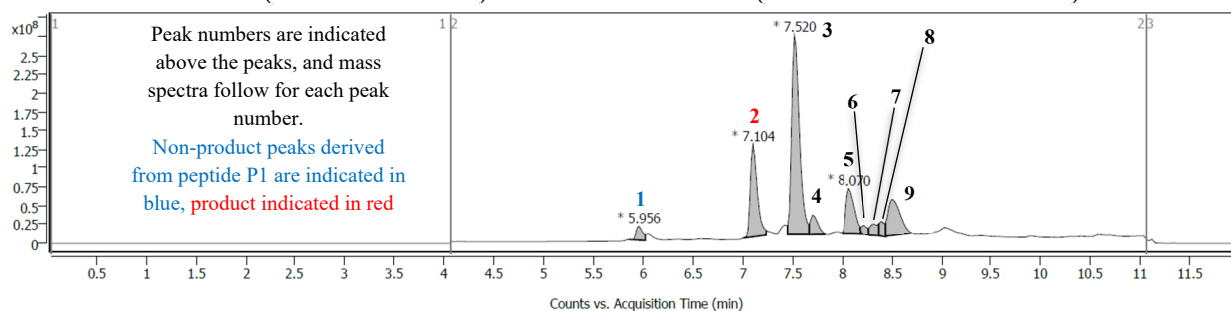


A solution of the palladium-peptide reagent (**1D**) in water (40 μM) was added to a solution of a peptide containing a single cysteine (20 μM) in TRIS buffer (0.1 M, pH 7.5). Note: if the palladium reagent was not readily soluble in H₂O, the slurry was sonicated for 10 s to facilitate this process and become fully solubilized. Final conditions: [Pd] = 20 μM; [R-SH] = 10 μM; After 6 h at 37 °C, 3-mercaptopropionic acid (3 equiv to the palladium complex solution in 6 μL of H₂O) was added to the reaction mixture to quench the remaining palladium species. The reaction was allowed to stand for 5 min and subsequently characterized by LC-MS.

Note: In the following pages, the full chromatogram is depicted alongside the extracted MS chromatogram from the associated peaks at the indicated time interval. All data was processed with Agilent MassHunter Qualitative Analysis 10.0. Conversion was assessed by integrating the peak on the chromatogram of the desired product divided by the sum total of the integration of the peaks of the starting thiol containing peptide + any observed products derived from the starting thiol containing peptide. Calculations are illustrated. All compounds were assigned based on their agreement with calculated masses generated using ChemDraw 20.0.



Conversion: Peak 2/(Peak 1 + Peak 2) * 100 = 593722764/(593722764 + 80274988) * 100 = 88%

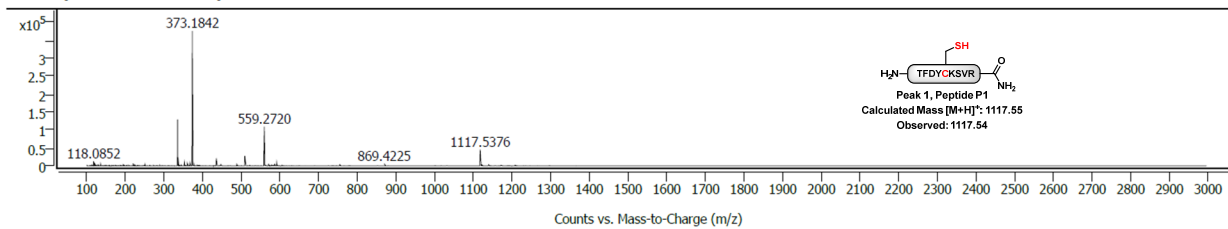


Chromatogram Peaks

Peak	Start	RT	End	Height	Area	Area %
1	5.856	5.956	6.022	18042101	80274988	5.52
2	7.004	7.104	7.237	123038222	593722764	40.85
3	7.454	7.520	7.670	265093448	1453552341	100.00
4	7.670	7.703	7.837	25276574	131500841	9.05
5	8.003	8.070	8.186	60801916	356172395	24.50
6	8.186	8.219	8.269	12604306	53484076	3.68
7	8.269	8.369	8.369	16354847	85734228	5.90
8	8.369	8.402	8.436	19764539	74298105	5.11
9	8.436	8.502	8.702	48693684	413106793	28.42

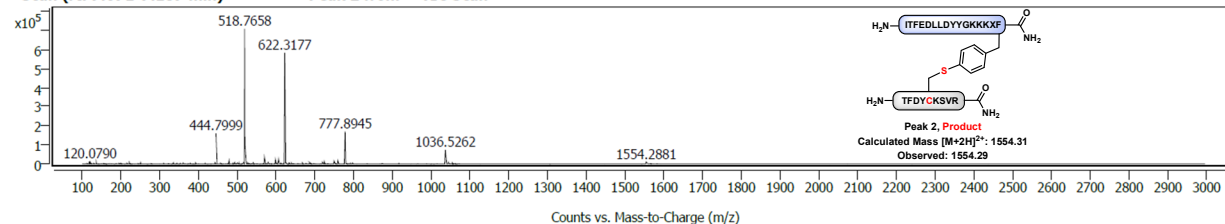
+ Scan (rt: 5.922-6.022 min)

Peak 1 from + TIC Scan



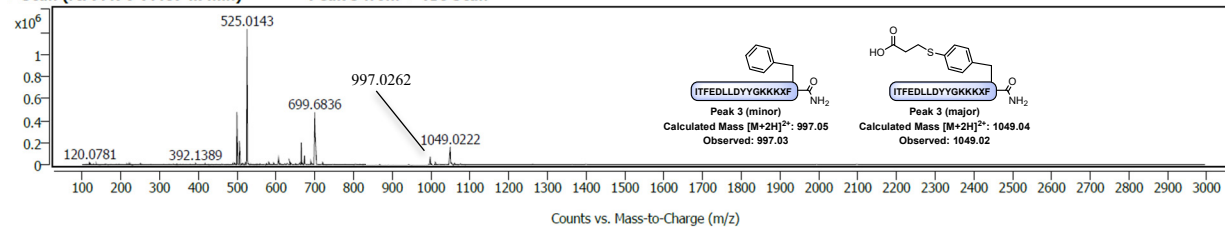
+ Scan (rt: 7.071-7.187 min)

Peak 2 from + TIC Scan



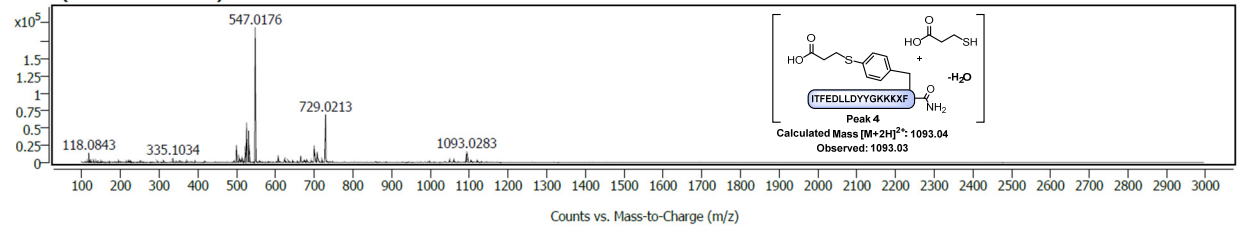
+ Scan (rt: 7.470-7.487 ... min)

Peak 3 from + TIC Scan



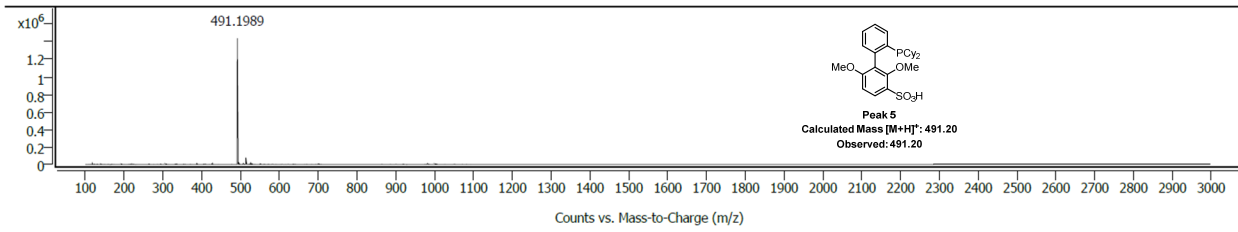
+ Scan (rt: 7.670-7.803 min)

Peak 4 from + TIC Scan



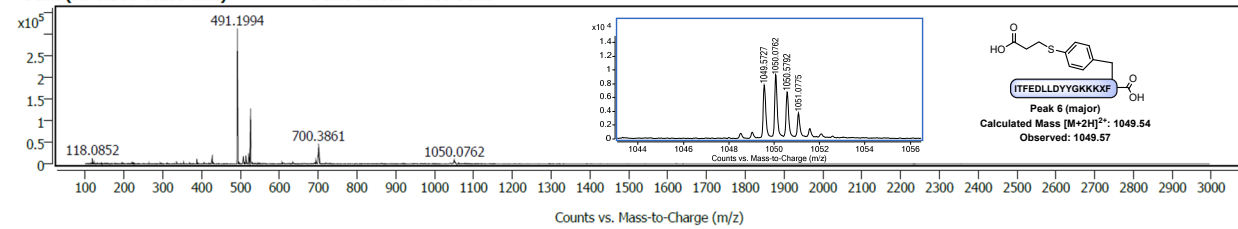
+ Scan (rt: 8.036 ... min)

Peak 5 from + TIC Scan



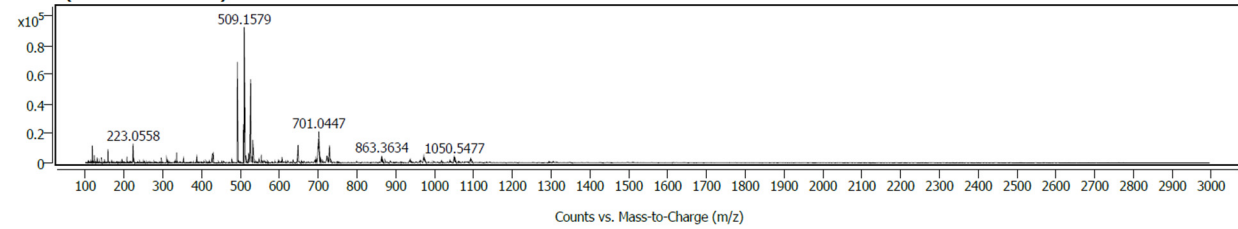
+ Scan (rt: 8.186-8.269 min)

Peak 6 from + TIC Scan



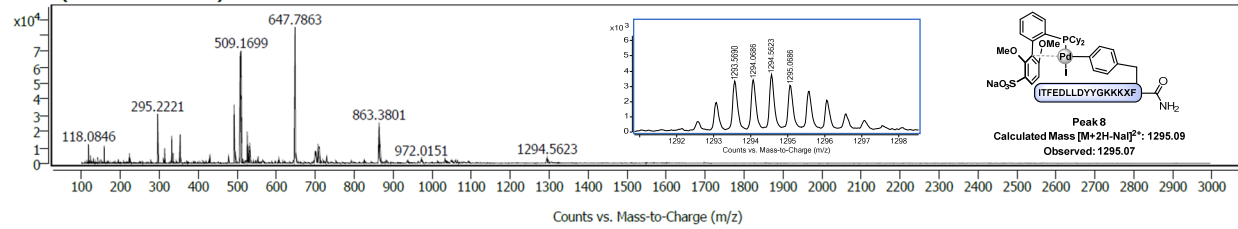
+ Scan (rt: 8.269-8.369 min)

Peak 7 from + TIC Scan



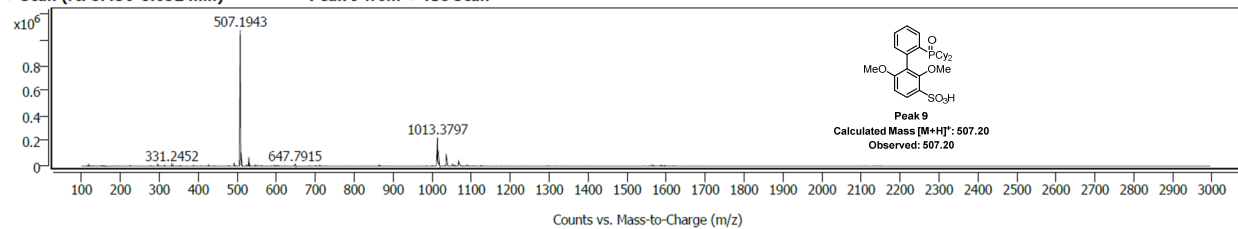
+ Scan (rt: 8.369-8.436 min)

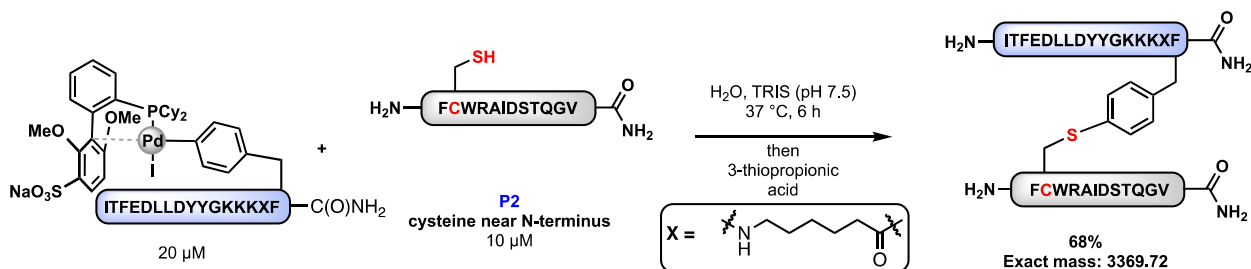
Peak 8 from + TIC Scan



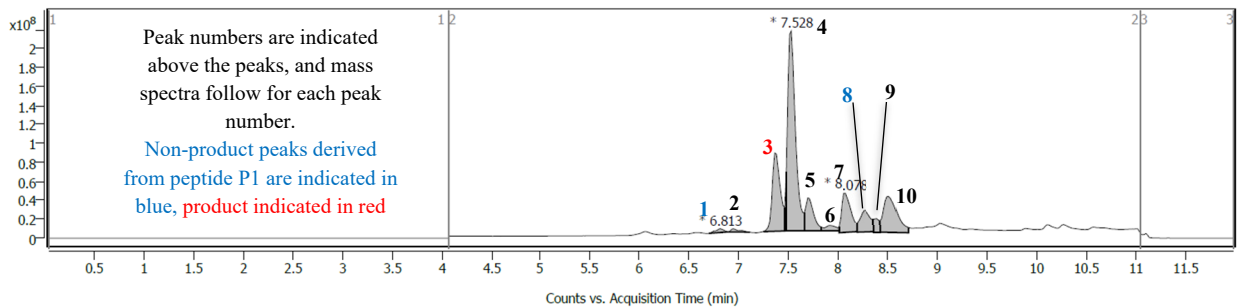
+ Scan (rt: 8.436-8.652 min)

Peak 9 from + TIC Scan



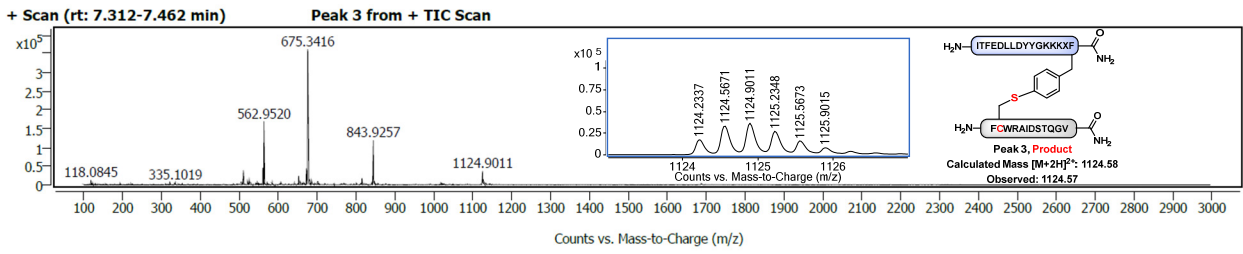
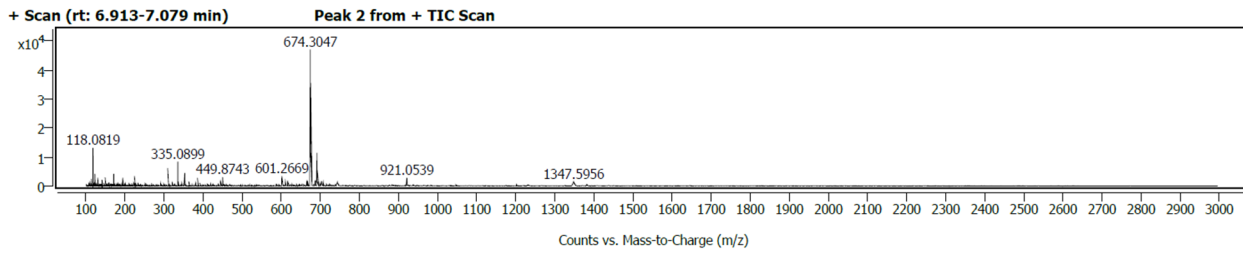
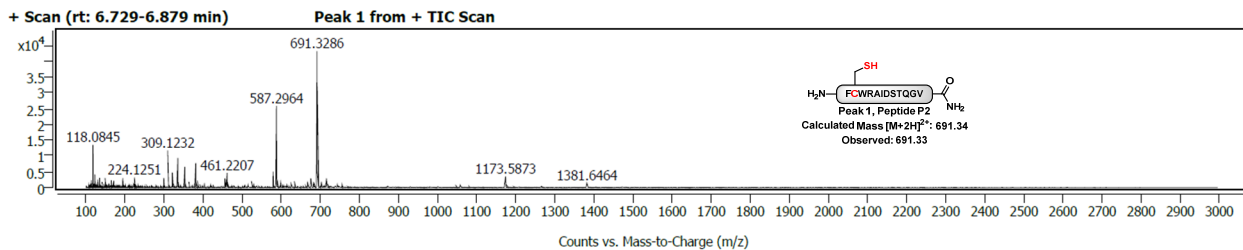


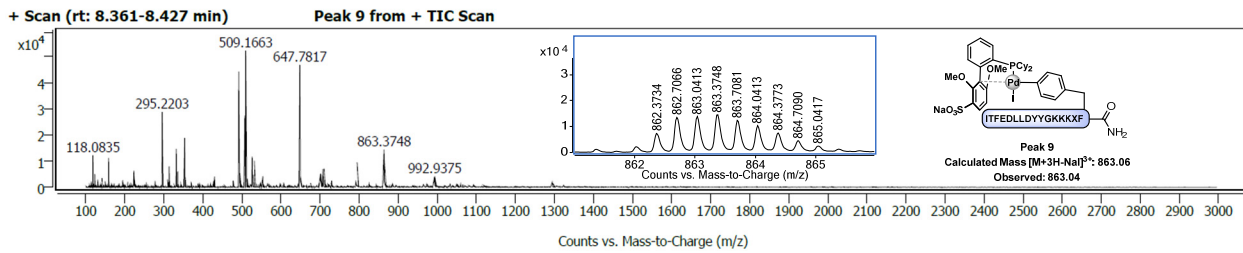
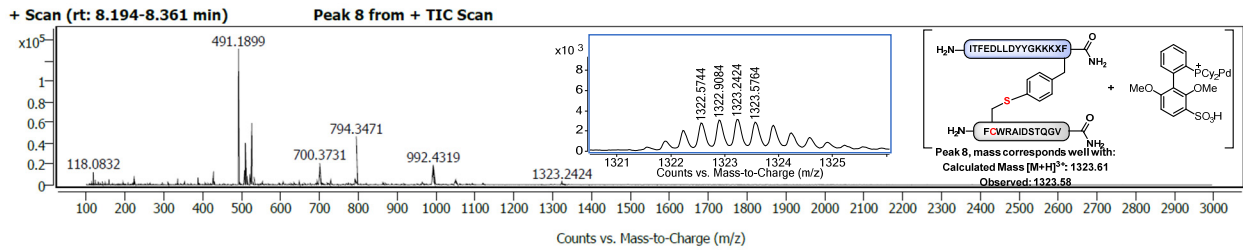
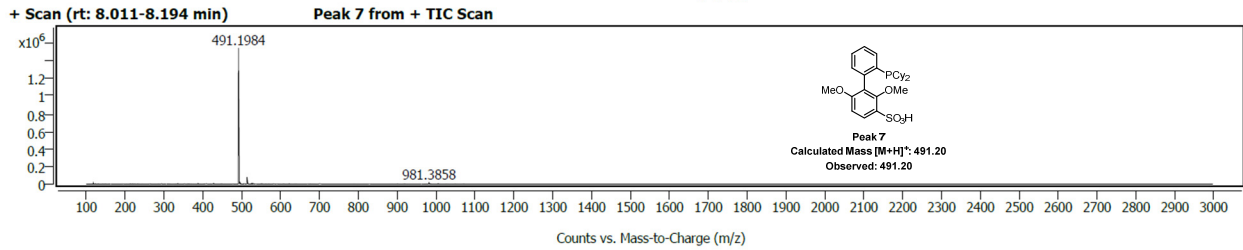
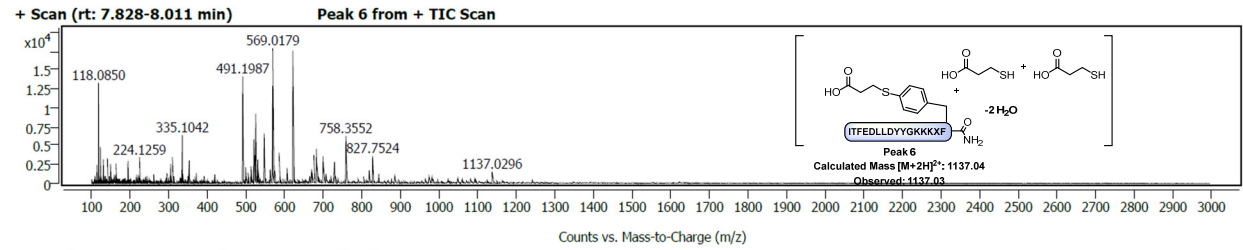
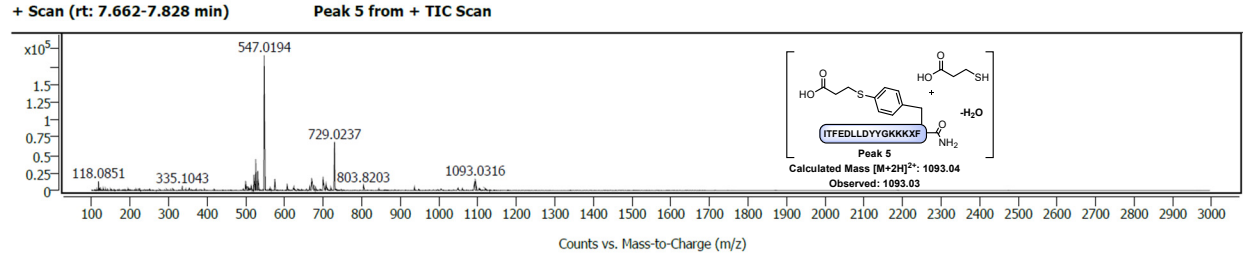
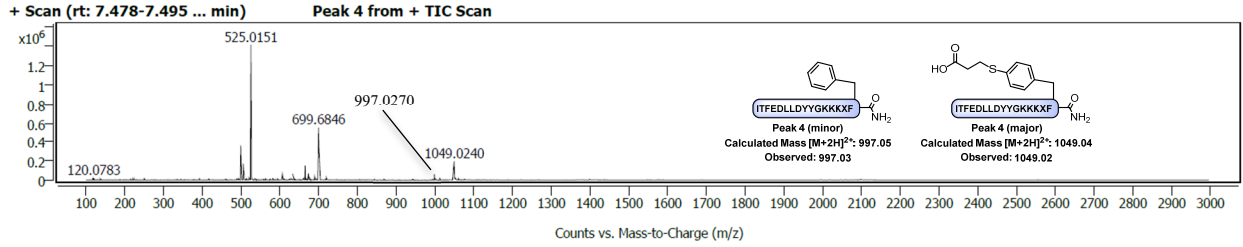
Conversion: $\text{Peak 3}/(\text{Peak 1} + \text{Peak 3} + \text{Peak 8}) * 100 = 469151812/(23098247+469151812+194446925) * 100 = 68\%$



Chromatogram Peaks

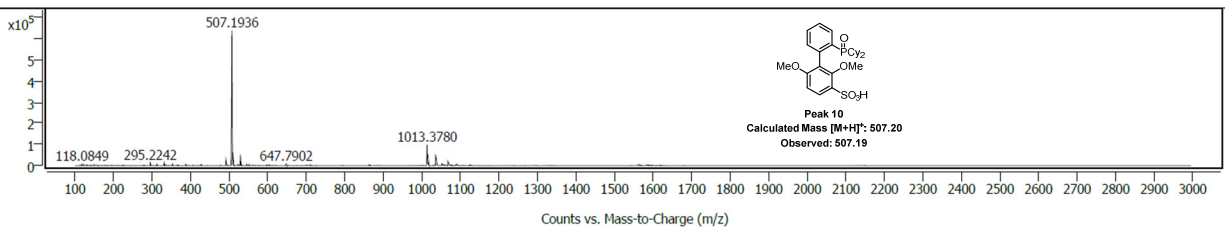
Peak	Start	RT	End	Height	Area	Area %
1	6.696	6.813	6.896	4018923	23098247	2.03
2	6.896	6.946	7.112	3340190	19472402	1.72
3	7.245	7.362	7.462	82585366	469151812	41.33
4	7.478	7.528	7.662	210904907	1135193528	100.00
5	7.662	7.695	7.828	34797263	197469572	17.40
6	7.828	7.911	8.011	5784359	49044964	4.32
7	8.011	8.078	8.194	43174554	285151408	25.12
8	8.194	8.261	8.361	24843971	194446925	17.13
9	8.361	8.394	8.427	16640596	62796028	5.53
10	8.427	8.510	8.710	39923603	383389420	33.77



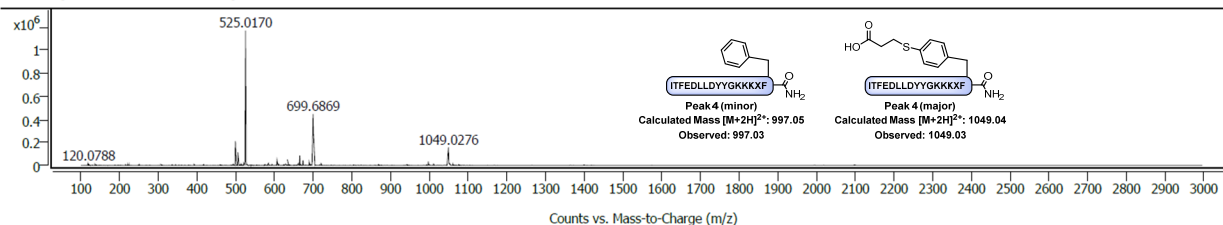


+ Scan (rt: 8.427-8.710 min)

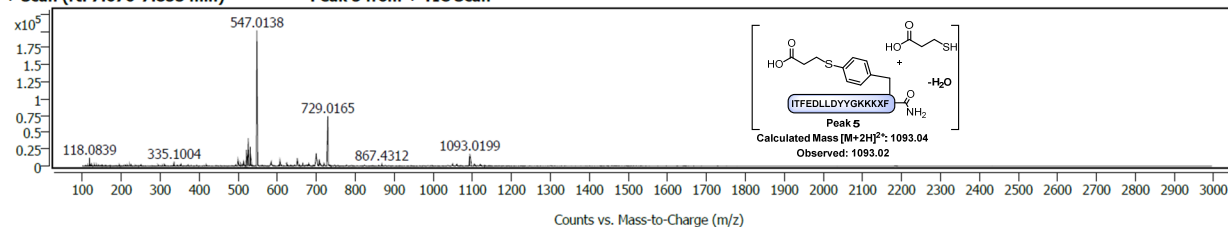
Peak 10 from + TIC Scan



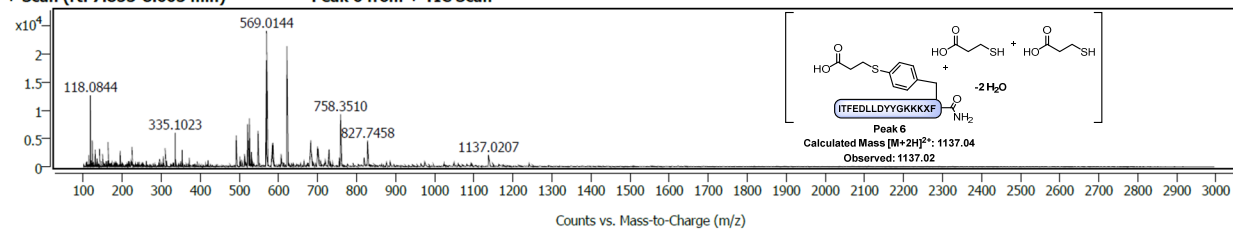
+ Scan (rt: 7.470-7.504 ... min) Peak 4 from + TIC Scan



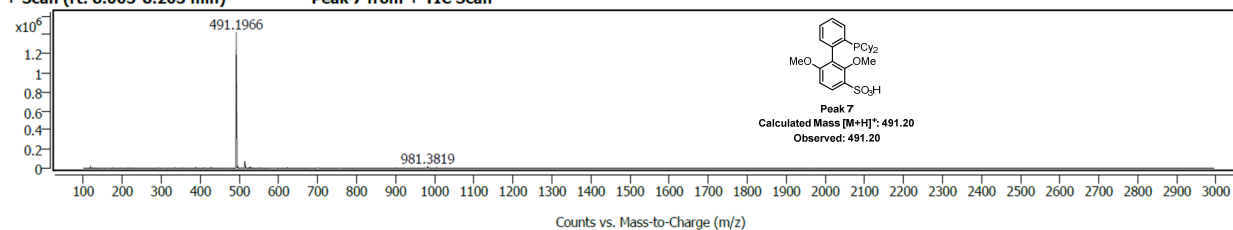
+ Scan (rt: 7.670-7.853 min) Peak 5 from + TIC Scan



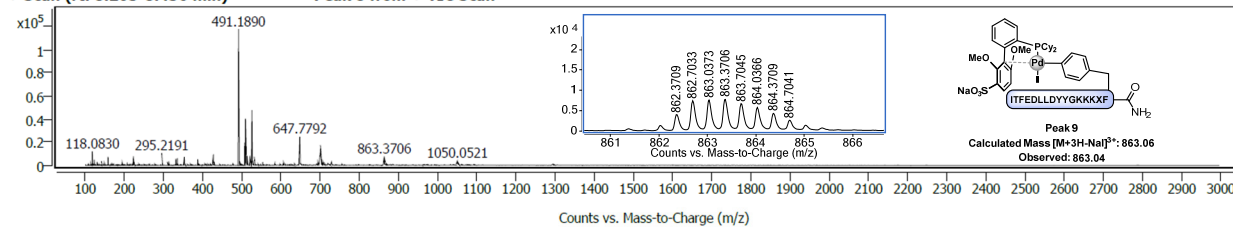
+ Scan (rt: 7.853-8.003 min) Peak 6 from + TIC Scan



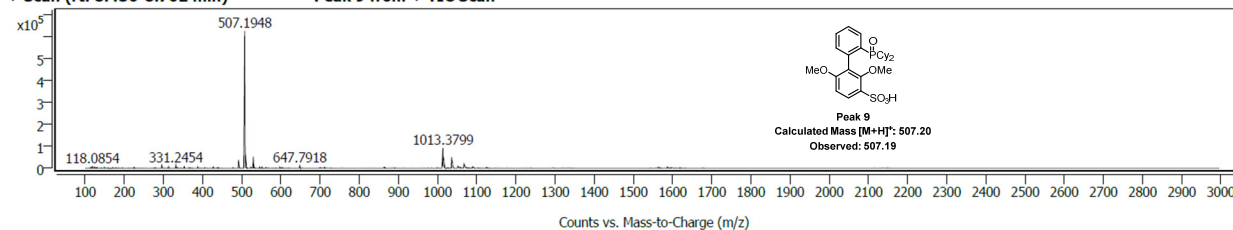
+ Scan (rt: 8.003-8.203 min) Peak 7 from + TIC Scan



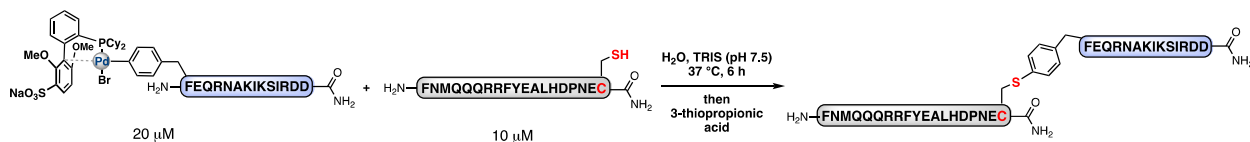
+ Scan (rt: 8.203-8.436 min) Peak 8 from + TIC Scan



+ Scan (rt: 8.436-8.702 min) Peak 9 from + TIC Scan



Large Scale Peptide-Peptide Ligation



Into a 250 mL round bottomed flask equipped with a magnetic stir bar, a solution of the palladium-peptide reagent in water (40 μM solution prepared by dissolving 1.75 mg of the Pd-OAC in 25 mL of water) was added to a solution of a peptide containing a single cysteine (20 μM solution prepared by solving 0.8 mg of peptide) in TRIS buffer (25 mL, 0.1 M, pH 7.5) and allowed to stir. Final conditions: [Pd] = 20 μM; [R-SH] = 10 μM; After 6 h at 37 °C, 3-mercaptopropionic acid (3 equiv to the palladium complex solution in 1 mL of H₂O) was added to the reaction mixture to quench the remaining palladium species. The reaction mixture was allowed to stand for 5 min, the solution was lyophilized. The resulting solid were then dissolved in water and acetonitrile containing 0.1% TFA, filtered through a 0.22 μm nylon filter and purified by mass-directed semi-preparative reversed-phase HPLC (RP-HPLC). Solvent **A** was water with 0.1% TFA additive and Solvent **B** was acetonitrile with 0.1% TFA additive. A linear gradient from 5-45% **B** changing a rate of 0.5% **B**/min was used. The peptides were purified on an Agilent Zorbax SB C3 column: 9.4 x 250 mm, 5 μm. Using the mass data collected for each fraction from the instrument, only pure fractions were combined and lyophilized. 1.54 mg of pure ligated peptide was obtained after purification (>99% conversion, 76% isolated yield).

8. PEPTIDE-PROTEIN LIGATION REACTIONS AND LC-MS CHARACTERIZATION

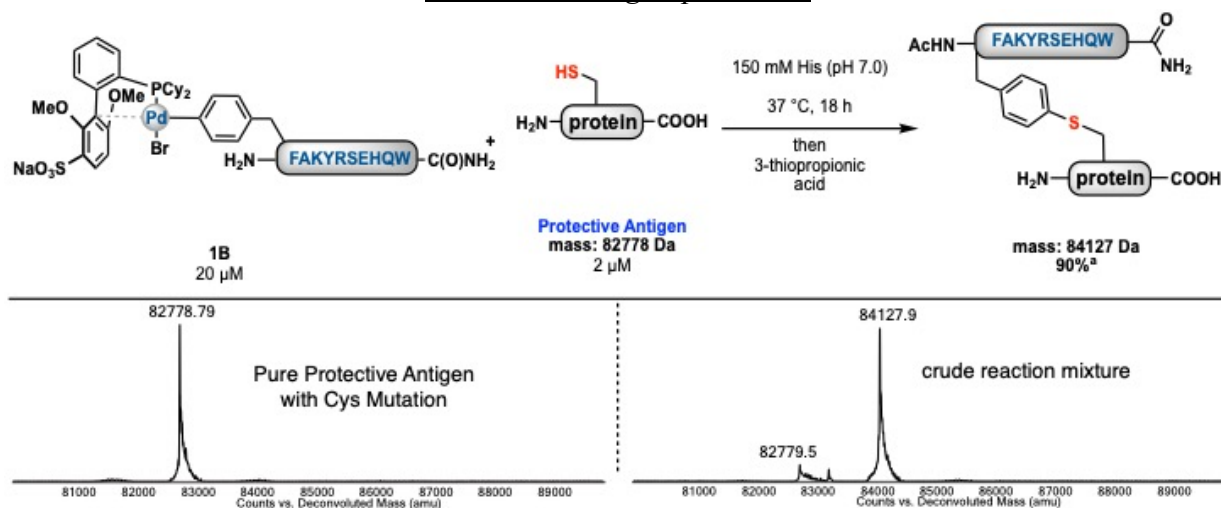
Protein Expression and Purification

pD444 PAC-CO plasmids were constructed as previously reported.³ Cysteine mutations were introduced by site-directed mutagenesis using QuickChange Lightning Single Site-directed Mutagenesis Kit (Agilent) following the manufacturer's instructions. Sequences of the generated protein construct are summarized in Table S2.

PA[K653C] was expressed in the periplasm of *E. coli* BL21(DE3) cells. Cells were grown in LB medium containing ampicillin (100 μg/mL) at 37 °C to an A₆₀₀ of 0.8. Expression was induced by addition of IPTG to final concentration of 0.4 mM, and the culture was grown overnight at 18 °C. The protein was purified by anion exchange chromatography followed by size exclusion chromatography.

The protein was analyzed by LC-MS confirming sample purity and molecular weight. Protein aliquots were flash frozen and stored in -80 °C freezer.

Protein Labeling Experiments



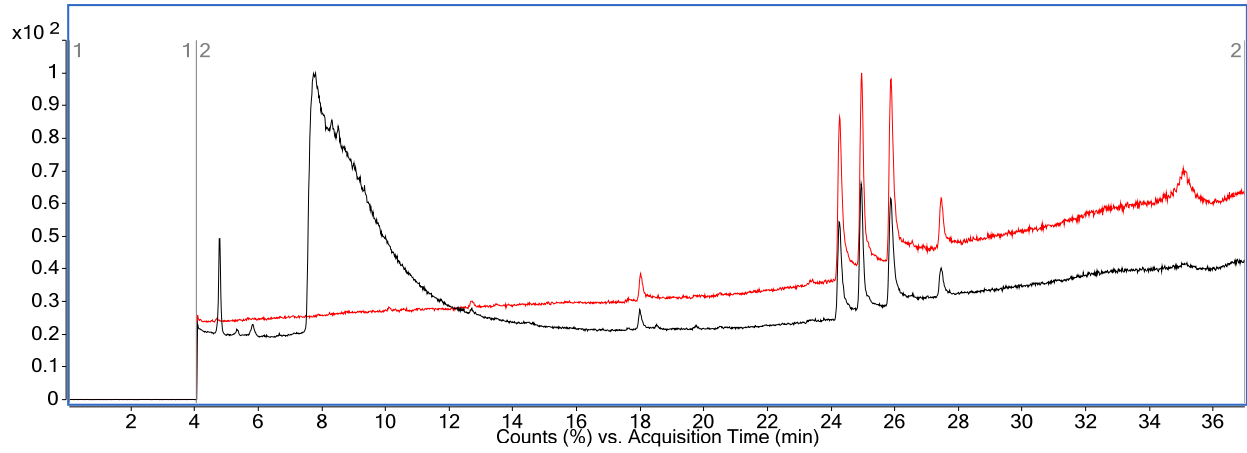
To a 1.6 mL Eppendorf tube was added His Buffer (200 μ L, 200 mM His at pH 7.0) followed by the addition of PA-cys (50 μ L, 1.0 mg/mL in 20 mM Tris, 150 mM NaCl at a pH of 7.5), and using the same pipette tip used to transfer the PA-cys, the solution was mixed by pipetting up and down 20x. Subsequently, peptide **1B** (12 μ L, 1.0 mg/mL in DMSO, see *Note* below) was added and the reaction was mixed by pipetting up and down 40x using the same pipette tip used to transfer the DMSO solution of peptide **1B**. The Eppendorf tube was then capped and placed in a preheated water bath at 37 °C for 18 h. The reactions were then quenched by the addition of the specified amount of 3-mercaptopropionic acid (20 μ L, 50 mM solution, prepared by adding 4 μ L of neat 3-mercaptopropionic acid to 912 μ L of Tris Buffer [20 mM Tris, 150 mM NaCl, pH 7.5]). All reactions were analyzed by injecting 100-200 μ g of protein utilizing *Method C*.

Note: The palladium-peptide **1B** did not fully dissolve in DMSO and created a slightly foggy solution. Efforts to perform this reaction in the absence of organic solvent led to variable conversion, which we attributed to the low solubility of the palladium-peptide. As a result, we chose to dissolve the peptide in DMSO.

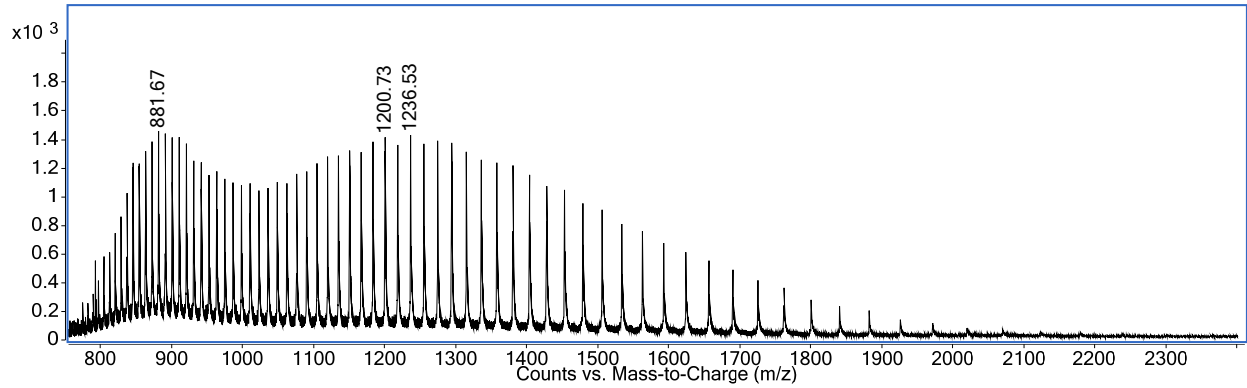
Reactions were analyzed using Agilent BioConfirm 10.0 and deconvoluted spectra were obtained using the maximum entropy algorithm with: a mass range of 20,000 Da to 100,000 Da; mass step of 0.5; utilizing a limited m/z range from 950.00-3000.00 Da; and with baseline subtraction of 7.0.

Chromatograms and mass spectra of PA-cys and the crude reaction mixture are on the following two pages.

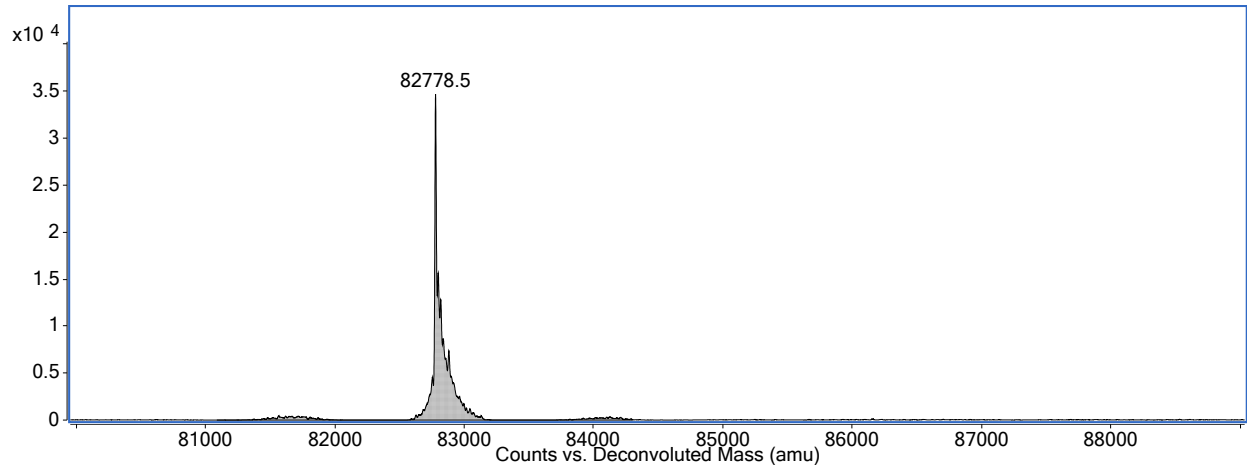
PA-Cys Starting Material



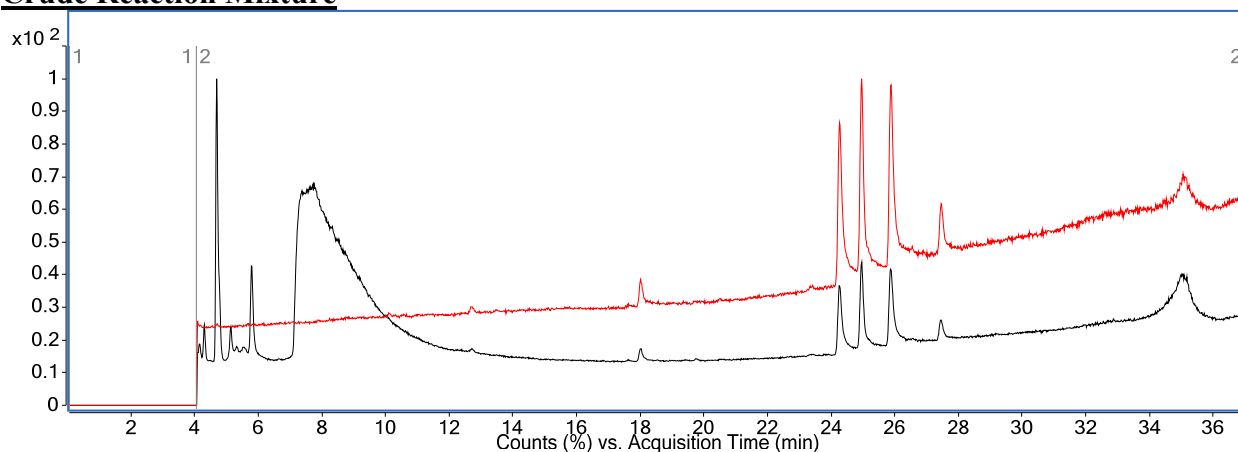
A background chromatogram is overlaid and depicted in red. The protein peak from 7.5-13 min was extracted to give the following chromatogram:



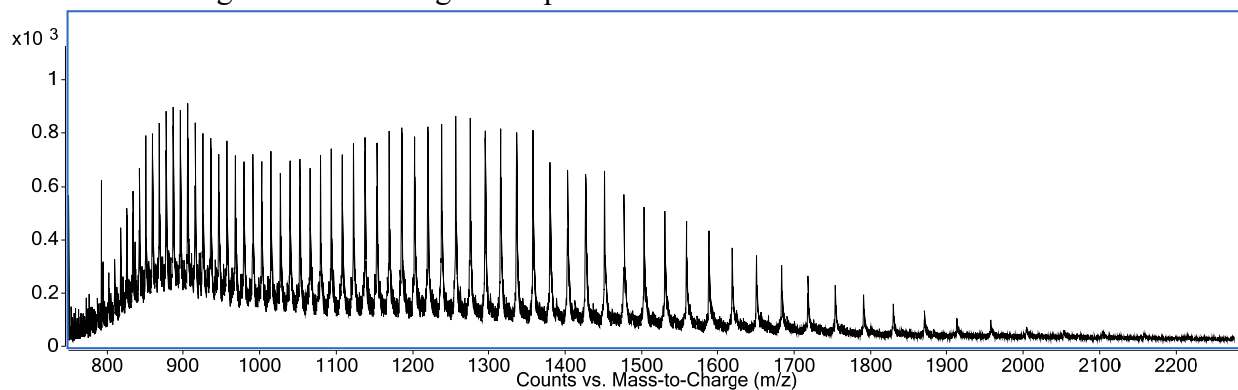
Deconvolution of this spectrum gave the following mass for PA-Cys:



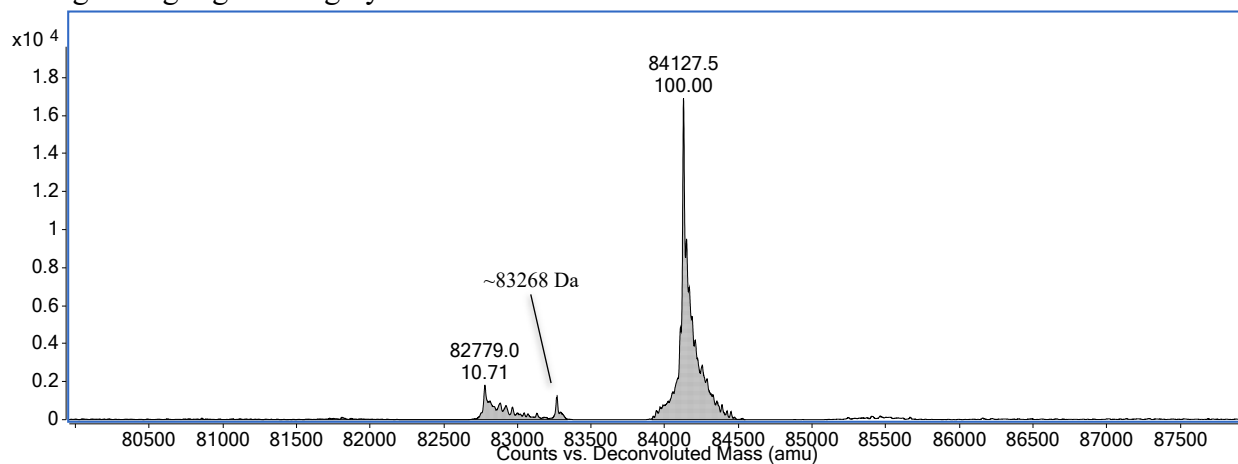
Crude Reaction Mixture



A background chromatogram is overlaid and depicted in red. The protein peak from 7.0-12.6 min was extracted to give the following mass spectrum:



Deconvolution as described above to give the following mass spectrum, with relative peak area of the region highlighted in grey written below the indicated mass.



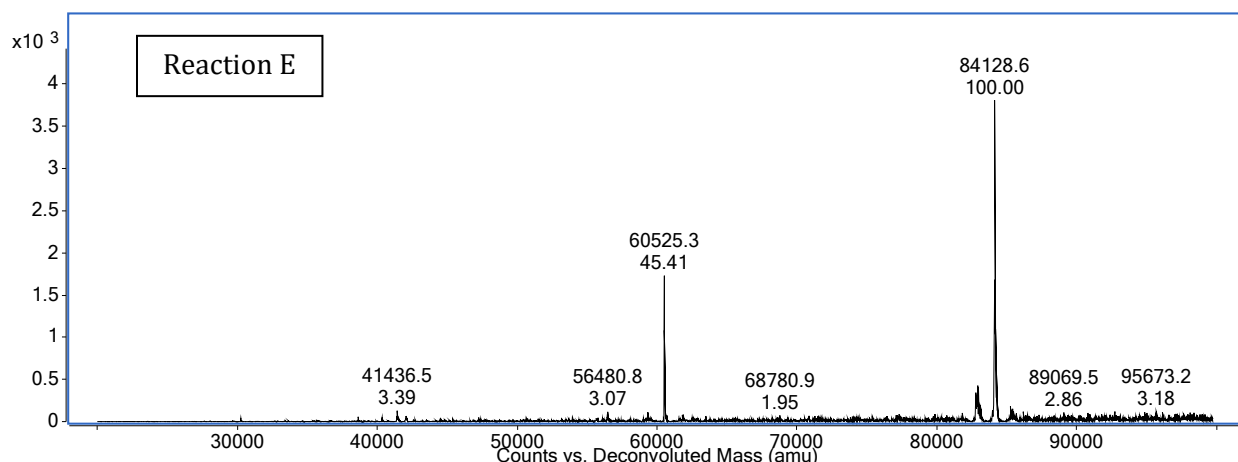
Conversion was calculated as follows: Area percent of product / (Area percent of all protein derived peaks) * 100 = 100 / (100 + 10.71) * 100 = 90% conversion

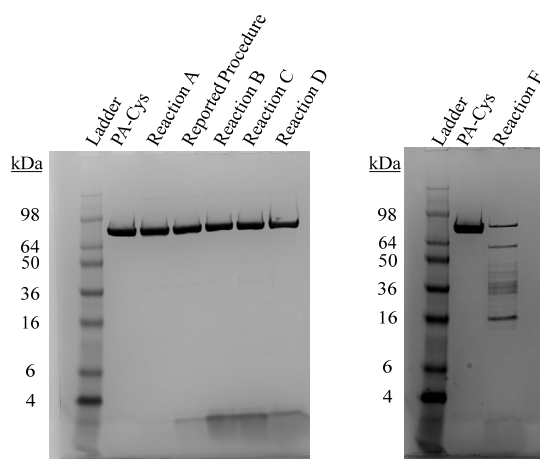
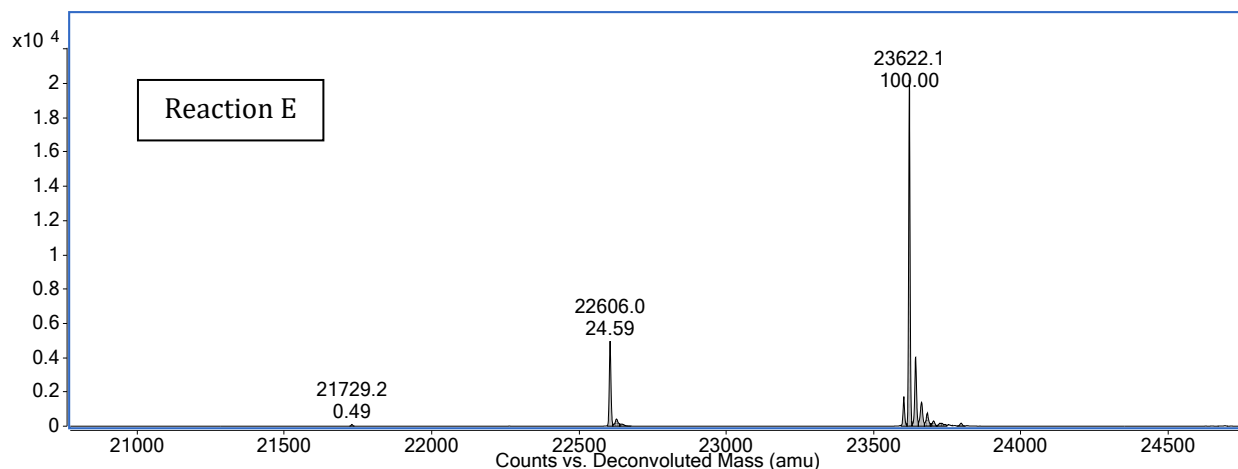
Note 1: When attempting the reaction without His buffer or without the use of DMSO, the reaction typically gave lower conversions and/or gave byproducts that were difficult to remove (a product whose mass corresponded to the product + Pd + sSPhos was observed). The use of DMSO was found to give reliable conversions and the use of His buffer was found to minimize the observation of this Pd + sSPhos adduct.

Note 2: During initial attempts using His buffer for the conjugation of peptide **1B** with PA-cys, a 500 mM, pH 6.1 buffer was used instead of the described 200 mM buffer used in the described protocol. In addition, 25 equivalents of the peptide **1B** were used. During this reaction, conversion was high (>90%). However, the protein was observed to fragment over the course of time to give a 22.6 kDa and a 60.5 kDa fragment. Decreasing the buffer concentration to 100-200 mM and increasing the pH to 7.0 was found to avoid this issue. As a result of this observed cleavage, SDS-PAGE analysis of the reaction mixtures were obtained to corroborate LC-MS data. The following is a summary of conditions and observations, with reaction B being the above procedure:

Buffer P is defined as: 20 mM Tris, 150 mM NaCl, pH 7.5

Reaction	Buffer Conditions	Volume of peptide 1B (1.0 mg/mL in DMSO)	Time	Conversion/Observations
A	200 mM His Buffer (pH 7.0) (200 μ L)	6 μ L (5 equiv)	18 h	78%
Reported Procedure	200 mM His Buffer (pH 7.0) (200 μ L)	12 μ L (10 equiv)	18 h	90%
B	200 mM His Buffer (pH 7.0) (200 μ L)	30 μ L (25 equiv)	18 h	91%
C	200 mM His Buffer (pH 7.0) (140 μ L) + Buffer P (60 μ L)	30 μ L (25 equiv)	18 h	90%
D	200 mM His Buffer (pH 6.1) (100 μ L) + Buffer P (100 μ L)	30 μ L (25 equiv)	13 h	93%
E	500 Mm His Buffer (pH 6.1) (528 μ L)	12 μ L (10 equiv)	15 h (mass spectral data shown below), SDS-PAGE run ~60 h after quenching the mixture.	Cleavage of the protein into two primary fragments: 22.6 kDa/60.5 kDa





SDS-PAGE depicting reactions A-E and the reported procedure. Reaction E appears to undergo degradation to predominantly form two major fragments (22.6 kDa and 60.5 kDa).

Table S1. Protective Antigen-Cys calculated cleavage site at tryptophan residue

Sequence ^a	Calculated mass
MEVKQENRLLNESESSQGLLGYYFSDLNFQAPMVVTS STTGDLSSIPSELENIPSENQYFQSAIWSGFIKVKKSDEYT FATSADNHVTMWVDDQEVINKASNSNKIRLEKGRLYQI KIYQRENPTKGLDFKLYWTD SQNKKEVISSDNLQLP ELKQKSSNSRKKRSTSAGPTVPDRDNDGIPDSLEVEGYT VDVKNKRTFLSPW	23622 Da (average) Observed: 23622 Da

ISNIHEKKGLTKYKSSPEKWSTASDPYSDFEKVTGRIDK
NVSPEARHPLVAAAYPIVHVDMENILSKNEDQSTQNTDS
ETRTISKNTSTSRHTHTSEVHGNAEVHASFFDIGGSVSAGF
SNSNSSTVAIDHSLSLAGERTWAETMGLNTADTARLNA
NIRYVNTGTAPIYNVLPTTSLVLGKNQTLATIKAKENQL
SQILAPNNYYPSKNLAPIALNAQDDFSSTPITMNYNQFL
ELEKTKQLRLDTDQVYGNIATYNFENGRVRVDTGSNW
SEVLPQIQETTARIIFNGKDLNLVERRIAAVNPSDPLETT
KPDMTLKEALKIAFGFNPNLQYQGKDITEFDNFNFD
QQT SQNIC(peptide)NQLAELNATNIYTVLDKIKLNAKMN
ILIRDKRFHYDRNNIAVGADESVVKEAHREVINSSTEGL
LLNIDKDIRKILSGYIVEIEDTEGLKEVINDRYDMLNISSL
RQDGKTFIDFKKYNDKLPLYISNPYKVVVYAVTKENT
IINPSENGDTSTNGIKKILIFSCKKGYEIG

60525 Da

(average)

Observed: 60525 Da

^aCysteine/Modification highlighted in red.

Control Experiment with Wild Type PA:

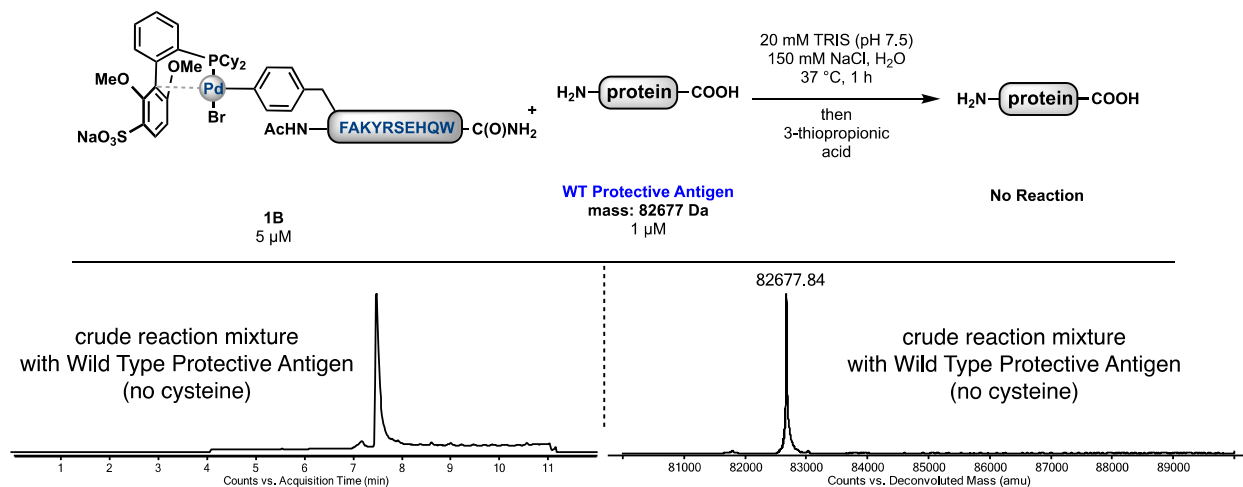


Table S2. Protective Antigen-Cys protein sequence and calculated mass

Sequence ^a	Calculated mass
MEVKQENRLLNESESSQGLLGYYFSDLNFQAPMVVTS STTGDLSSIPSELENIPSENQYFQSAIWSGFIKVKKSDEYT FATSADNHVTMWVDDQEVINKASNSNKIRLEKGRLYQI KIYQRENPTTEKGLDFKLYWTDSONKKEVISSDNLQLP ELKQKSSNSRKKRSTSAGPTVPDRDNDGIPDSLEVEGYT VDVKNKRTFLSPWISNIHEKKGLTKYKSSPEKWSTASDP YSDFEKVTGRIDKNVSPEARHPLVAAPIVHVDMENIIL SKNEDQSTQNTDSETRTISKNTSTSRHTTSEVHGNAEVH ASFFDIGGSVSAGFSNSNSSTVAIDHSLSLAGERTWAET MGLNTADTARLNANIRYVNTGTAPIYNVLPTTSLVLGK NQLATIKAKENQLSQILAPNNYPSKNLAPIALNAQDD FSSTPITMNYNQFLELEKTKQLRLDTDQVYGNIATYNFE NGRVRVDTGSNWSEVLPQIQETTARIIFNGKDLNLVERR IAAVNPSDPLETTKPDMLKEALKIAFGFNPNLQYQ GKDITEFDNFDDQQT SQNICNQLAELNATNIYTVLDKIK LNAKMNILIRDKRFHYDRNNAVGADES VVKEAHREVI NSSTEGLLL NIDKDIRKILSGYIVEIEDTEGLKEVINDRYD MLNISSLRQDGKTFIDFKKYNDKLPYISNPNYKVN AVTKENTIINPSENGDTSTNGIKKILIFS KKGYEIG	82781.31 Da (average)

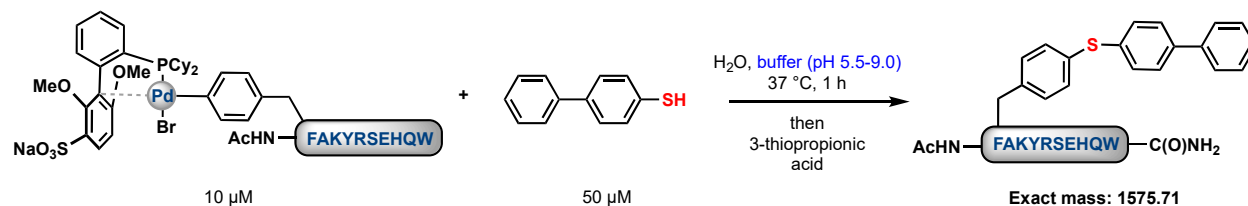
^aCysteine residue highlighted in red.

Table S3. Wild Type Protective Antigen protein sequence and calculated mass

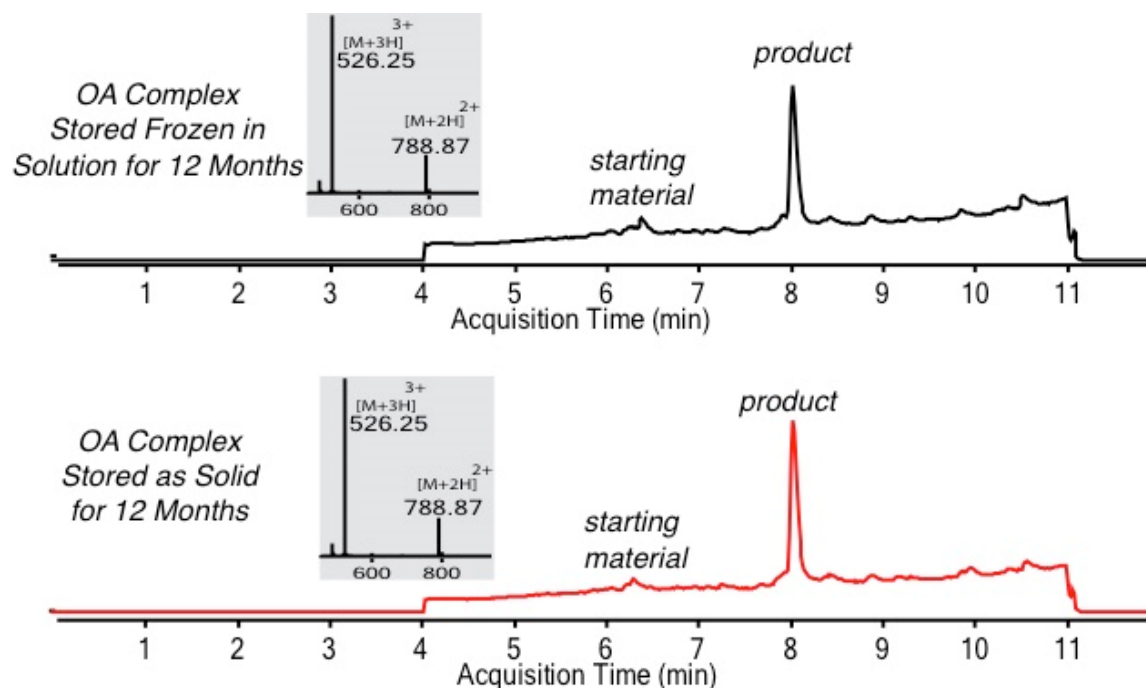
Sequence ^a	Calculated mass
<p>MEVKQENRLLNESESSSQGLLGYYFSDLNFQAPMVVTS STTGDLSSIPSELENIPSENQYFQSAIWSGFIKVKKSDEYT FATSADNHVTMWVDDQEVINKASNSNKIRLEKGRLYQI KIYQRENPTKGLDFKLYWTDSONKKEVISSDNLQLP ELKQKSSNSRKKRSTSAGPTVPDRDNDGIPDSLEVEGYT VDVKNKRTFLSPWISNIHEKKGLTKYKSSPEKWSTASDP YSDFEKVTGRIDKNVSPEARHPLVAAAYPIVHVDMENIIL SKNEDQSTQNTDSETRTISKNTSTSRHTHTSEVHGNAEVH ASFFDIGGSVSAGFSNSNSSTVAIDHSLSLAGERTWAET MGLNTADTARLNANIRYVNTGTAPIYVNLPTTSLVLGK NQTLATIKAKENQLSQILAPNNYYPKLNLAIALNAQDD FSSTPITMNYNQFLELEKTKQLRLDTDQVYGNIATYNFE NGRVRVDTGSNWSEVLPQIQETTARIIFNGKDLNLVERR IAAVNPSDPLETTKPDMTLKEALKIAFGFNPNLQYQ GKDITEFDNFQDQTSQNIKNQLAELNATNIYTVLDKIK LNAKMNILIRDKRFHYDRNNIAVGADESVVKEAHREVI NSSTEGLLLNIKDIRKILSGYIVEIEDTEGLKEVINDRYD MLNISSLRQDGKTFIDFKKYNDKLPLYISNPNYKVNVEY AVTKENTIINPSENGDTSTNGIKKILIFSCKKGYEIG</p>	<p>82806.35 Da</p> <p>82675.15 Da (<i>N</i>-terminal methionine excision)</p>

9. OXIDATIVE ADDITION COMPLEX STABILITY

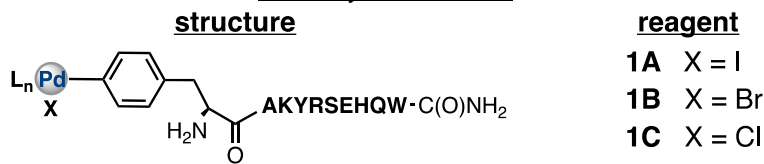
When stored as a solid or kept frozen in solution, the palladium-peptide oxidative addition complexes display remarkable stability for upwards of 12 months and show no diminished reactivity. This is confirmed via a set of experiments wherein the oxidative addition complexes were stored as either a frozen solution or solid and then, after 12 months, allowed to react with a small molecule thiol. The reaction conversions are comparable to that of a freshly prepared palladium-peptide oxidative addition complex.



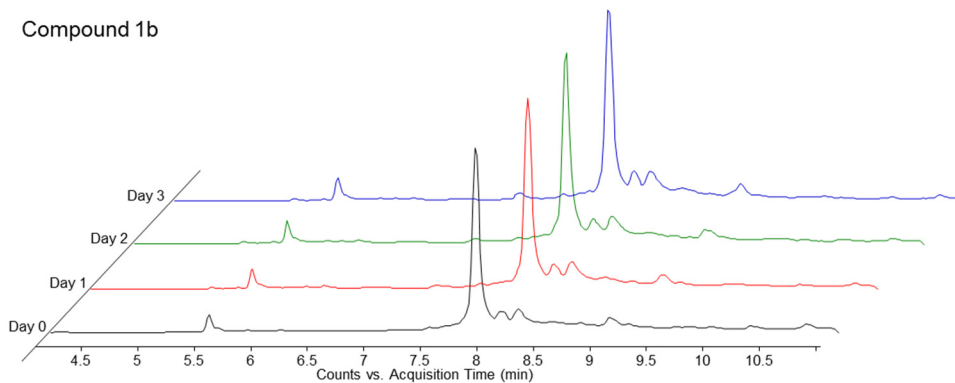
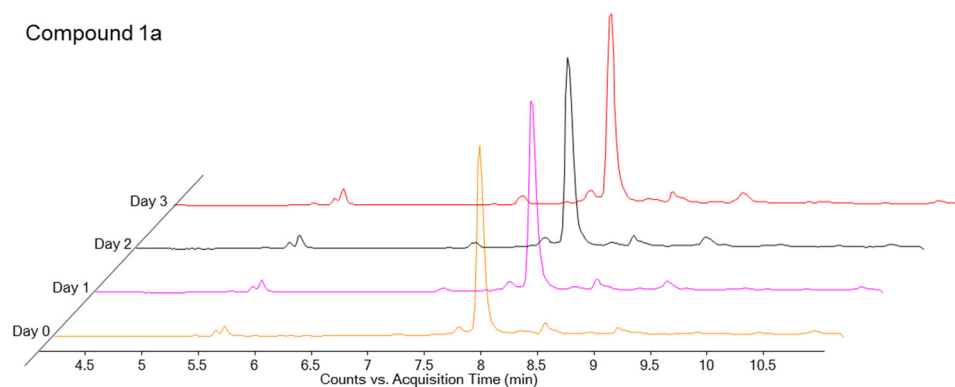
A solution of the palladium-peptide reagent **1B** (20 μM) in water was added to an equal volume of a solution containing biphenyl-4-thiol (100 μM) in TRIS buffer (0.1 M, pH 7.5). The palladium reagents were sonicated for 10 s to ensure the reagents were fully dissolved. Final conditions: $[\text{Pd}] = 10 \mu\text{M}$; $[\text{biphenyl-SH}] = 50 \mu\text{M}$; After 1 h at 37 $^\circ\text{C}$, 3-mercaptopropionic acid (3 equiv) dissolved in H_2O was added to the reaction mixture to quench the remaining palladium species. The reaction was allowed to stand for 5 min and subsequently characterized by LC-MS.



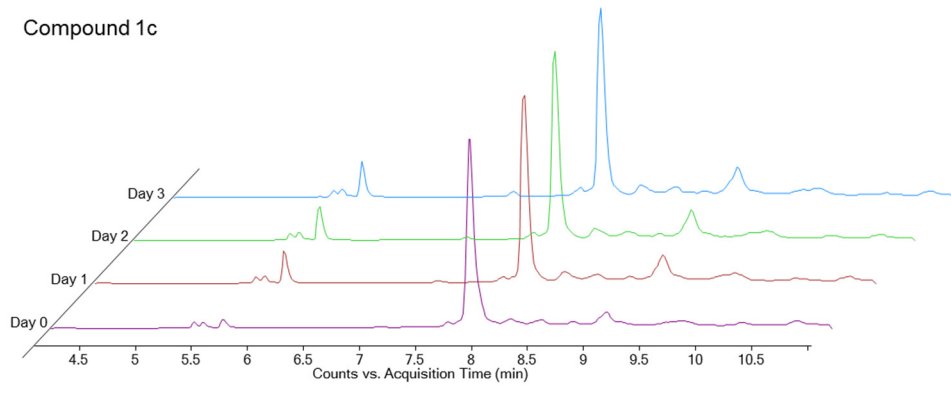
Stability in Solution



The three palladium-peptide oxidative addition complexes (**1A**, **1B**, and **1C**) were dissolved in 50% water / 50% acetonitrile containing 0.1% TFA at a concentration of 300 nanograms / μL . The solutions were analysed by LC-MS using method A after 1, 2, and 3 days. For compounds **1A**, **1B**, and **1C**, the peaks ~ 5.6 minutes have mass 1349.7 Da and 1374.7 Da, which corresponds with replacement of Pd+X+Ligand with either a hydrogen (-H) or nitrile group (-CN). For compound **1C**, the peak ~ 5.7 minutes corresponds to peptide **P6**.

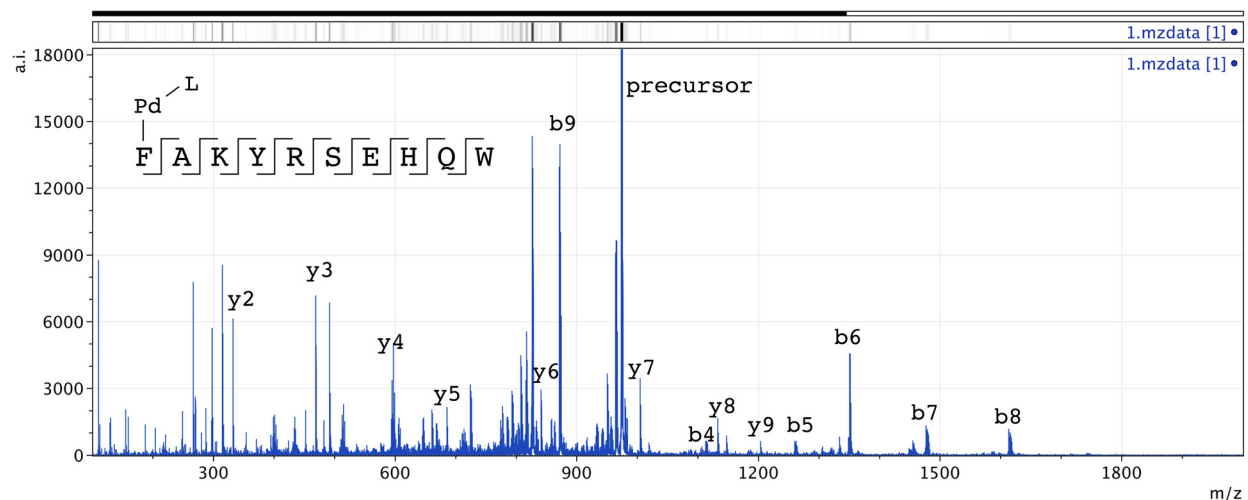


Compound 1c



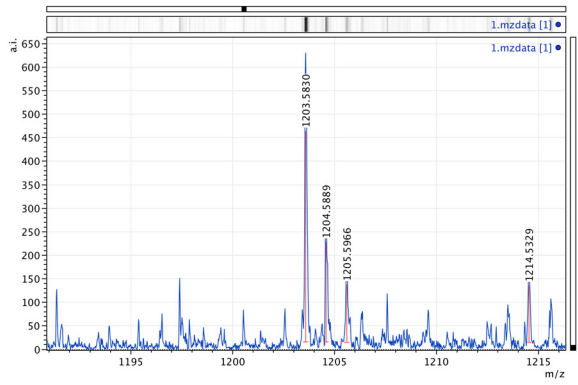
10. COMPLEX **1B** MS/MS CHARACTERIZATION

To confirm that the palladium is located at the N-terminal 4-bromophenylalanine residue, and not elsewhere on the peptide, we subjected oxidative addition complex **1B** to LC-MS/MS analysis. Method A was modified to acquire secondary MS spectra targeting specific ions. Ions with $z = +2$ and $m/z = 973.87$ or 973.37 Da were selected for secondary MS. Shown below is the secondary MS spectrum at 7.95 minutes for the 973.37 Da ion, with CID at 37.3.

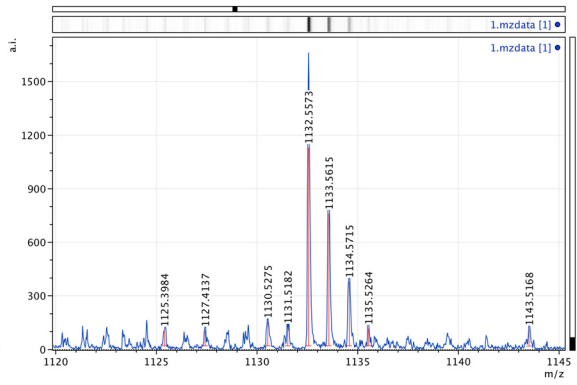


The data were analysed using mMass software. The presence of palladium makes comprehensive analysis of the MS/MS data challenging due its isotopic abundance (deisotoping algorithms do not account for the multiple Pd isotopes). Therefore, a few selected ions are shown below. Critically, no y-ions exhibited an isotope pattern suggestive of palladium, as would be expected for a palladium complex on the N-terminal residue. Additionally, the b-ions exhibited the characteristic palladium isotope pattern.

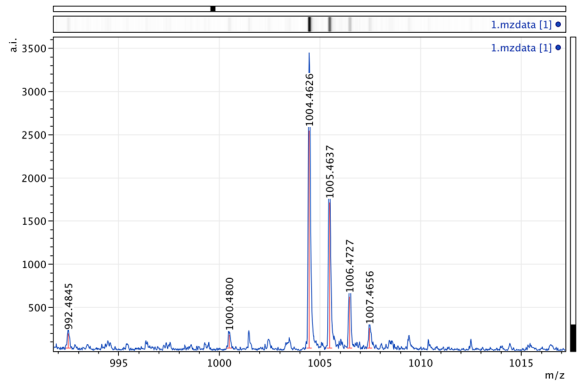
Ion	Fragment	Expected Monoisotopic Mass ($z = +1$)
y ₉	-AKYRSEHQW	1203.60
y ₈	-KYRSEHQW	1132.56
y ₇	-YRSEHQW	1004.47
y ₆	-RSEHQW	841.41
b ₉	[Pd]FAKYRSEHQ-	871.33 ($z = +2$)
b ₅	[Pd]FAKYR-	1260.45



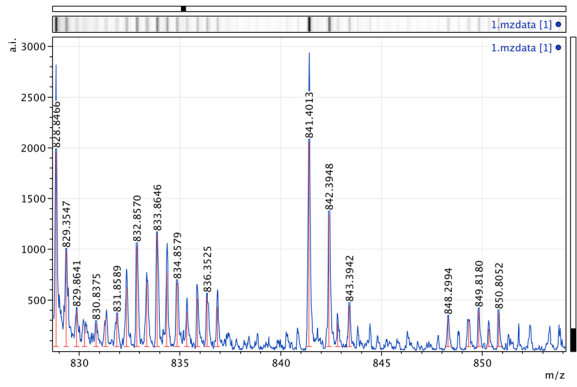
Y9



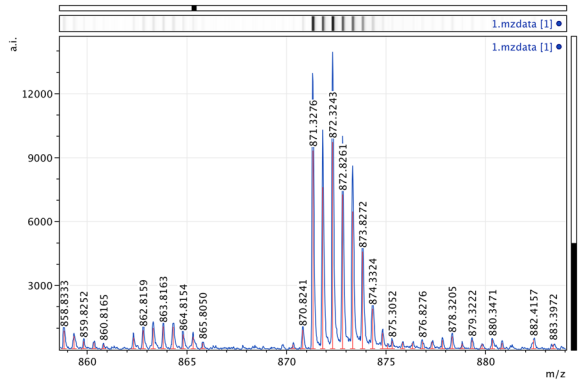
Y8



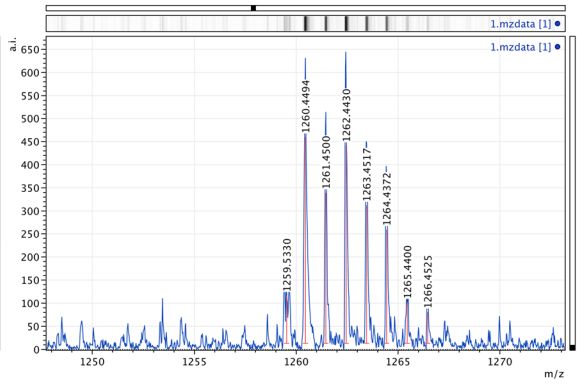
Y7



Y6



b9



b5

11. NMR STRUCTURE ANALYSIS OF PEPTIDE-OAC

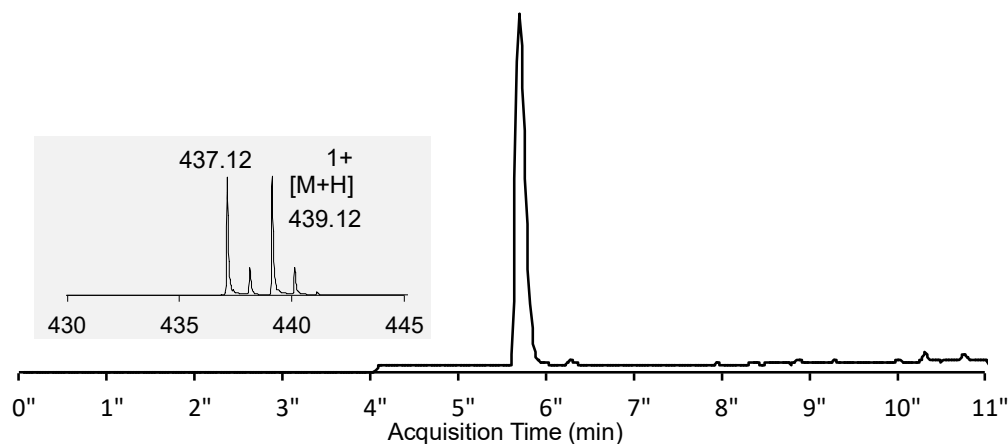
11.1. Synthesis of peptides and corresponding OAC

11.1.1. Synthesis of H-Pro-Pro-Phe(4-Br)-NH₂ (2A)

Tripeptide H-Pro-Pro-Phe(4-Br)-NH₂ was prepared by standard manual solid-phase peptide synthesis as follows:

H-Rink Amide-ChemMatrix resin (1.0 g) was placed in DMF for 30 min to swell, then the swelled resin was loaded into a hand coupling vessel. For the first coupling, the resin was treated with 6 mL of 0.38 M HATU solution in DMF containing Fmoc-protected 4-Br-phenylalanine (1.165 g, 2.5 mmol) and 1.25 mL of DIEA (reaction time: 20 min). Then the solution was drained using a vacuum line, the resin washed extensively with DMF (5×), and drained. Deprotection was performed with 20% piperidine solution in DMF (2 × 10 mL, 5 min each). After deprotection, the resin was washed extensively with DMF (5×) and drained. For the second and third couplings, the resin was treated with 12 mL of 0.38 M HATU solution in DMF containing Fmoc-protected proline (1.685 g, 5.0 mmol) and 2.5 mL of DIEA (reaction time: 20 min). After the final deprotection, the resin was washed extensively with DMF, CH₂Cl₂ and dried under vacuum. The peptide was cleaved from the resin by treatment with 30 mL of the cleavage solution (TFA : H₂O : TIPS= 9.65 : 0.25 : 0.1) at 60 °C for 10 min. The resulting solution was then triturated and washed with cold diethyl ether (3×). The obtained solid was dissolved in a solution of 50% H₂O and 50% acetonitrile containing 0.1% TFA and lyophilized. The crude peptide was purified using the general purification protocol described previously (see **Section 2.2**).

HRMS (ESI) calc. C₁₉H₂₆BrN₄O₃⁺ [M+H]⁺: 437.1183. Found: 437.1193.

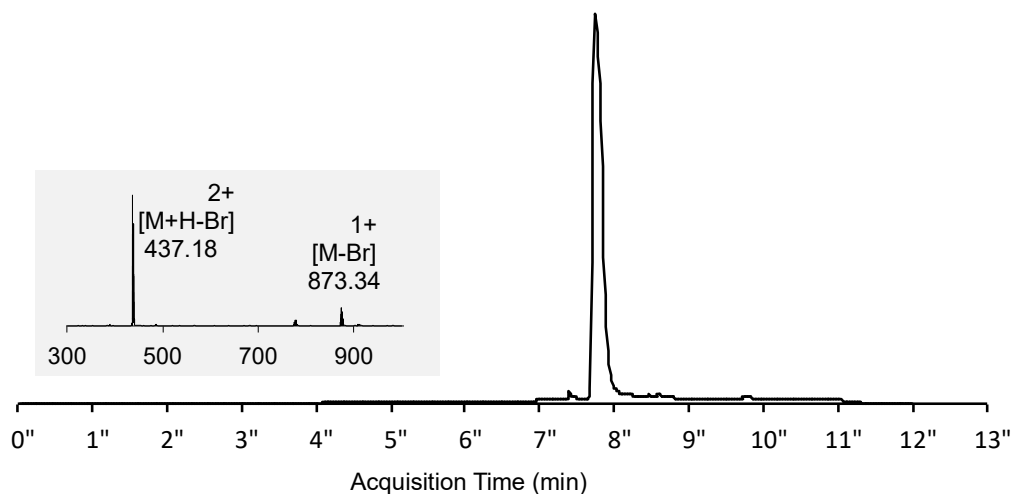


Total ion count chromatogram and mass spectrum (inset) of peptide **2A**

11.1.2. Synthesis of H-Pro-Pro-Phe(4-Br)-NH₂ -OAC (**2B**)

Following the general procedure (**Section 4**), a scintillation vial (5 mL) in a nitrogen filled glovebox was charged with SPhos (16 mg, 0.039 mmol), peptide **2A** (8.5 mg, 0.015 mmol), and DMSO-THF 1:1 (1 mL). Solid (cod)Pd(CH₂SiMe₃)₂ (15 mg, 0.039 mmol) was added rapidly in one portion as a solution in THF (0.1 mL) and the resulting solution was stirred for 1 h at room temperature. Subsequently, the reaction mixture was flash frozen in liquid nitrogen and lyophilized. The crude peptide was purified using the general purification protocol described previously (see **Section 2.2**) to give **2B** (11.0 mg, 73%).

HRMS (ESI) calc. C₄₅H₆₀N₄O₅PPd⁺ [M-Br]⁺: 873.3331. Found: 873.3350.



Total ion count chromatogram and mass spectrum (inset) of peptide-OAC **2B**

11.2. NMR Spectroscopic Experiments

11.2.1. General Experimental

NMR spectra were measured on a Bruker AVANCE Neo 600 MHz spectrometer equipped with a 5 mm QCI-F cryoprobe. Unless otherwise noted spectra were recorded at 25 °C. Standard COSY, TOCSY, ¹³C-HSQC, ¹³C-HMBC, and multiplicity-edited ¹³C-HSQC spectra were recorded for resonance assignment. ROESY spectra were recorded with a mixing time of 400 ms for H-Pro-Pro-Phe(4-Br)-NH₂ and 200 ms for H-Pro-Pro-Phe(4-Br)-NH₂-OAC.

11.2.2. Sample Preparation and NMR Analysis

Spectra of **2A** were recorded using a 9 mM solution in H₂O:D₂O 9:1 (10 mM sodium acetate, pH 5.0) with acetic acid as internal reference (CH₃COOH: δ 2.08). Spectra of **2B** were recorded using a 3 mM solution in H₂O:D₂O 9:1 (10 mM sodium acetate, pH 5.0) with acetic acid as internal reference (CH₃COOH: δ 2.08).

11.2.3. Acquisition Parameters of 2D NMR Experiments

Table S4. Acquisition and processing parameters of 600 MHz 2D NMR spectra of **2A** (9 mM solution in H₂O:D₂O 9:1). The water signal was suppressed by presaturation or excitation sculpting.

Experiment	o1p/o2p [ppm]	SW [ppm]	TD	DS/NS	D1 [s]	SI
COSY	6.000	12/12	2k/256	16/2	1.0	1k/1k
TOCSY	4.700	10/10	2k/256	16/8	1.5	1k/1k
¹³ C-HSQC	6.000/80	12/160	2k/256	32/8	1.0	1k/1k
ROESY	4.700	10/10	2k/256	16/8	1.0	1k/1k

Table S5. Acquisition and processing parameters of 600 MHz 2D NMR spectra of **2B** (3 mM solution in H₂O:D₂O 9:1). The water signal was suppressed by presaturation or excitation sculpting.

Experiment	o1p/o2p [ppm]	SW [ppm]	TD	DS/NS	D1 [s]	SI
COSY	6.000	12/12	2k/256	16/2	1.0	1k/1k

TOCSY	4.700	10/10	2k/256	16/4	1.5	1k/1k
¹³ C-HSQC	6.000/80	12/160	2k/256	32/8	1.0	1k/1k
ROESY	4.700	10/10	2k/256	16/48	1.0	1k/1k

11.3. Tabulated NMR Data

11.3.1. Chemical Shifts of H-Pro-Pro-Phe(4-Br)-NH₂ (2A)

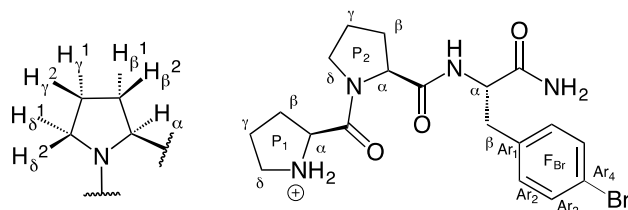


Fig. S1. Designation of pyrrolidine protons in the proline residues and protons of 4-bromophenylalanine residue.

Table S6. The ¹H and ¹³C chemical shifts and coupling constants of H-Pro-Pro-Phe(4-Br)-NH₂ in H₂O:D₂O (9:1) pH 5.0 at 25 °C. For overlapping signals, proton chemical shifts were extracted from ¹³C-HSQC spectrum.

Residue	Designation	δ _H (ppm), mult. (J, Hz)	δ _C (ppm)
P ₁	α	4.65, dd (8.5, 7.1)	58.4
	β	2.60–2.54, m ^{a)}	27.6
		2.00, m ^{b)}	
	γ	2.06, m ^{c)}	23.1
	δ	3.51–3.43, m ^{c)}	46.0
	CO	-	167.5
P ₂	α	4.47, dd (8.4, 5.9)	59.7
	β	2.32–2.27, m ^{a)}	28.4
		1.88, dq (13.0, 6.8) ^{b)}	
	γ	2.03, m ^{c)}	23.7
	δ	3.71, dt (10.0, 6.7) ^{a)}	46.8
3.60, dt (10.1, 7.1) ^{b)}			
	CO	-	172.6
F _{Br}	α	4.63–4.56, m	53.8
	β	3.17–3.07 m ^{c)}	35.6

Ar ₁	-	119.6
Ar ₂	7.25, dd (8.3, 2.2)	130.4
Ar ₃	7.58, dd (8.4, 2.0)	130.8
Ar ₄	-	134.7
NH	8.36, d (7.1)	-
NH ₂	7.59, s	-
	7.11, s	-
CO	-	174.6

a) Refers to H_β¹, H_γ¹ or H_δ¹ protons. b) Refers to H_β², H_γ² or H_δ² protons. c) For geminal protons which could not be resolved single chemical shift is given.

11.3.2. Chemical Shifts of Peptide H-Pro-Pro-Phe(4-Br)-NH₂-OAC (2B)

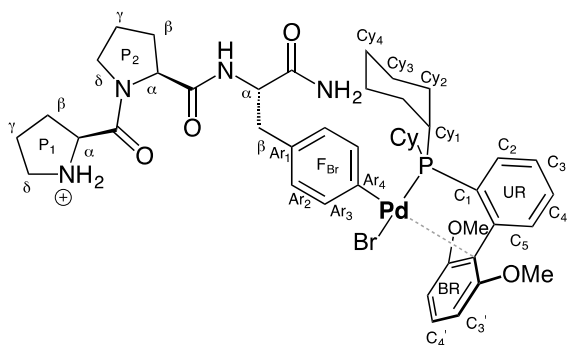


Fig. S2. Designation of protons in H-Pro-Pro-Phe(4-Br)-NH₂-OAC.

Table S7. ¹H NMR chemical shifts of **2B**

Residue	Designation	δ _H (ppm), mult. (J, Hz), number of H	δ _C (ppm)
P ₁	α	4.69–4.65, m, 1H	58.8
	β	2.60, m, 1H ^{a)}	28.0
		2.09, m (overlap), 1H ^{b)}	-
	γ	2.11, m, (overlap), 2H ^{c)}	23.5
	δ	3.50–3.42, m, 2H ^{c)}	46.4
CO	-	-	167.9

P ₂	α	4.50–4.45, m (overlap), 1H	60.2
	β	2.36–2.27, m (overlap), 1H ^{a)}	29.0
		1.89, dq, (13.4, 6.8), 1H ^{b)}	-
	γ	2.05, m (overlap), 2H ^{c)}	24.2
	δ	3.74, dt (9.8, 6.7) ^{a)} , 1H	47.3
		3.63, dt (9.8, 7.1) ^{b)} , 1H	-
	CO	-	172.9
F _{Br}	α	4.50-4.45, m (overlap), 1H	54.8
	β	3.08-2.96 m ^{c)} , 1H	35.7
	Ar ₁	-	132.9
	Ar ₂	7.09-7.02, m, 2H	128.4
	Ar ₃	7.25-7.17, m, 2H	135.7
	Ar ₄	-	136.8
	NH	8.35, d (6.4), 1H	-
	NH ₂	7.50, s, 1H	-
		6.99, s, 1H	-
		CO	-
UR ^{d)}	C ₁	-	141.6 ^{e)}
	C ₂	7.96, m, 1H	132.1
	C ₃	7.60, m, 1H	127.6
	C ₄	7.06, m (overlap), 1H	130.4
	C ₅	7.66, m, 1H	132.3
	C ₆	-	134.1
BR ^{f)}	MeO	3.92, s, 6H	55.7
	C ₁ '	-	105.6

	C ₂ '	-	160.5, 160.6
	C ₃ '	6.91, d (7.9), 2H	105.0
	C ₄ '	7.78, t (8.4), 1H	136.2
Cy ^{g)}	Cy ₁ ^{h)}	2.36–2.27, m (overlap), 2H	33.7, 33.9
	Cy ₂ -Cy ₄	1.94–1.89 (m, 1H), 1.83–1.57 (m, 1H), 1.40–1.30 (m, 2H), 1.28–1.18 (m, 2H), 1.15–1.08 (m, 2H), 0.78–0.70 (m, 1H), 0.67–0.60 (m, 1H),	25.1, 25.9, 26.2, 27.1, 27.6

a) Refers to H_β¹, H_γ¹ or H_δ¹ protons. b) Refers to H_β², H_γ² or H_δ² protons. c) For geminal protons which could not be resolved a single chemical shift is given. d) UR = “upper ring”. e) C₁ was assigned based on analogy to known SPhos-Pd complexes. f) BR = “bottom ring”. g) The chemical shifts of protons and carbons in cyclohexyl groups were reported for the combination of Cy₂-Cy₄. h) Chemical shift of Cy₁ protons were determined from ¹³C-HSQC.

¹³C and ³¹P spectra of 2B

¹³C NMR (125 MHz, H₂O+D₂O, chemical shifts standardized to acetate (177.2 ppm for carbonyl carbon)) δ 174.9, 172.9, 167.9, 160.6, 160.5, 141.6*, 136.8, 136.2, 135.7, 134.1, 132.9, 132.3, 132.1, 130.4, 128.4, 127.6, 105.6, 105.0, 60.2, 58.8, 55.7, 54.8, 47.3, 46.4, 35.7, 33.9*, 33.7*, 29.0, 28.0, 27.6, 27.1, 26.2*, 25.9*, 25.1, 24.2, 23.5.

*The asterisk indicates observed peak splitting due to ³¹P–¹³C coupling.

Additional peaks associated with sodium acetate or trifluoroacetate in attached spectra: δ 162.3 (q, *J* = 35.6 Hz, TFA), 115.9 (q, *J* = 291.8 Hz, TFA), 177.2 (sodium acetate), 20.6 (sodium acetate).

³¹P NMR (162 MHz, H₂O+D₂O) δ 45.1.

11.4. Determination of NOE-Derived Distances

The ROESY cross-peaks integration was performed with MestReNova 7.1.2, The volumes of cross-peaks were converted into corresponding distances using Eq.(1)⁶:

$$r_{ij} = a + b(V_{ij})^{-1/6} \quad (1)$$

where $a = \frac{r_{ref2}(V_{ref1})^{-1/6} - r_{ref1}(V_{ref2})^{-1/6}}{(V_{ref1})^{-1/6} - (V_{ref2})^{-1/6}}$, and $b = \frac{r_{ref2} - r_{ref1}}{(V_{ref1})^{-1/6} - (V_{ref2})^{-1/6}}$

The distances between H_α and H_β located on the same side of pyrrolidine rings of proline residues were assumed to correspond to 2.4 Å.⁶ The distance between two geminal protons was assumed to be equal to 1.8 Å. For H-Pro-Pro-Phe(4-Br)-NH₂ (**2A**) and H-Pro-Pro-Phe(4-Br)-NH₂ -OAC (**2B**) the averaged P₁α - P₁β¹ and P₂α - P₁β¹ peaks as well as P₂β¹- P₂β² were used for calibration. If the cross-peaks from both sides of the diagonal could be integrated, they were separately converted into distances and then averaged. The volume integrals used to estimate distances scale with the sixth power of distance. As such, the error estimates are expected to be small.

11.5. NOE-Derived Distances

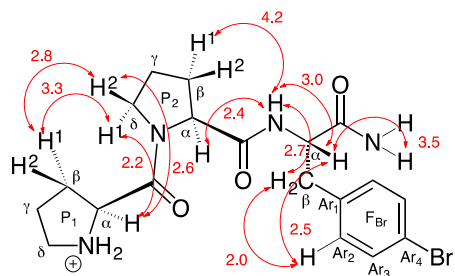


Fig. S3. Summary of NOEs of **2A** with distances in Å.

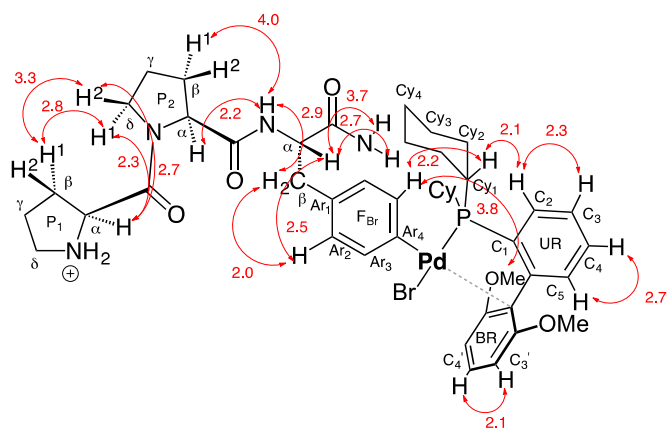


Fig. S4. Summary of NOEs of **2B** with distances in Å.

12. CONFORMATIONAL ANALYSIS OF A TRIPEPTIDE OXIDATIVE ADDITION COMPLEX VIA DFT

General Computational Considerations

All reported DFT calculations were performed using the ORCA software⁴ or Gaussian 03.⁵ Images of the 3D structures were rendered using CYLView.⁶ The geometry of all reactants and transition states were optimized using the B3LYP^{7,8} functional in the gas phase. In these geometry optimizations, a mixed basis set of SDD^{9,10} for Pd and 6-31G(d)^{11,12,13} for all other atoms was used. Ground state geometries were validated by vibrational analysis at the same level. These frequencies were also used to calculate zero-point and thermal energies at 298 K using the standard rigid-rotor and harmonic approximations in Gaussian 03. Higher-level single point energies were obtained for each stationary point using the B3LYP functional with a mixed basis set of SDD for Pd and 6-311+G(d,p) for all other atoms. In these calculations, the SMD implicit solvation model¹⁴ with water as solvent ($\epsilon = 80.4$) was applied. The estimated Gibbs free energies of solvation are reported as a composite of this higher-level electronic energy (SDD/6-311+G(d,p), SMD) plus all other contributions from the lower level (SDD/6-31G(d), gas phase).

Generation of Candidate Conformations

Using the Confab utility,¹⁵ conformations of the peptide **2A** were systematically generated by a torsion driving approach. This procedure sampled ~2 million geometries, which were reduced to a set of 438 unique candidates with energies within 20 kcal/mol of the minimum energy conformer, as assessed using the MMFF94 forcefield.¹⁶ Next, gas phase DFT optimization of this set (B3LYP/6-31G(d)/SDD(Pd)) led to a further reduction to 48 unique conformations. Assessment of the solution-phase Gibbs free energies (B3LYP/6-311+G(d,p)/SDD(Pd)/SMD(water)) revealed **Conf 61** to be lowest in energy, with the remaining members spanning a roughly 12 kcal/mol range of energies above **Conf 61**. Notably, many of the bond distances in **Conf 61** agree with ROESY measurements for the peptide, shown below.

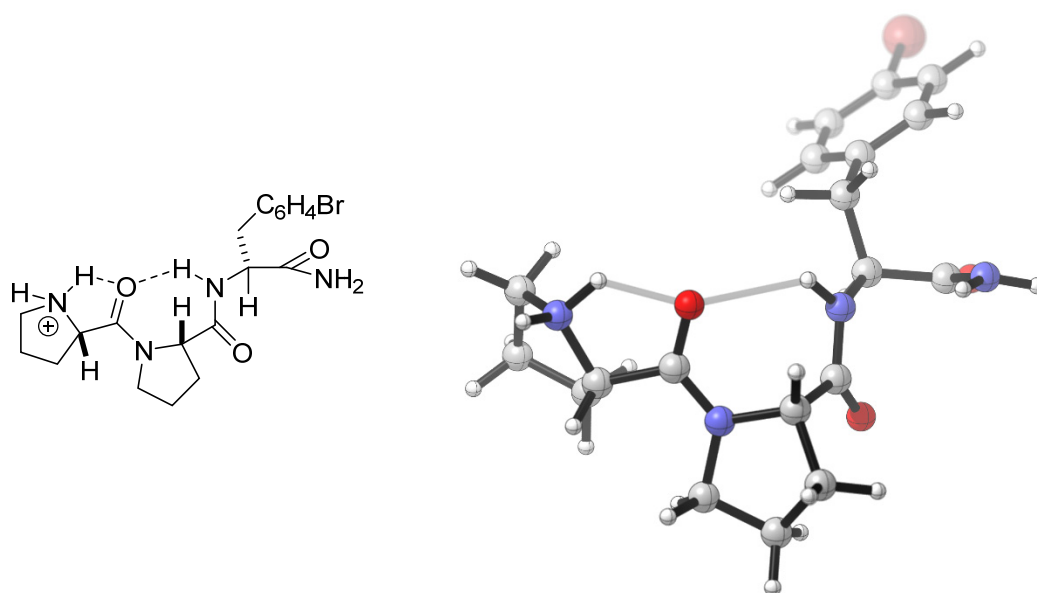
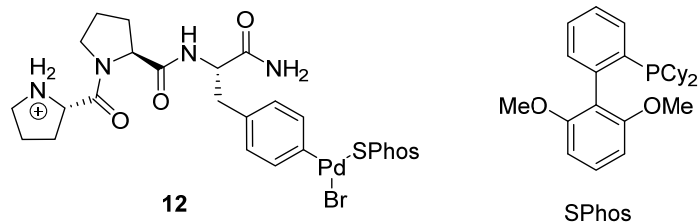


Fig. S5. Favored conformation (**Conf 61**) of the peptide **2A**.

Table S8. H-H distances in H-Pro-Pro-Phe(4-Br)-NH₂ obtained from ROESY experiment and computed distances

ROESY Correlation (H-H)	Experimental Distance (Å)	Computed Distance (Å) in Conf 61A
P ₁ α - P ₁ β ¹	2.4	2.41
P ₁ α - P ₂ δ ¹	2.2	2.50
P ₁ α - P ₂ δ ²	2.6	2.80
P ₁ β ¹ - P ₂ δ ²	2.8	2.35
P ₁ β ¹ - P ₂ δ ¹	3.3	3.50
P ₂ β ¹ - F _{Br} NH	4.2	4.54
P ₂ α - F _{Br} NH	2.4	2.29
F _{Br} α - F _{Br} NH	3.0	2.81
F _{Br} β - F _{Br} NH	2.7	2.57
F _{Br} β - F _{Br} Ar ₂	2.0	2.45
F _{Br} α - F _{Br} Ar ₂	2.5	2.92
F _{Br} α - F _{Br} CONH ₂	3.5	3.55



Based on these preliminary results, we set out to perform a similar conformational search for the palladium oxidative-addition complex derived from this peptide (**2B**, above). We inserted SPhosPd into each of the 48 candidate conformations of peptide **2A** with several different geometries for the Pd-containing fragment. Following the results in a previous theoretical study, it was important to assess both the “O-bound” and “C-bound” conformations of SPhosPd, which were similar in energy for several model compounds (within 1 kcal/mol).¹⁷ Furthermore, the -PCy₂ group could display several similar conformations, differing by rotation about the P–C bonds. Finally, rotation around the C(aryl)–Pd bond needed to be considered for each complex. The entire set of Pd-containing candidates was subjected to gas phase DFT optimization (B3LYP/6-31G(d)/SDD(Pd)) then ranking by approximate solution phase Gibbs free energy (B3LYP/6-311+G(d,p)/SDD(Pd)/SMD(water)). The energies of the 100 most stable conformations are displayed in Table S9.

Table S9. Summary of highest probability results from conformational search for **2B**.

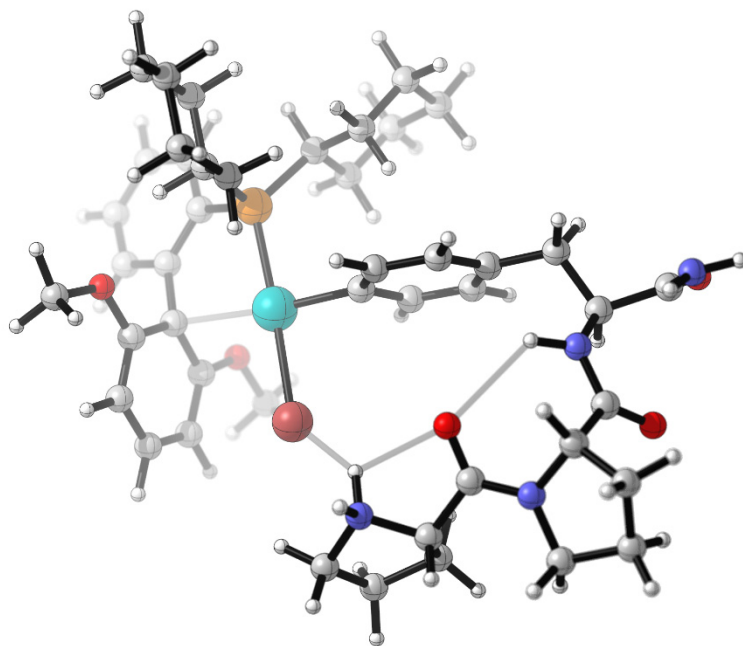
Conformation Label	Relative Energy (kcal/mol)						
354A	0.00	43B	3.52	146B	4.42	113C	5.06
354B	0.08	58B	3.52	128B	4.52	245A	5.07
354C	0.19	61B	3.57	113D	4.58	245D	5.08
264E	0.27	280E	3.60	332E	4.62	127E	5.11
209D	0.30	43C	3.61	82B	4.63	19B	5.15
354D	0.52	162E	3.62	250E	4.74	32E	5.18
264D	0.87	61E	3.63	250C	4.75	275B	5.19
209A	1.92	114E	3.64	82A	4.76	275A	5.19
61A	1.96	58C	3.68	409E	4.76	102E	5.19
6A	2.27	162C	3.79	280C	4.80	409D	5.24
1A	2.28	332B	3.81	32C	4.86	227C	5.29
162A	2.31	250A	3.83	43D	4.88	1D	5.30
19E	2.58	21E	3.88	227A	4.88	245E	5.30
58E	2.82	146E	3.88	115A	4.89	19D	5.33

67B	2.85	274E	3.88	146A	4.89	102B	5.36
43A	2.86	162B	3.94	274A	4.90	1E	5.37
58D	2.99	6B	3.99	32B	4.92	29E	5.41
354E	3.02	32A	4.00	274D	4.93	32D	5.42
58A	3.06	280B	4.06	146D	4.94	183B	5.43
19A	3.11	6D	4.09	115B	4.94	3D	5.48
113B	3.17	67D	4.14	227B	4.95	280D	5.50
162D	3.29	250D	4.16	332D	4.95	332A	5.51
250B	3.30	113A	4.40	114B	4.99	1C	5.51
409B	3.30	67A	4.40	409A	5.00	6E	5.52
6C	3.35	274B	4.42	280A	5.06	102A	5.53

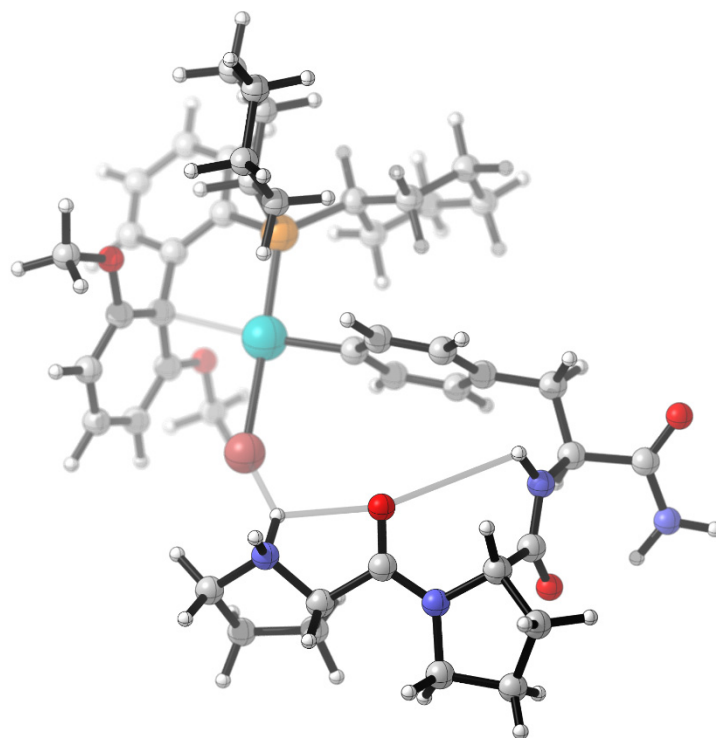
Comparison of Most Probable Ground State Conformations to ROESY Data

The highlighted entries of Table S9 correspond to the five lowest energy conformations of **2B** that are consistent with the ROESY data (see below for details). 3D representations are displayed on the following pages.

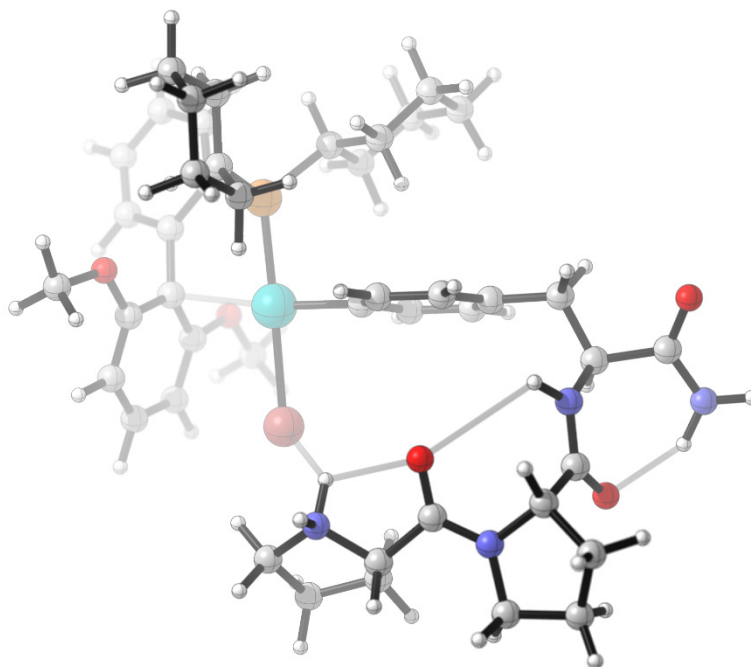
Conf 61A



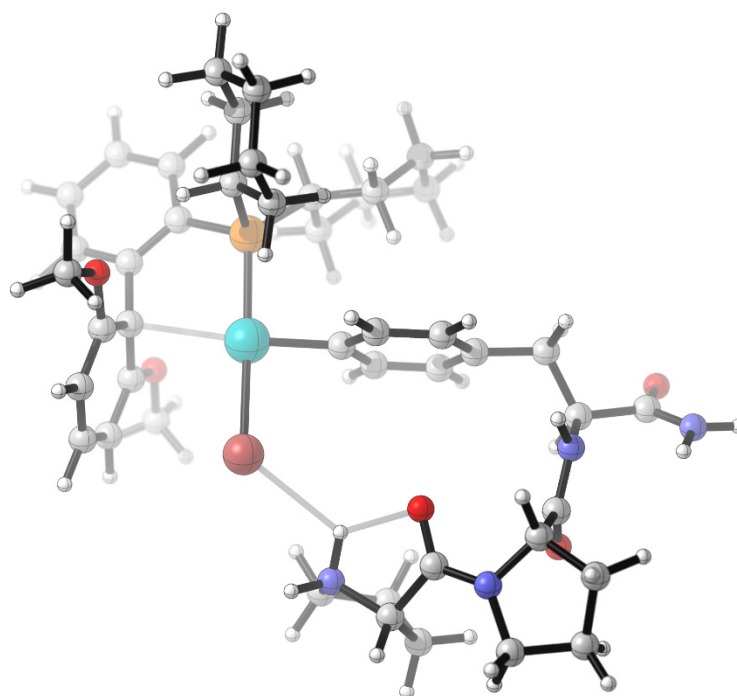
Conf 6A



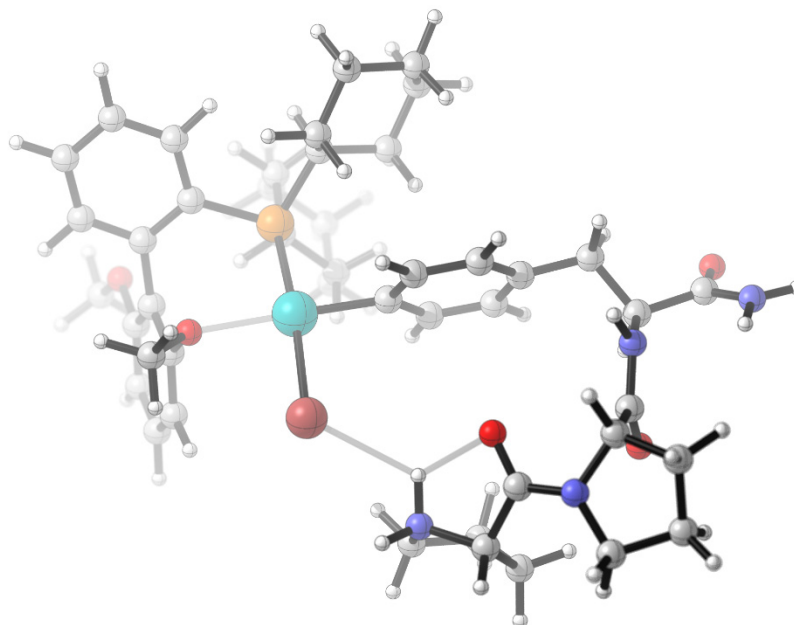
Conf 1A



Conf 162A



Conf 162D



The first three conformers (61A, 1A, 6A) differ primarily by rotation of the C-terminal amide group and are very similar in energy. Thus, we assigned **Conf 61A** as the most probable ground state conformation, with contributions from amide rotamers **Conf 6A** and **Conf 1A**. The consistency of this assignment with ROESY data is supported by the values in Table S10.

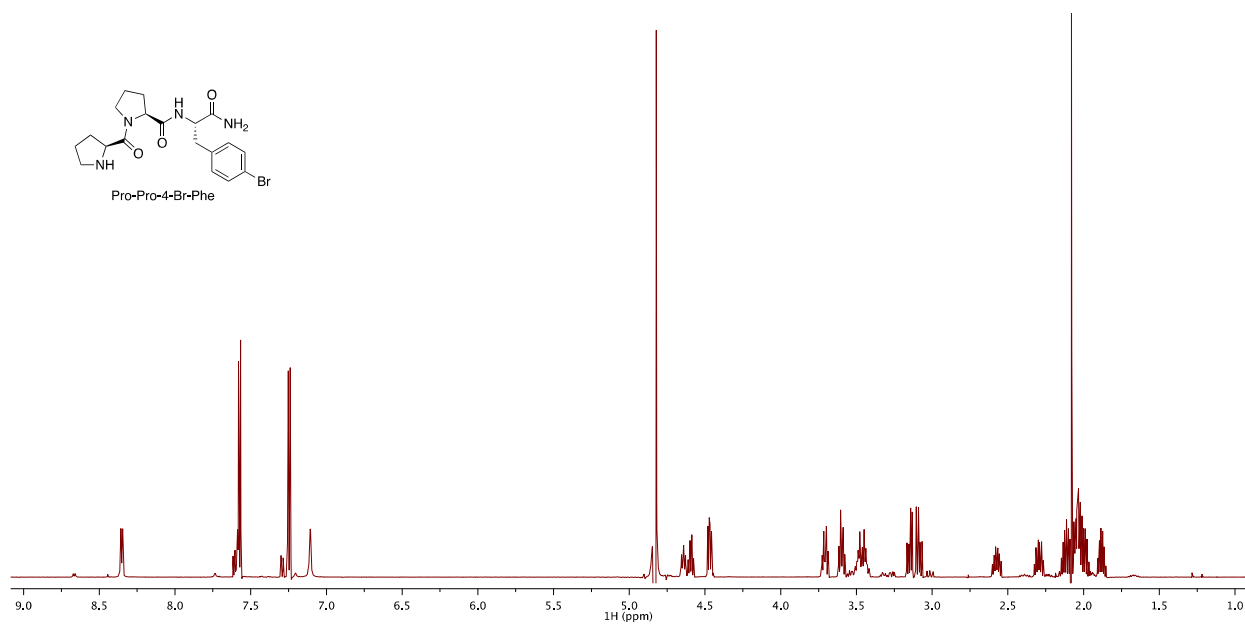
Table S10. H-H distances in H-Pro-Pro-Phe(4-Br)-NH₂-OAC obtained from ROESY experiment and computed distances

ROESY Correlation	Experimental Distance (Å)	Computed Distance (Å) in Conf 61A
(H-H)		
P ₁ α - P ₁ β ¹	2.4	2.45
P ₁ α - P ₂ δ ¹	2.3	2.37
P ₁ α - P ₂ δ ²	2.7	2.73
P ₁ β ¹ - P ₂ δ ¹	2.8	2.34
P ₁ β ¹ - P ₂ δ ²	3.3	3.49
P ₂ β ¹ - F _{Br} NH	4.0	4.24

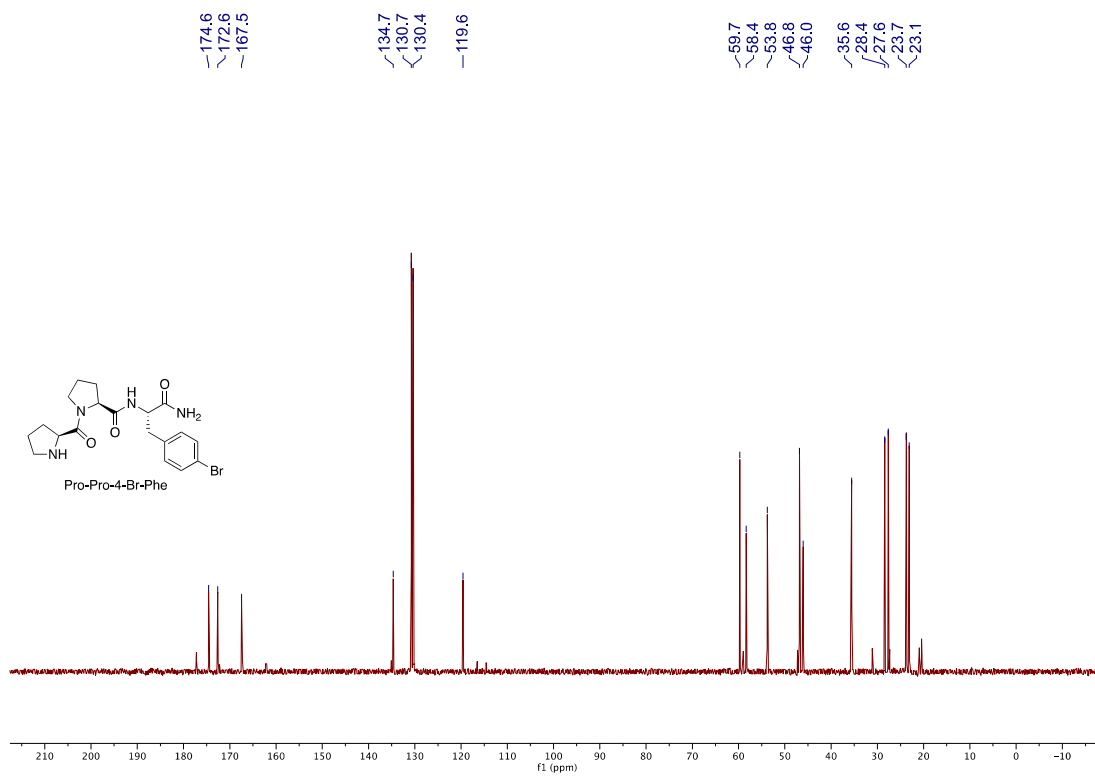
$P_2 \alpha - F_{Br} NH$	2.2	2.29
$F_{Br} NH - F_{Br} \beta$	2.9	2.68
$F_{Br} \alpha - F_{Br} Ar_2$	2.5	2.71
$F_{Br} \beta - F_{Br} Ar_2$	2.0	2.41
$F_{Br} \alpha - F_{Br} CONH_2$	2.7, 3.7	3.55, 4.08
		Conf 6A: 2.42, 3.58
		Conf 1A: 2.48, 3.61
$Cy1 - UR C_2$	2.1	2.01
$F_{Br} Ar_3 - MeO$	3.8	4.01
$MeO - BR C_3'$	2.1	1.6–2.3 (methyl rotation)
$BR C_3' - BR C_4'$	2.1	2.46
$UR C_2 - UR C_3$	2.3	2.45
$UR C_4 - UR C_5$	2.7	2.47

13. NMR SPECTRA

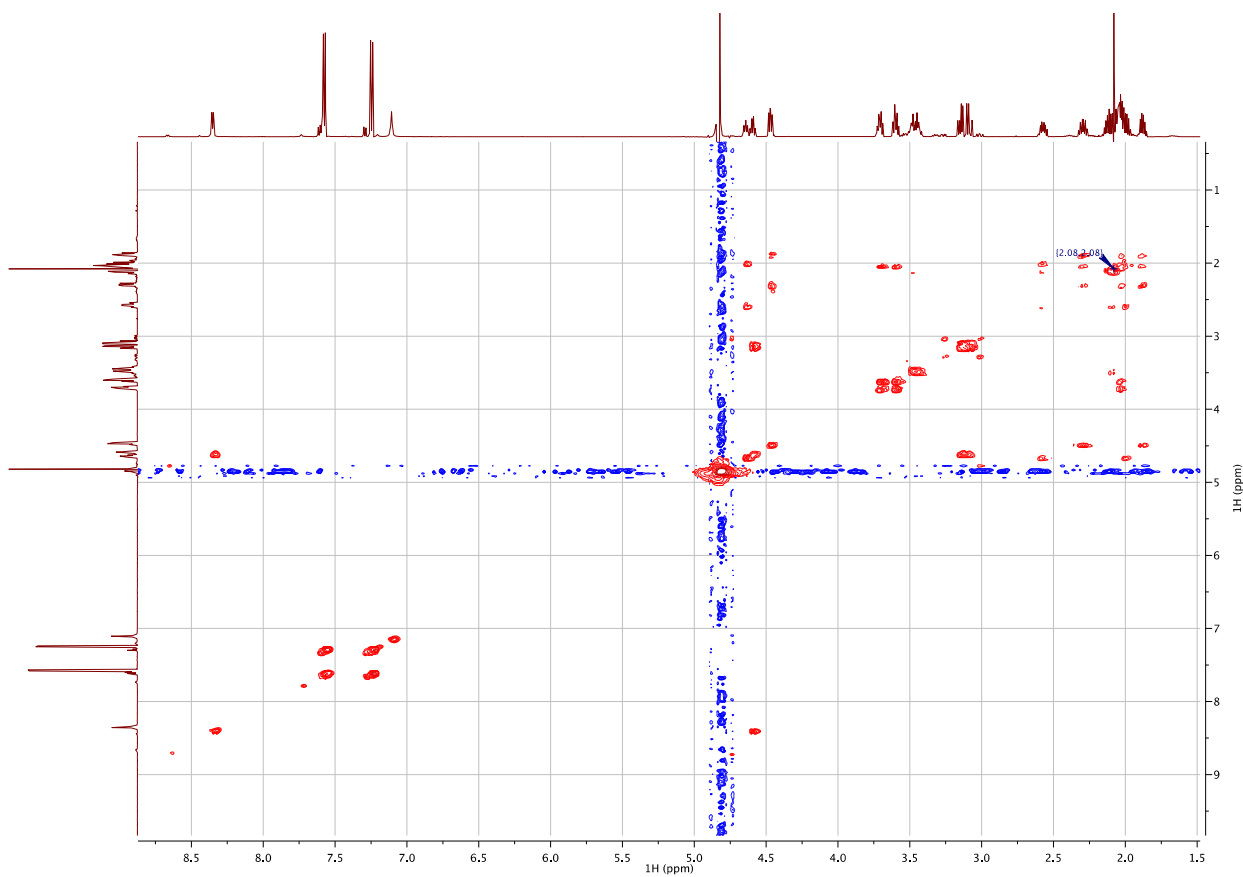
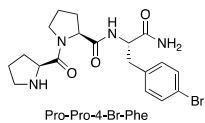
13.1 NMR Spectra of H-Pro-Phe(4-Br)-NH₂ (2A)

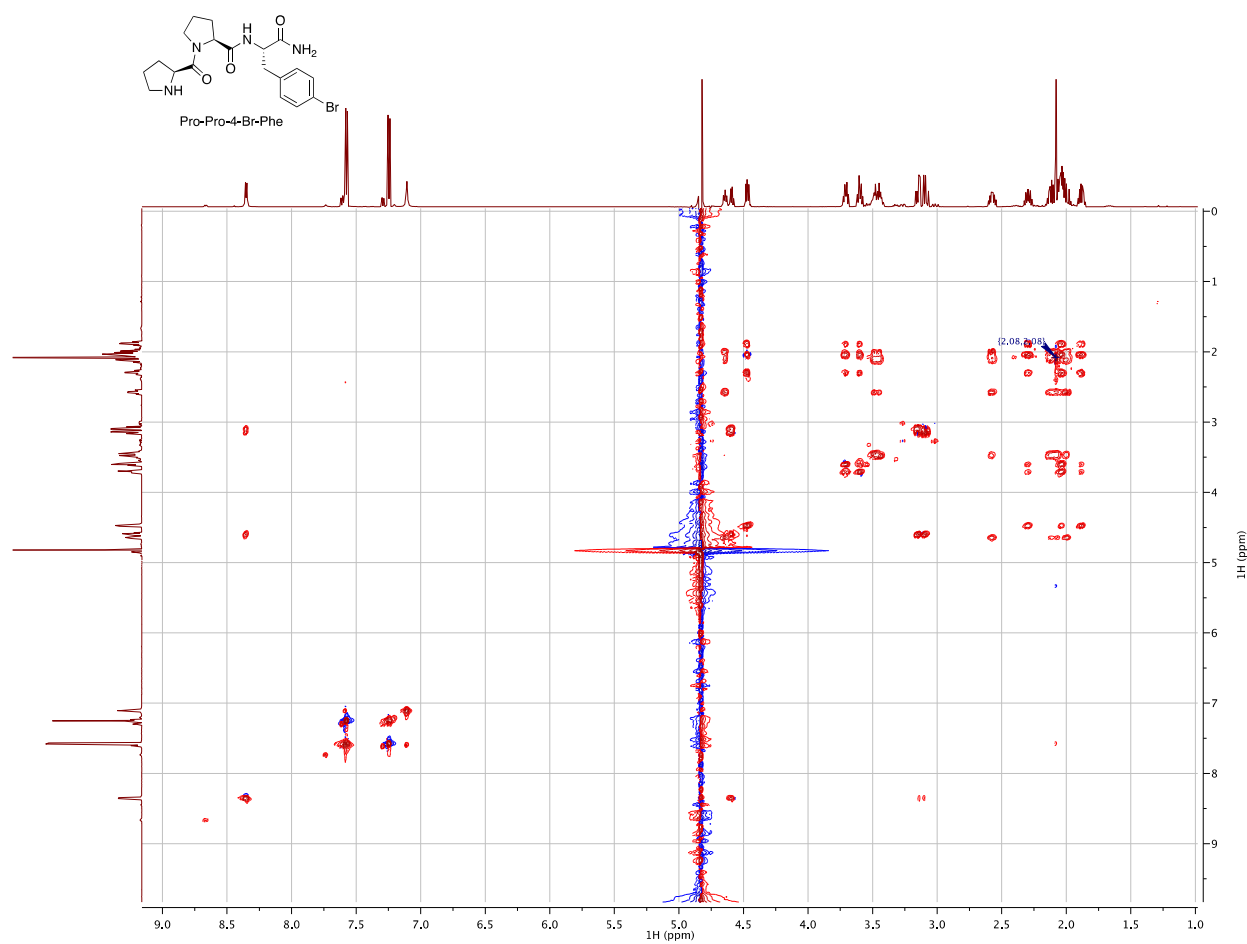


600 MHz ¹H spectrum of **2A** in H₂O:D₂O 9:1 pH 5.0 (9 mM) at 25 °C. The minor peaks from the F_{Br} residue are associated with an uncharacterized isomer of **2A**.

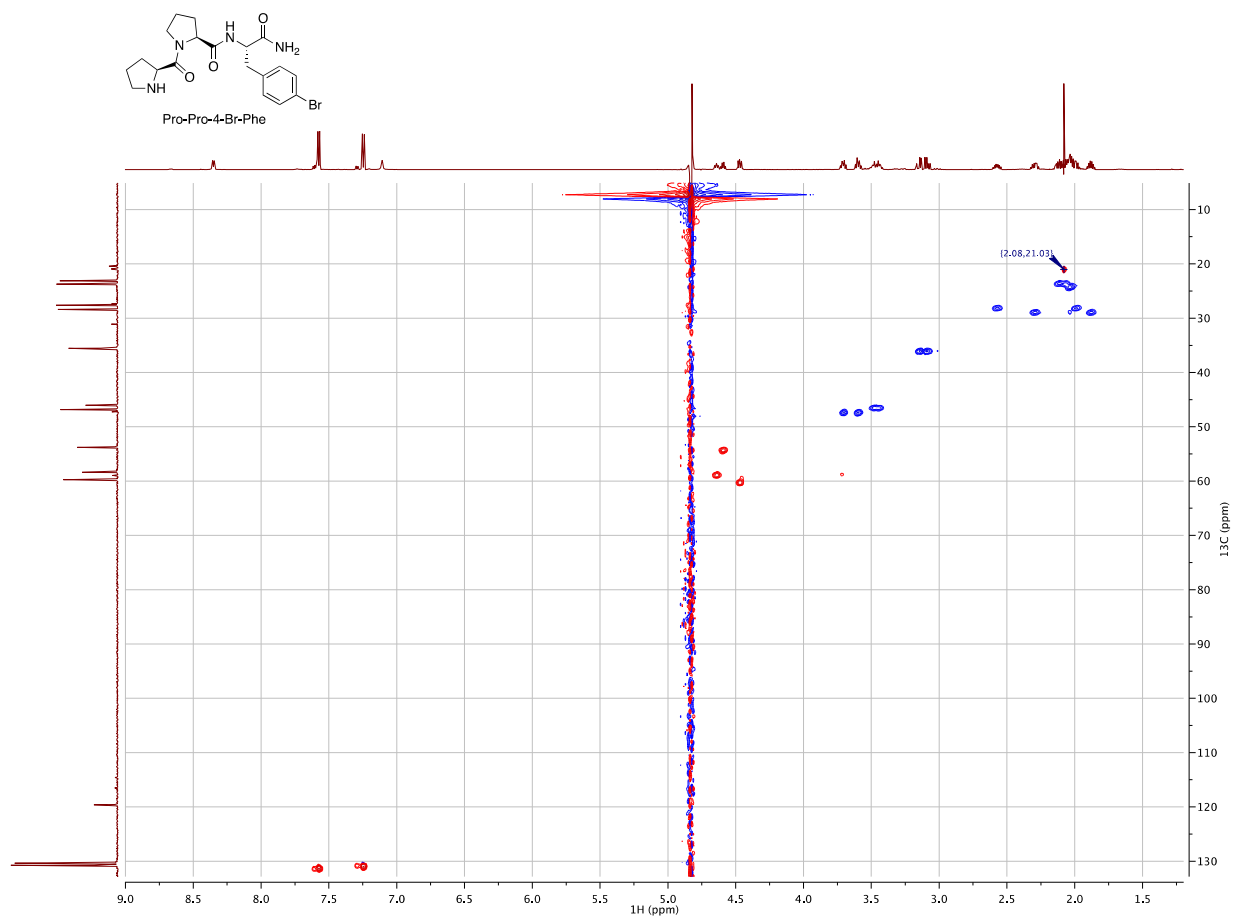


151 MHz ^{13}C spectrum of **2A** in $\text{H}_2\text{O}:\text{D}_2\text{O}$ 9:1 pH 5.0 (9 mM) at 25 °C. The minor peaks from the F_{Br} residue are associated with an uncharacterized isomer of **2A**.

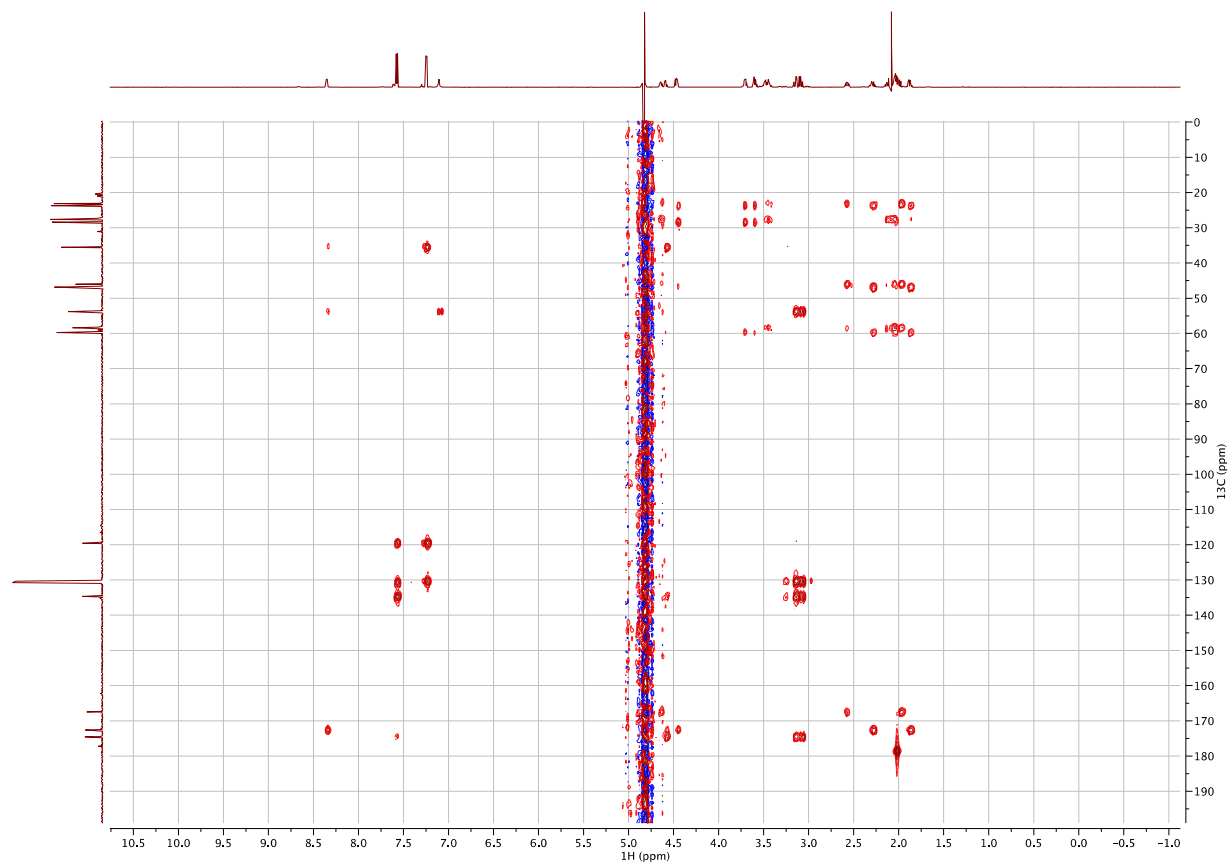




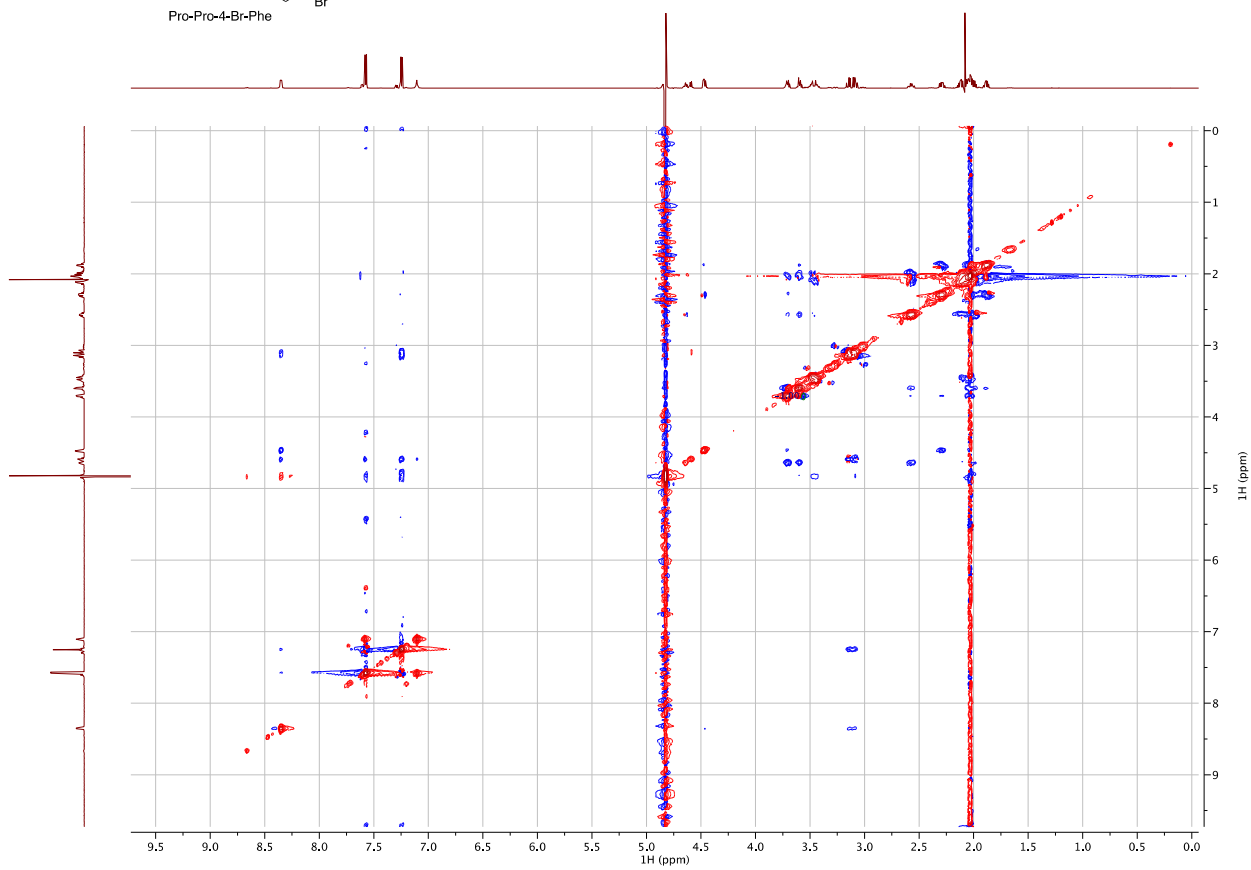
600 MHz TOCSY spectrum of **2A** in H₂O:D₂O 9:1 pH 5.0 (9 mM) at 25 °C.



600 MHz multiplicity-edited ^{13}C -HSQC spectrum of **2A** in $\text{H}_2\text{O}:\text{D}_2\text{O}$ 9:1 pH 5.0 (9 mM), 25 °C.

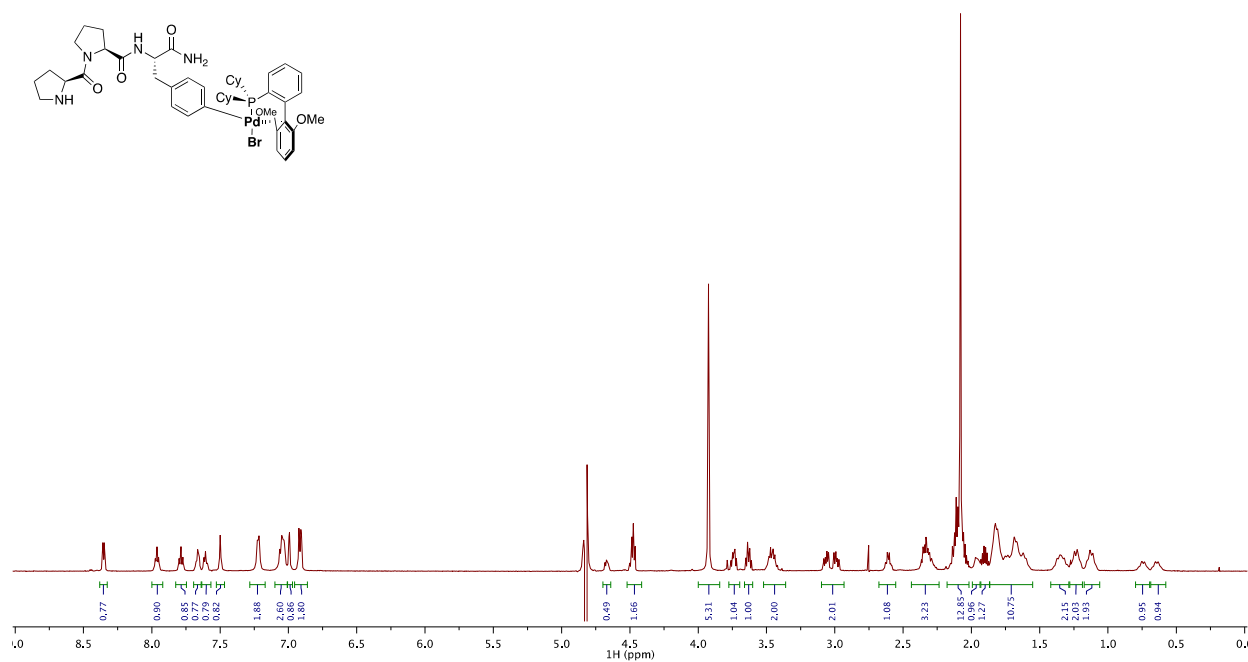


600 MHz ^{13}C -HMBC spectrum of **2A** in $\text{H}_2\text{O}:\text{D}_2\text{O}$ 9:1 pH 5.0 (9 mM) at 25 °C.

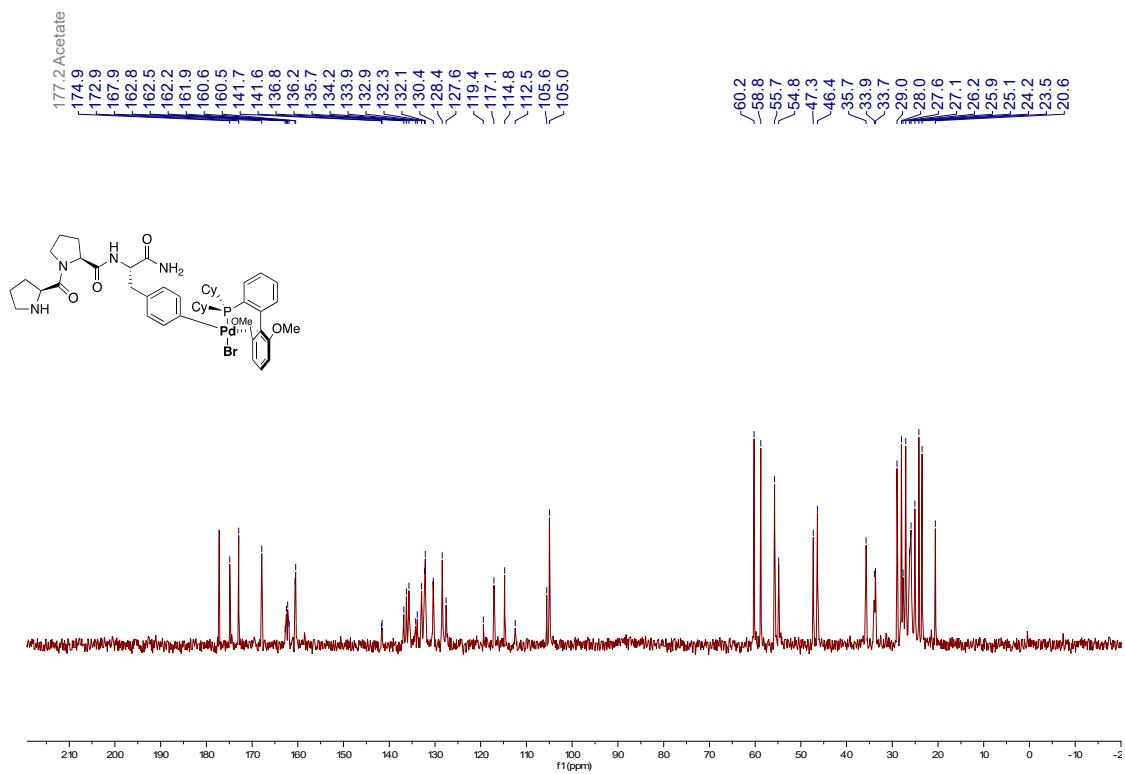


600 MHz ROESY spectrum of **2A** in $\text{H}_2\text{O}:\text{D}_2\text{O}$ 9:1 pH 5.0 (9 mM) at 25 °C.

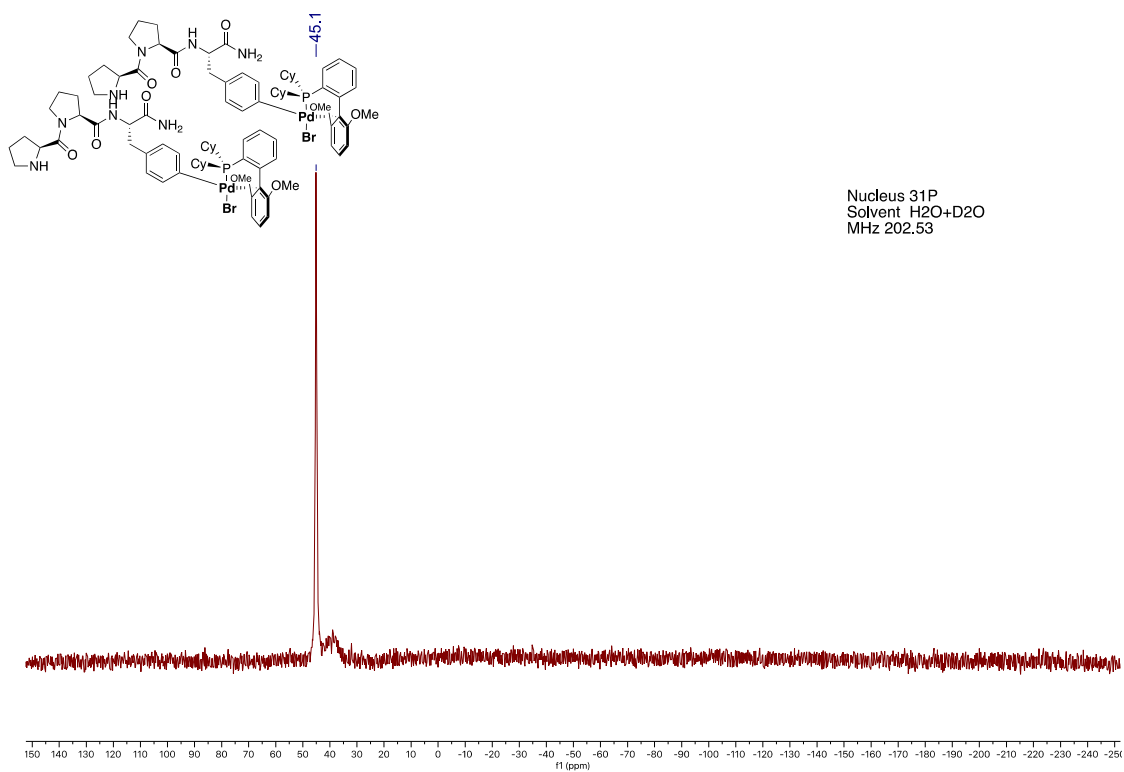
13.2. NMR Spectra of H-Pro-Phe(4-Br)-NH₂-Oxidative Addition Complex (**2B**)



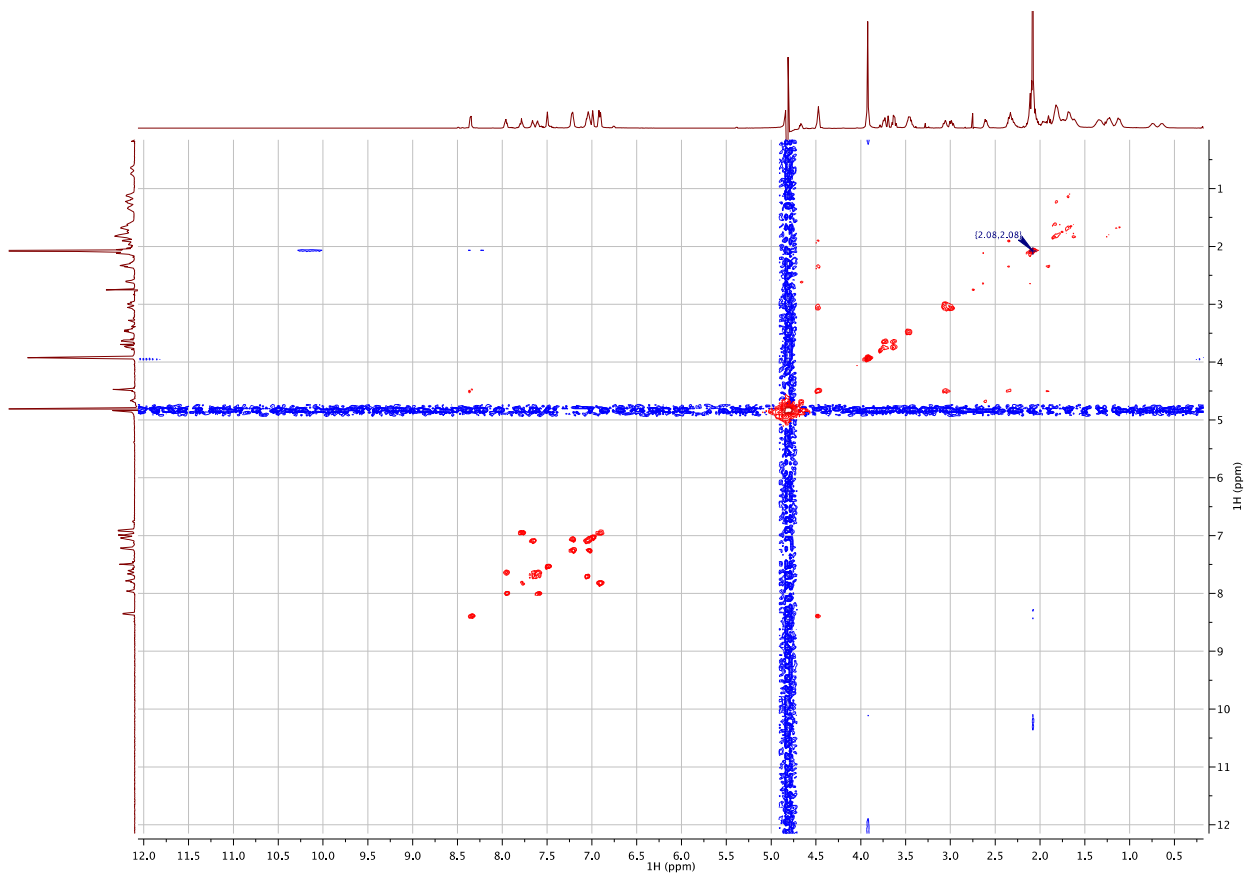
600 MHz ¹H spectrum of **2B** in H₂O:D₂O 9:1 pH 5.0 (3 mM) at 25 °C.



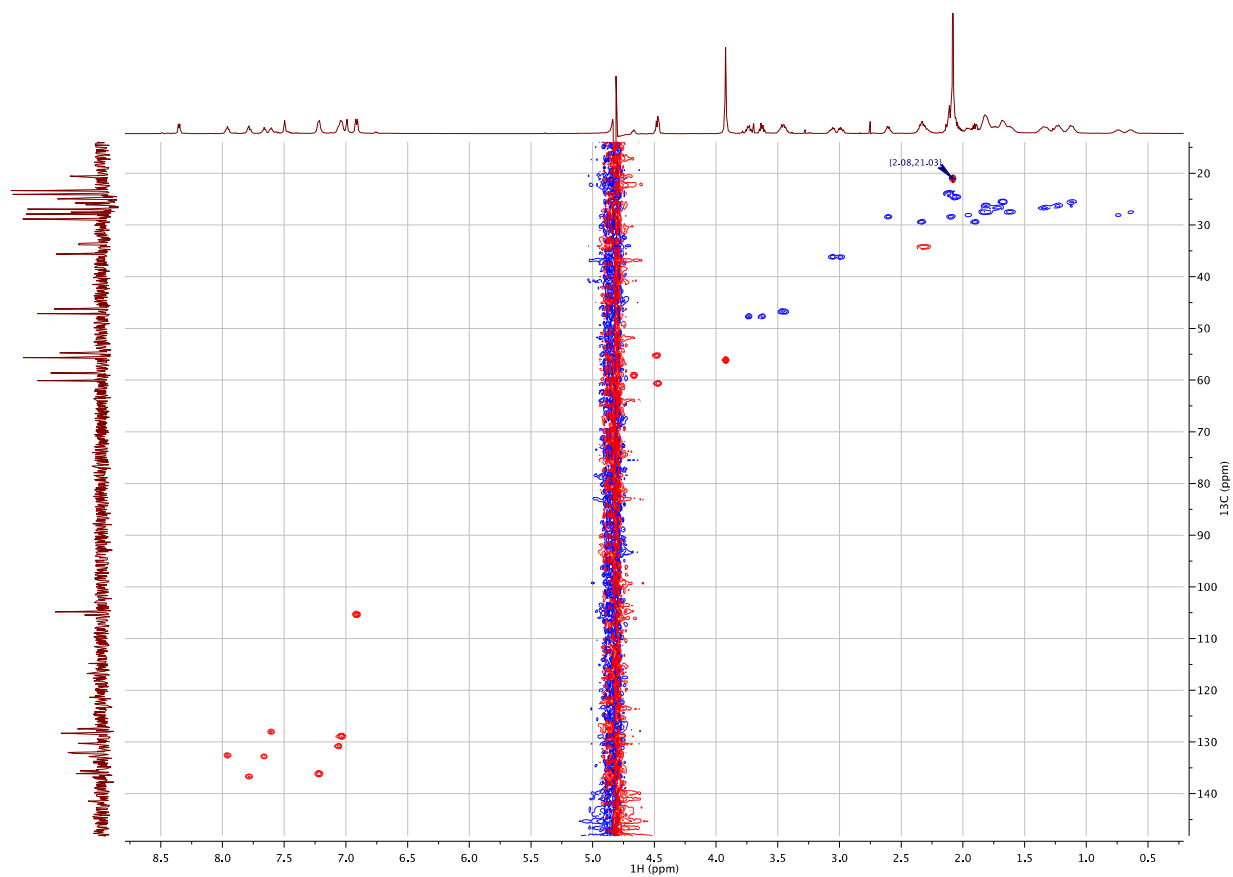
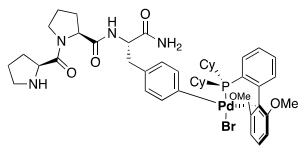
126 MHz ^{13}C spectrum of **2B** in $\text{H}_2\text{O}:\text{D}_2\text{O}$ 9:1 pH 5.0 (3 mM) at 25 °C.



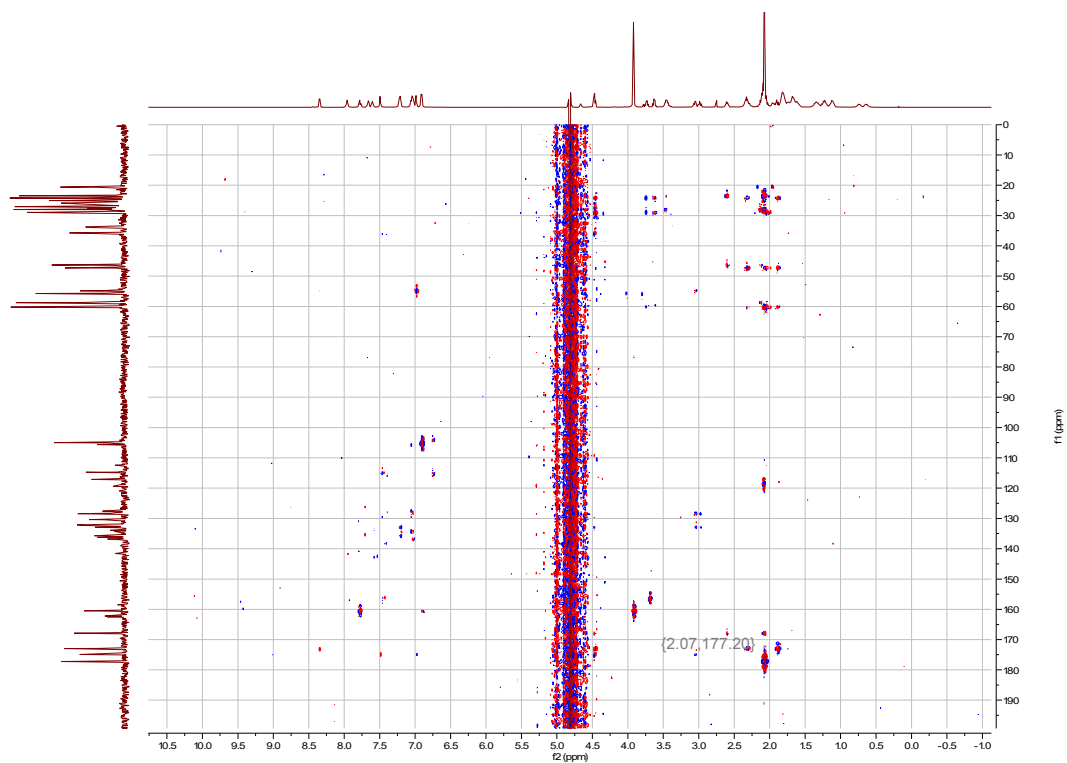
203 MHz ^{31}P spectrum of **2B** in $\text{H}_2\text{O}:\text{D}_2\text{O}$ 9:1 pH 5.0 (3 mM) at 25 °C.



600 MHz COSY spectrum of **2B** in $\text{H}_2\text{O}:\text{D}_2\text{O}$ 9:1 pH 5.0 (3 mM) at 25 $^\circ\text{C}$.



600 MHz multiplicity-edited ^{13}C -HSQC spectrum of **2B** in $\text{H}_2\text{O}:\text{D}_2\text{O}$ 9:1 pH 5.0 (3 mM), 25 °C.



600 MHz ¹³C-HMBC spectrum of **2B** in H₂O:D₂O 9:1 pH 5.0 (3 mM) at 25 °C.

14. REFERENCES

1. Vinogradova, E. V., Zhang, C., Spokoyny, A. M., Pentelute, B. L., Buchwald, S. L. *Nature*, 526, 687–691 (2015).
2. Mijalis, A. J.; Thomas III, D. A.; Simon, M. D.; Adamo, A.; Beaumont, R.; Jensen, K. F.; Pentelute, B. L. *Nat. Chem. Biol.*, 13 (5), 464–466 (2017).
3. Su, L.; Pan, Y.; Huang, Y.; Cho, C.; Chen, C.; Huang, S. *J. Biol. Chem.*, 286 (39), 34101–34120 (2011).
4. F. Neese, *The ORCA program system. WIREs Comput. Mol. Sci.* **2**, 73-78 (2012).
5. M. J. Frisch, G. W. Trucks, H. B. Schlegel, G. E. Scuseria, M. A. Robb, J. R. Cheeseman, J. A. Montgomery Jr., T. Vreven, K. N. Kudin, J. C. Burant, J. M. Millam, S. S. Iyengar, J. Tomasi, V. Barone, B. Mennucci, M. Cossi, G. Scalmani, N. Rega, G. A. Petersson, H. Nakatsuji, M. Hada, M. Ehara, K. Toyota, R. Fukuda, J. Hasegawa, M. Ishida, T. Nakajima, Y. Honda, O. Kitao, H. Nakai, M. Klene, X. Li, J. E. Knox, H. P. Hratchian, J. B. Cross, V. Bakken, C. Adamo, J. Jaramillo, R. Gomperts, R. E. Stratmann, O. Yazyev, A. J. Austin, R. Cammi, C. Pomelli, J. W. Ochterski, P. Y. Ayala, K. Morokuma, G. A. Voth, P. Salvador, J. J. Dannenberg, V. G. Zakrzewski, S. Dapprich, A. D. Daniels, M. C. Strain, O. Farkas, D. K. Malick, A. D. Rabuck, K. Raghavachari, J. B. Foresman, J. V. Ortiz, Q. Cui, A. G. Baboul, S. Clifford, J. Cioslowski, B. B. Stefanov, G. Liu, A. Liashenko, P. Piskorz, I. Komaromi, R. L. Martin, D. J. Fox, T. Keith, M. A. Al-Laham, C. Y. Peng, A. Nanayakkara, M. Challacombe, P. M. W. Gill, B. Johnson, W. Chen, M. W. Wong, C. Gonzalez, J. A. Pople, *Gaussian 03, Revision C.02*. Gaussian, Inc., Wallingford CT (2004).
6. C. Y. Legault, *CYLView, 1.0b*. University of Sherbrooke (2009).
7. A. D. Becke, *J. Chem. Phys.* **98**, 5648-5652 (1993).
8. C. Lee, W. Yang, R. G. Parr, *Phys. Rev. B* **37**, 785-789 (1988).
9. P.C. Harihan, J. A. Pople, *Theoret. Chimica Acta* **28**, 213-222 (1973).
10. M. M. Francl, W. J. Pietro, W. J. Hehre, J. S. Binkley, M. S. Gordon, D. J. DeFrees, J. A. Pople, *J. Chem Phys.* **77**, 3654-3665 (1982).
11. R. Krishnan, J. S. Binkley, R. Seeger, J. A. Pople. *J. Chem. Phys.* **72**, 650-654 (1980).
12. A. D. McLean, G. S. Chandler, *J. Chem. Phys.* **72**, 5639-5648 (1980).
13. L. A. Curtiss, M. P. McGrath, J.-P. Blandeau, N. E. Davis, R. C. Binning, L. Radom, *J.*

Chem. Phys. **103**, 6104-6113 (1995).

14. A. V. Marenich, C. J. Cramer, D. G. Truhlar, *J. Phys. Chem. B* **113**, 6378-6396 (2009).

15. N. M. O'Boyle, T. Vandermeersch, C. J. Flynn, A. R. Maguire, G. R. Hutchison, *J. Cheminform.* **3**:8 (2011).

16. T. A. Halgren, *J. Comput. Chem.* **17**, 490-519 (1996).

17. T. E. Barder, M. R. Biscoe, S. L. Buchwald, *Organometallics* **26**, 2183-2192 (2007).
